Chapter One
Introduction

1-1 What is nuclear structure ?

Nuclear structure physics has been an active field of research since the discovery of the nucleus. Rutherford found that most of all matter was concentrated in a very small core at the center of the atom in 1911 [1]. Perhaps the next great milestone was the discovery of the neutron by the associate and doctoral student of Rutherford, Chadwick in 1932 [2]. It is noteworthy that by this time special relativity, quantum mechanics, and the relativistic formulation of quantum mechanics were already developed. The existence of the positron was postulated by Dirac in his relativistic formulation of quantum mechanics in 1928 [3, 4] and it was subsequently discovered in 1932 by Anderson [5], the same year the neutron was discovered. I would thus list the finding of the neutron as a relatively modern discovery. The proton and neutron have since been used as the fundamental building blocks in describing the nature of the atomic nucleus to this day.

A number of models have been developed to describe the large array of phenomena and properties displayed by atomic nuclei. The liquid drop model, first proposed by Gamow in 1928 [6], viewed the nucleus as drop of liquid whose constituent particles were held together by surface tension. This model was able to describe some bulk properties of nuclei. Using the ideas of the liquid drop model, von Weiz̈acker developed a semiempiral mass formula [7] to predict nuclear masses. A large breakthrough in nuclear theory came in 1949 when Maria Goeppert-Mayer [8] and independently Jensen, Haxel and Suess [9] were able to explain the magic numbers in nuclei, where nuclei would exhibit an increased stability, by including a spin-orbit interaction term in a Hamiltonian that considered all nucleons to be orbiting essentially freely in an average field created by all the other nucleons. The magic numbers correspond to closed shells in nuclei analogous to the filling of electron shells in atoms. Excited states were found that correspond to the excitation of a nucleon into an orbit of a higher lying shell as predicted by the model. The shell model, as this model is called, has been one of the most fundamental ways to describe atomic nuclei. It has since been used extensively in the analysis of experimental data.

Apart from the single-particle excitations found in nuclei, another type of excitation, collective excitation, was soon explained. In 1950, Rainwater observed that spherical nuclei could easily be deformed [10]. This led the way in the 1950's for more ground breaking work done by Bohr and Mottelson [11, 12] and also Hill and Wheeler [13] when they presented models for collective motion in nuclei. These models used shapes to parameterize the nucleus and used their dynamics to derive the collective phenomena that was observed. Since the discoveries of single-particle and collective motion, these have been the two ways in which excitations in nuclei have been classified. The interplay between single-particle and collective degrees of freedom has long been and continues to be an active field of study. One example is perhaps a variation of the shell model, which was proposed by Nilsson in 1955 [14] where he considered the average potential of the shell model to be deformed. This lead to the idea of changing shell structure with deformation.

In 1975, the Interacting Boson Model (IBM), the model used in the present work, was proposed by Iachello and Arima [15] , where interacting bosons are used to describe collective excitations in nuclei. From the symmetry properties of the model's boson hamiltonian, three types of idealized nuclei were found whose properties can be calculated analytically. These three limits of nuclei can be used as benchmarks with which to classify different nuclei. It was found that different regions of the nuclear chart exhibit properties that are similar to one of these idealized limits.

The above account of nuclear physics is very brief and highlights only a few of the main accomplishments in nuclear physics in the twentieth century. Although brief, it can be seen that there is not one single comprehensive theory in nuclear physics, but several models tailored to describe specific phenomena. A quote taken from the book of Eisenbud and Wigner [16] published in 1958 describes the state of nuclear theory in the following way :

"Internucleon forces are not yet completely known and it is clear that they have a complex character. Even the consequences of a simple interaction are difficult to obtain for a system containing a large but finite number of particles. A good deal of effort has been expended, therefore, in the search for simple models in terms of which the broad regularities satisfied by nuclei could be understood. This search has led to a number of interesting but only partially successful models; these have proved very fruitful for the stimulation of experimental research, and for the development of further ideas on nuclear structure. One can hope that future investigations will clarify the limitations of these models and provide an understanding of the validity of different models for different groups of phenomena".

Although written in 1958, the ideas set forth in this quote still serve as an description of present day research in nuclear physics. It is with the aim of better understanding the "broad regularities satisfied by nuclei" and "understanding the validity of different models for different groups of phenomena" that the topic of this present work is introduced. One of the broad regularities in nuclei that will be investigated is the existence of a certain class of collective excitations called mixed-symmetry states defined within the Interacting Boson Model. The data obtained from the experimental investigations of these states will help elucidate the extent of the validity of the Interacting Boson Model.

1.2 Historical Survey

1- *Kr* isotopes

The even–even $^{76-90}Kr$ are the members of the chain existing around the mass region $A \cong 80$ and they are settled away from both the proton closed-shell number at 28 and neutron closed shell at 50. The interacting boson model-2 (IBM-2) has recently been applied to many light isotopes of Kr with emphasis on the energy levels and on the electromagnetic transition rates.

Several theoretical and experimental studies of even-even *Kr* isotopes have been carried out: Kaup and Gelberg [17] , have performed systematic analysis of *Kr* isotopes in IBM-2, reproduced energy levels. Helleister *et al.*, [18] studied the energy levels and Electric transition probabilities and made comparison with experimental

data. Meyer *et al.,* [19] investigated the nuclear structure of the ^{82}Kr isotope, using ion-beam spectroscopy studies and compared the experimental data with the results of IBM-2.

Glannatiempo *et al.,* [20] studied the life-time of the 0_2^+ level in the ^{80}Kr isotope and compared the result with the calculated value of IBM-2. Deibaksh *et al.,* [21] have performed IBM-2 calculations on *Kr* isotopes , using two-different approaches. The first approach based on the energy of bosons as $\varepsilon_\pi = \varepsilon_\nu$, and the second approach was based on the difference between the energy of proton boson and energy of neutron boson $\varepsilon_\pi \neq \varepsilon_\nu$. The results of IBM-2 were found to be in good agreement with experimental data except for the state 2_3^+. Giannatiempo *et al.,* [22] have studied the symmetry property of the bands in $^{74\text{-}82}Kr$ isotopes by calculating *F*-spin and the n_d component of the wavefunction of the states of these bands.

Shi Zhu-Yii *et al.,*[23] have studied *Kr* isotopes by using a microscopic *sd* IBM-2 +2q.p. approach; the levels of the ground-band, γ-band and partial two-quasiparticle bands for $^{72\text{-}84}Kr$ isotopes were calculated. The data obtained are in good agreement with the experimental results, and successfully reproduce the nuclear shape phase transition of $^{72\text{-}84}Kr$ isotopes at zero temperature. The ground-state band is described successfully up to $J^\pi = 18^+$ and E_x=10 MeV. Based on this model, the aligned requisite minimum energy has been deduced. The theoretical calculations indicate that no distinct change of nuclear states is caused by the abruptly broken pair of a boson, and predict that the first backbending of *Kr* isotopes may be the result of aligning of two quasi-neutrons in orbit $g_{9/2}$, which gains the new experimental support of the measurements of *g*- factors in the $^{78\text{-}86}Kr$ isotopes.

Al-Khudair and Gui-Lu [24] studied the level structure of $^{76\text{-}82}Kr$ isotopes within the framework of IBM-2 , and performed that the $J^\pi = 2^+$ (one-phonon mixed symmetry state) and $J^\pi = 1^+, 2^+, 3^+$ (two-phonons mixed symmetry states), and have been identified by analyzing the wavefunction of *M1* transition.

Turkan *et al.,* in 2006 [25] determined the most appropriate Hamiltonian that is needed for present calculations of nuclei in the $A \cong 80$ region by the view of Interacting Boson Model-2 (IBM-2). After obtaining the best Hamiltonian parameters, level energies and B(E2) probabilities of some transitions in $^{88\text{-}90}Kr$ nuclei were estimated. Results were compared with previous experimental and theoretical data and it was observed that they are in good agreement.

Turkan *et al.,* in 2009 [26] studied The quadrupole moments of $^{76,78,80,82,84,88}Kr$ and $^{74,76,78,80,82}Se$ isotopes in terms of the interacting boson model (IBM), and it was found that a good description of them can also be concluded in this model. Before the quadrupole moments were calculated, the positive-parity states and electromagnetic-transition rates (*B*(*E*2)) of even-mass *Kr* nuclei have also been obtained within the framework of IBM. It was seen that there is a good agreement between these results and the previous experimental data. The quadrupole moments of the neighboring Se - isotopes were also obtained and it was seen that the results are satisfactorily agree well with the previous experimental data.

2- Xe Isotopes

The Interacting Boson Model enables one to classify the nuclei according to the dynamical symmetries of the *IBM* Hamiltonian. Three symmetries are most relevant for the description of excited states of quadrupole-collective nuclei: *U(5)* for vibrational nuclei [27], *SU(3)* for axially deformed nuclei [28], and *O(6)* for deformed nuclei with soft triaxiallity [29]. In the *A* = 130 mass region, the *Xe* isotopes exhibit excitation spectra close to the *O(6)* symmetry. After some theoretical investigations [30,31,32,33,34], it was concluded that the xenon isotopes should lie in a transitional region from *U(5)*- to an *O(6)*-like structure as the neutron number decreases from the closed shell *N*=82. This was later supported by Casten and von Brentano [35] who presented the evidence for an extensive region of nuclei near *A*= 130 resembling the *O(6)* symmetry. The evolution of the one-quadrupole phonon 2_m^+ state with *F*-spin value $F = F_{max} - 1$ in a *U(5)-O(6)* transition is still unknown. Thus *Xe* was a good candidate for exploring this *U(5)-O(6)* transitional region.

The low-lying states showing a rich collective structure in this region, were investigated extensively in terms of various models, such as the interacting boson model (IBM) [35,36,37,38,39,40,41], the fermion dynamical symmetry model (FDSM) [42,43], the pair-truncated shell model (PTSM) [44,45] and the nucleon-pair shell model [46,47,48,49].

The *Xe* , region with the mass number $A \approx$ 120–130 has recently been studied experimentally and interpreted by several models [50,51,52,53]. In ref.[54], the general Bohr Hamiltonian (GBH) is applied to describe the low-lying collective excitations in even–even isotopes of *Te, Xe, Ba, Ce, Nd* and *Sm*, and the low-lying collective states of even–even nuclei were investigated along the region of 50 < Z, N < 82. The ground state properties of even–even *Xe* isotopes have been the subject of theoretical [55] and experimental studies [56-63] involving in-beam γ-ray spectroscopy.

Maras *et al*.,[64] have investigated, the ground state, quasi beta and quasi gamma band energies of $^{114,116,118,120}Xe$ isotopes by using both IBM-1 and IBM-2 versions of the interacting boson model (IBM). In calculations, the theoretical energy levels have been obtained by using PHINT and NPBOS program codes. The results compared with the experimental data in respective tables and figures. It was seen that the obtained theoretical results were in good agreement with the experimental data.

Laurent Coquard [65] have studied the evolution of the one-quadrupole phonon 2_{1M}^+ mixed-symmetry state in *Xe* isotopes and showed that collective nuclei are characterized by rotational and vibrational states due to a common and, therefore, "collective" behavior of the two constituents of the nucleus: protons and neutrons. The evolution of the collectivity (spontaneous deformation) is governed by the proton-neutron interaction in the valence shell. Nuclear states, that are particularly sensitive to the proton-neutron interaction in the valence shell, are the so called mixed symmetry states. In their work they determined the fundamental evolution *i.e.,* the

one-quadrupole phonon 2_{1M}^+ state, in a transitional region from vibrational nuclei (^{134}Xe) to γ-soft nuclei reflecting the O(6)-like structure of the IBM-2 ($^{124,126}Xe$). Projectile-Coulomb excitation of *Xe* isotopes has been performed at Argonne National Laboratory (ANL) using the Gammasphere array for the detection of γ-rays.

Turkan and Maras in 2011 [66], have studied the energy levels and transition probabilities *B(E2)* of some even-even Te (*Z*=52, *N*=68-80 and *N*=84) and even-even *Xe* nuclei (*Z*=54, *N*=68-80 and *N*=84-88) by using the interacting boson model (IBM-1 and IBM-2). The results were compared with some previous experimental and theoretical values. It was seen that an acceptable degree of agreement between the predictions of the model, (IBM-1 and IBM-2) and experiment was achieved.

Eid and Diab [67] in 2012 studied the potential energy surfaces, $V(\beta, \gamma)$, for a series of Xenon isotopes $^{122-134}Xe$. The relatively flat potential to ^{130}Xe and energy ratio $E(4_1^+)/E(2_1^+) = 2.2$ show E(5) symmetry to the nucleus which is lying in the transition region from γ-soft to vibrational characters. The interacting boson model ($IBM-1$) has been used in calculating levels energies and electromagnetic transition probabilities $B(E2)'s$. Backbending is observed for $^{122-130}Xe$. The calculated values were compared to the available experimental data and showed a reasonable agreement.

3- *Nd* Isotopes

Neodymium isotopes are the members of the chain of nuclei around $A \approx 140$ and they represent an ideal case for studying the influence of the shape transition from spherical to deformed nuclei. The nuclei around mass 140 have many interesting features such as high-spin isomers, backbending phenomena, even–odd energy staggering of quasi-bands caused by a soft triaxial deformation, and features recently referred to as 'chiral bands'. These nuclei belong to a typical transitional region between spherical and deformed shapes.

It has been recognized that in order to be able to judge any model on the nuclear structure of even–even *Nd* nuclei, more accurate theoretical details are necessary. This has led to a wealth of theoretical studies , that were performed in the last 15 years, with many probes and the *B(E2)* values of some low-lying collective states were obtained.

Manio and Ventura [68] have studied the even-even $^{136-154}$Nd in the IBM . They discovered all three limiting cases of the IBM and transitional nuclei between the limits in the isotopic chain. Chuu *et al*., [69] studied the ^{148}Nd nucleus in the interacting boson model in the context of an *N*=88 isotones. Gupta [70] studied the $^{144-150}Nd$ isotopes in IBM-1. In this study the level structure is analyzed taking into account of the available experimental information, with respect to the symmetries of IBM-1**.** The level energies, B(E2) values, and interband B(E2) ratios were compared with available data The adopted level schemes of $^{144-150}Nd$ and the varying limitations of the interacting boson model in these isotopes were discussed.

Eurogam-I and Gammasphere experiments have established new level scheme for $^{152\text{-}156}Nd$ isotopes [71]. New experimental levels in $^{146\text{-}150}Nd$ isotopes were also obtained [72]. Static's moments have been measured over the years [73].

Long Guilu *et al.,*[74] studied the spectra and *E*2 properties of $^{146\text{-}156}Nd$ using the IBM-2. They found that $^{146\text{-}150}Nd$ are in the transition from vibrational to rotational (*SU*(5) to *SU*(3)). From ^{152}Nd onward the isotopes are nearly perfect rotors. Possible deformation saturation is discussed in the interacting boson model.

It was recently shown that a signature of phase transition is observed in the chain of *Sm*, *Mo* and *Nd* isotopes, where isotopes are ^{152}Sm, ^{104}Mo and ^{150}Nd [74,75,76]. ^{150}Nd display the predicted features of the *X*(5) symmetry and marks critical point. However, more detailed studies and experiments are needed to get ideas about this signature.

In 2007 Turkan and Inci [77] studied some even–even neodymium nuclei using IBM-2. In their study, they determined the most appropriate Hamiltonian that is needed for their calculations of nuclei in the $A \approx 130$ region, by the view of projection of IBM-2 parameters onto IBM-1. The interacting boson model has been widely used for describing the quadrupole collective states of the medium heavy nuclei and no distinction is made between proton and neutron variables, when the first version IBM-1 is applied. So, triaxiality can be described explicitly, through the introduction of cubic terms in the boson operators. However, the microscopic foundations state is very important to describe the proton and neutron variables explicitly. This is also a generalized definition of the second version of the IBM-model ,IBM-2 model. Using the best-fitted values of parameters in the Hamiltonian of the IBM-2, they calculated the energy levels and *B*(*E*2) values for a number of transitions in $^{144,146,148,150,152,154}Nd$. The results were compared with the previous experimental and theoretical data which showed. Many *B*(*E*2) values, that are still not known so far, are stated and the set of parameters, used in these calculations, are the best approximation that has been carried out so far. It has turned out that the interacting boson model is fairly reliable for the calculation of spectra in the entire set of $^{144,146,148,150,152,154}Nd$ isotopes.

Inan *et al*., [78] in 2008 studied the *X*(5) symmetry which take place when moving continuously from the pure U(5) symmetry to the SU(3) symmetry and it implies a definite relations among the level energies and among the E2 transition strengths. It was recently shown that a signature of phase transition is observed in the chain of Sm, Mo and Nd isotopes, where ^{152}Sm, ^{104}Mo and ^{150}Nd display the predicted features of the X(5) symmetry and mark therefore the critical point. However, more detailed studies and experiments are needed to get ideas about this signature. Without entering into detail they have firstly compared the results obtained in their previous study [15] of $^{144\text{-}154}Nd$ with that of the limits in *X*(5) symmetry and then given a clear description about the validity of the Hamiltonian parameters used in the study. At the end, they have concluded that some of the *Nd* isotopes display *X*(5) symmetry features.

Turkan and Inci [79] compared some predictions between Davidson-like potentials and Interacting Boson Model: $X(5)$ behavior of even–even $^{128-140}$Nd Isotopes, they denote that the level scheme of the transitional nuclei $^{128-140}$Nd also presents the characteristic $X(5)$ pattern, not only in the ground-state band, but also in some low-lying bands. An adequate point of the model leading to the $X(5)$ symmetry was therefore confirmed. They have also carried out calculations of positive-parity states of even-mass *Nd* nuclei within the framework of the interacting-boson model, and then the calculated energy values were compared with the experimental data along with the Davidson potential predictions. By comparing transitional behavior in the *Nd* nuclei with the predictions of an $X(5)$ critical symmetry, and investigated an achievable degree of agreement between the predictions of the model leading to this symmetry and the interacting-boson model IBM-1 and IBM-2. Their rsults agree well experimental predictions.

4 - *Ge* Isotopes

Even-even *Ge* isotopes, with $Z = 32$ and $32 \leq N \leq 50$, have a collective quadrupole excitation strongly dependant on the number of nucleons outside the closed shells 28 and 50, and the neutron-proton interaction is known to have a great influence on nuclear properties. These isotopes are part of an interesting region including *Se* and *Kr*, which has and is likely to attract many experimental and theoretical works [80–83]. Hsieh *et al.*, [84] found that the spectra of those nuclei can not be explained in terms of simple versions of the rotational or vibrational models, with shape coexistance, for and there is a transition from spherical to weakly deformed shape with different types of deformations.

The previous work of configuration mixing by Duvail *et al.*, [85] using a version of the IBM-2 with configuration mixing, has shown that a good description of the stable *Ge* nuclei can be obtained. In this work they applied the standard, two-particle two-hole, IBM-2 with configuration mixing to the stable nuclei and extrapolate the model predictions to the recently explored radioactive neutron-rich isotopes $^{78-80}$Ge and the single-closed shell nucleus ^{82}Ge.

Padilla-Rodal *et al.*, [86] showed that the low energy spectra, electric quadrupole transitions, and quadrupole moments for the *Ge* isotopes can be determined in the framework of the IBM-2 with configuration mixing. These calculated observables reproduce well the available experimental information including the newly obtained data for radioactive neutron-rich $^{78-82}$Ge isotopes. Using a matrix formulation, a geometric interpretation of the model was established. The two energy surfaces determined after mixing, carry information about the deformation parameters of the nucleus. For the even-even *Ge* isotopes the obtained results are consistent with the shape transition that takes place around the neutron number $N = 40$.

The irregular neutron-dependence of important observables such as the excitation energy of the 0_2^+ states, the relative values of the electric transition probability and the population cross sections in two-neutron-transfer reactions. Vergnes *et al.*, [87] have suggested that a structural change takes place around $N = 40$ for *Ge* isotopes. In combination with the measurement of the electric quadrupole moments associated with the 2_1^+ and 2_2^+ states [88,89], thies experimental data have

been taken as evidence of a shape transition and the coexistence of two different kinds of deformations for this isotopic chain [90].

Turkan and Maras [91] have been studied the sufficient aspects of model leading to the E(5) symmetry and proved by presenting $E(5)$ characteristic of the transitional nuclei $^{64-80}Ge$. The positive parity states, of even-even Ge nuclei within the framework of Interacting Boson Model (IBM) , have been calculated and compared with the Davidson potential predictions along with the experimental data. It can be said here that the set of parameters used in these calculations are the best approximation that has been carried out so far. Hence, the Interacting Boson Model is fairly reliable for the calculation of spectra in such set of Ge isotopes.

Subber [92] has been used Interacting Boson Models IBM-1and IBM-2, to calculate energy levels and nuclear properties of the even-even $^{64-80}Ge$ isotopes. Energy levels of the low lying states of these nuclei were produced, the electric quadruple reduced transition probabilities also were calculated as well. Mixing ratios $\delta(E2/M1)$ for transitions with $\Delta I = 0$, $I \neq 0$ are calculated. All these results were compared with the available experimental data and other IBM their versions calculations. Satisfaction agreements were obtained.

In this work, we have carried out the level scheme of the transitional nuclei $^{64-80}Ge$ showing the characteristic $E(5)$ pattern in their some low-lying bands. The positive parity states of Ge isotopes also stated within the framework of the Interacting Boson Model. By comparing transitional behavior in the Ge isotopes with the predictions of an $E(5)$ critical symmetry, an achievable degree of agreement has been obtained. Configuration mixing of bosons have been used to study the nuclear structure and electromagnetic properties of Ge isotopes.

1.3 Scientific Motivation

The aims of the present work are as follows:

1- To study the nuclear structure and electromagnetic transitions $B(E2)$, $B(M1)$, mixing ratio $\delta(E2/M1)$, monopole transitions, isomer shifts and isotopic shifts for even-even Kr, Xe, Nd and Ge isotopes by means of the Interacting Boson Model -2 (IBM-2).

2- A certain class of collective states arise in the the Interacting Boson Model called mixed-symmetry states , which can be thought of as states in which the protons and neutrons oscillate out of phase with respect to one another. This mode of excitation should be sensitive to the proton-neutron interaction in the valence shell because of its isovector character. Seeing how these states evolve as a function of proton and neutron number can give insight into the strength of the proton-neutron interaction for a given mass region. The proton-neutron interaction in the valence shell of nuclei has been attributed as being responsible for the formation of collectivity in Kr and Xe , Nd and Ge isotopes .

New classes of symmetries have also been defined to describe the nucleus -3 at the phase transitional point. These are the symmetries of the geometric Bohr Hamiltonian and are denoted as E(5) and X(5). There has been a lot of work going on

in finding out the nucleus belonging to different mass regions to obey these kinds of critical point symmetry. There are many experimental signatures for the nucleus to lie at the phase transitional point; these are listed in a very ordered manner by Clark [93]].

4- To study the configuration mixing character for *Ge* isotopes which are of special interest because of the coexistence of two-sets of bands, of a very different character in these isotopes when the IBM-2 configuration mixing provides a good description of both states. Also the Interacting Boson Model (IBM) with configuration mixing can be give a geometrical interpretation, when ones used in conjunction with a (matrix) coherent-state method. This approach can also be used to study the geometric aspects of shape coexistence in nuclei, as well as the phase space diagrams associated to this phenomenon.

1.4 Outline

Finally, a brief outline of the remainder of this work will be given. In Chapter Two, some background on the collective models, briefly vibrational and rotational models and in details the Interacting Boson Model, mixed-symmetry states and configuration mixing will be presented. The results are discussed in Chapter Three. Chapter four gives the concluding remarks and suggestions for future work.

3.4 Ge Isotopes

3.4.1 Hamiltonian Interaction Parameters

Table (3-25) contains the IBM-2 Hamiltonian parameters (in MeV) used in the present study to calculate the energies of the positive parity low-lying levels of $^{64-80}$Ge. N_π =2 (first configuration or normal configuration 2π) and N_v changes from 4 to 7 for $^{64-72}$Ge and finally varies from 6 to 3 for $^{74-80}$Ge. The Hamiltonian parameter values of IBM-2 were estimated by fitting to the experimental energy levels and it was made by allowing one parameter to vary while keeping the others constant. This procedure was carried out iteratively until an overall fit was achieved. The computer program *NPBOS* [124], was used to make the Hamiltonian diagonal. In principle, all parameters can be varied independently in fitting the energy spectrum of one nucleus. As a results calculations, we find that the structure of the spectra determined almost by four quantities ε , K , χ_v and χ_π. These quantities may in general depend both on the proton boson number N_π and neutron boson number N_v, guided by the microscopic calculations of [114]. We have assumed that only ε and K depend on N_π and N_v i.e., $\varepsilon(N_\pi, N_v)$, $\kappa(N_\pi, N_v)$ while χ_π depends only on N_π constant for all isotopes and χ_v on N_v . Thus a set of isotopes have the same value of χ_π. The parameterization allows one to correlate a large number of experimental data. Similarly, when a proton-proton interaction $V_{\pi\pi}$ and neutron-neutron interaction V_{vv} is added, the coefficients C_L are taken as $C_L^\pi(N_\pi)$ and $C_L^v(N_v)$ i.e., the proton-proton interaction will only depend on N_π and neutron-neutron on N_v**.**

Table (3-25): IBM-2 Hamiltonian parameters (N_π = 2), all parameters in MeV units except χ_π .and χ_v are dimensionless

Isotopes	ε	κ	χ_v	χ_π	C_{0v}	C_{2v}	C_{4v}	$C_{0\pi}$	$C_{2\pi}$	$C_{4\pi}$	$\xi_1 = \xi_3$	ξ_2
Ge-64	1.235	-0.220	1.250	0.7-	0.0	0.0	-0.33	0.0	0.0	0.0	0.061	-0.060
Ge-66	1.370	-0.235	1.200	-0.7	0.0	0.0	0.0	0.0	0.0	0.0	0.061	-0.055
Ge-68	1.401	-0.200	1.225	-0.7	-1.50	0.0	0.21	0.0	0.0	0.0	0.051	-0.040
Ge-70	1.425	-0.195	1.325	0.7-	-0.19	-0.38	0.17	0.0	0.0	0.0	0.022	-0.039
Ge-72	1.300	-0.245	1.150	-0.7	-2.41	0.0	0.16	0.0	0.0	0.0	0.021	-0.030
Ge-74	1.090	-0.210	1.100	-0.7	-1.21	-1.21	-0.22	0.0	0.0	0.0	-0.021	-0.029
Ge-76	0.945	-0.215	1.100	0.7-	0.0	0.0	-0.90	0.0	0.0	0.0	-0.021	-0.021
Ge-78	0.930	-0.215	1.100	-0.7	0.0	0.0	-0.22	0.0	0.0	0.0	-0.011	-0.018
Ge-80	1.200	0.225	1.000	-0.7	0.0	-0.9	0.0	0.0	0.0	0.0	-0.100	-0.013

The alternate configuration used for the germanium isotopes involves a two-particle-four-hole excitation in the shell model proton space. This corresponds to two proton boson particles and one proton boson hole in the IBM space. For simplicity, the proton boson particles and hole are treated equivalently, even though the underlying fermion pair degrees of freedom originate in different major shells.

The values of the parameters used for the present calculations are given in table (3-26). The value of the parameter ε for the N_π =4 configuration, $\varepsilon^{4\pi}$, is changed smoothly for all isotopes. The K trends for both configurations follow the microscopic predictions. The values of χ_π, $\xi_1 = \xi_2 = \xi_3$, $\alpha_2 = \beta_2$ are kept constant for all isotopes and χ_v is taken the same for the normal and intruder configurations. The

variation of Δ as a function of the neutron number is linear, Our Δ values are larger than the ones given in [85] because we are assuming that the intruder configuration originates from the excitation of one proton pair across the $Z = 28$ shell gap instead of a proton pair within the same valence space.

The parameter $C_{0\nu}$, $C_{2\nu}$ and $C_{4\nu}$ in the $V_{w\nu}$ interaction term, is varied smoothly from one isotope to another. The same values are used for both configurations. These parameters are used in NPMIX code to evaluate the energy levels after mixing.

Table (3-26): IBM-2 Hamiltonian parameters ($N_\pi = 4$), all parameters in MeV units except χ_π .and χ_ν are dimensionless

Isotopes	$\mathcal{E}$	κ	χ_ν	χ_π	$C_{0\nu}$	$C_{2\nu}$	$C_{4\nu}$	$C_{0\pi}$	$C_{2\pi}$	$C_{4\pi}$	$\alpha_2 = \beta_2$	ξ_k	Δ
Ge-64	1.60	-0.260	1.250	1.39-	0.0	0.0	-0.33	0.0	0.0	0.0	0.118	0.055	4.3
Ge-66	1.55	-0.255	1.200	1.39-	0.0	0.0	0.0	0.0	0.0	0.0	0.118	0.055	4.0
Ge-68	1.45	-0.250	1.225	-1.39	-1.50	0.0	0.21	0.0	0.0	0.0	0.118	0.055	3.8
Ge-70	1.33	-0.240	1.325	1.39-	-0.19	-0.38	0.17	0.0	0.0	0.0	0.118	0.055	3.0
Ge-72	1.15	-0.240	1.150	1.39-	-2.41	0.0	0.16	0.0	0.0	0.0	0.118	0.055	2.8
Ge-74	1.08	-0.230	1.100	-1.39	-1.21	-1.21	-0.22	0.0	0.0	0.0	0.118	0.055	1.02
Ge-76	1.30	-0.240	1.100	1.39-	0.0	0.0	-0.90	0.0	0.0	0.0	0.118	0.055	0.04
Ge-78	1.20	-0.250	1.100	1.39-	0.0	0.0	-0.22	0.0	0.0	0.0	0.118	0.055	-0.99
Ge-80	1.10	-0.260	1.000	-1.39	0.0	-0.9	0.0	0.0	0.0	0.0	0.118	0.055	-1.22
Ge-82	1.25	-0.280	1.000	-1.39	0.0	0.0	0.0	0.0	0.0	0.0	0.120	0.055	-1.22

Having considered the spectrum in some detail, it is of interest to compare the number of levels predicted with the number of free parameters used. There are ten parameters in the IBM-2 Hamiltonian, Eq.(2-42), and three in the mixing Hamiltonian, Eq.(2.75). Since the 4π parameters could conceivably all be different from those for the 2π case, there are 23 possible parameters for each isotope, an enormous number. However, six of these are not used: $C_{2\nu}^{4\pi}$, $C_{4\nu}^{4\pi}$ and $\xi_{,3}$ for both configurations. Four parameters, χ_ν both χ_π's and ξ_2 are determined from microscopic calculations or established from the *Ge* isotones. Also, χ_ν, $C_{0\nu}$ and ξ_2 are identical for both configurations. This reduces the number of free parameters to ten. Six of these are constant across the shell: $C_{2\nu}^{4\pi}$, $C_{4\nu}^{4\pi}$, $\varepsilon^{4\pi}$, α, β and Δ. Hence, the only free parameters which a allowed to vary from one isotope to another are $\varepsilon^{2\pi}, \kappa^{2\pi}, \kappa^{4\pi}$ and $C_{0\nu}$.

With four free parameters per isotope, more than fourteen energy levels are predicted (including the 2π ground state) for each germanium isotope.

3.4.2 Energy Spectra

The calculated energy spectra, before mixing and after mixing, are presented along with the experimental spectra in figures(3.23-31) before mixing. The figure (3.32-40) includes the after mixing (intruder configuration).

We have applied the model describe in the previous section to the calculation of the energy levels of the isotopic chain $^{64-80}_{32}Ge$ in major shell 28 and 50. The results are shown in (figs. 3.23-31). A detailed comparison with experimental data is shown in the figures. As it can be seen from these results, the agreement between the experimental data and theoretical results are quite good and the general features are reproduced well, especially for the members of the ground-state band. The value of $R_{4/2}$ as it is seen in table (3-30) it increases gradually from about 2.28 to 2.60. The agreement between the experimental values and IBM-2 for $E(4_1^+)/E(2_1^+)$ ratios of all *Ge* isotopes and the results show that $R_{4/2} > 2$ for all *Ge* isotopes. It means that their structure seems to be varying from Harmonic Vibrator (HV) to along gamma soft rotor (SU(5)→O(6)). So, the energy levels of the $^{64-80}Ge$ nuclei can be situated between the pure vibrational and rotational limit [20], are also trying to get a solution of potentials for the $E(5)$ and $X(5)$ models of the Bohr Hamiltonian by comparing the findings with the experimental data as well as the previous results.

Table (3-27): Values $E(J_1^+/2_1^+)$ for *Ge* Isotopes in normal configuration ($N_\pi = 2$)

Isotopes	$E(4_1^+/2_1^+)$			$E(6_1^+/2_1^+)$			$E(8_1^+/2_1^+)$		
	[Exp.[117	(E(5	IBM-2	[Exp.[117	(E(5	IBM-2	[Exp.[117	(E(5	IBM-2
Ge-64	2.275	2.3	2.225	3.8	5.3	3.318	5.7	5.3	5.253
Ge-66	2.273	2.3	2.184	3.8	5.2	3.623	-	5.2	5.730
Ge-68	2.233	2.2	2.214	3.6	5	3.567	4.8	5.0	4.760
Ge-70	2.072	2.1	2.075	3.5	4.3	3.467	-	4.3	4.542
Ge-72	2.071	2.1	2.465	3.3	4.3	3.913	4.8	4.3	4.732
Ge-74	2.458	2.5	2.508	-	6.6	4.166	-	6.6	7.114
Ge-76	2.508	2.5	2.536	-	7	4.227	-	7	6.478
Ge-78	2.536	2.5	2.560	-	7	4.413	-	7	5.986
Ge-80	2.643	2.5	2.619	-	7	3.607	-	7	4.885

The normal configuration for germanium involves $N_\pi = 2$ (sometimes denoted as 2π, two proton bosons), counting from the $Z = 28$ closed shell. The neutron configuration for $^{64}Ge_{32}$ for example, is $N_v = 2$ (two neutron boson), counting from the $N = 28$ closed shell. The vibrational spectra can be calculated by diagonalizing the *IBM*-2 Hamiltonian, Eq.(2.42), in the space of two proton and N_v neutron s and d bosons. In order to describe the rotational states, an alternative configuration must be specified and a separate set of *IBM* calculations made, based on that configuration. The alternate configuration used for the germanium isotopes involves a two-particle-four-hole excitation in the shell model proton space. This corresponds to two proton boson particles and two proton boson hole in the IBM space. For simplicity, the proton boson particles and holes are treated equivalently, even though the underlying fermion-pair degrees of freedom originate in different major shells.

93

Figure (3-23): Comparison between experimental and calculated energy levels for ^{64}Ge. The experimental data are taken from ref. [117].

Figure (3-24): Comparison between experimental and calculated energy levels for ^{66}Ge. The experimental data are taken from ref. [117].

Figure (3-25): Comparison between experimental and calculated energy levels for ^{68}Ge. The experimental data are taken from ref. [117].

Figure (3-26): Comparison between experimental and calculated energy levels for ^{70}Ge. The experimental data are taken from ref. [117].

Figure (3-27): Comparison between experimental and calculated energy levels for ^{72}Ge. The experimental data are taken from ref. [117].

Figure (3-28): Comparison between experimental and calculated energy levels for ^{74}Ge. The experimental data are taken from ref. [117].

Figure (3-29): Comparison between experimental and calculated energy levels for ^{76}Ge. The experimental data are taken from ref. [117].

Figure (3-30): Comparison between experimental and calculated energy levels for ^{78}Ge. The experimental data are taken from ref. [117].

Figure (3-31): Comparison between experimental and calculated energy levels for ^{80}Ge. The experimental data are taken from ref. [117].

Once *IBM* calculations have been done in model spaces with $N_\pi = 2$ and $N_\pi = 4$ to describe the vibrational and rotational states, respectively, the two calculations are combined using Eq.(2-76).

For each isotope, separate IBM-2 calculations were done for the $N_\pi = 2$ and $N_\pi = 4$ configurations, in which Eq.(2-42) was numerically diagonalized in the appropriate space using the computer code NPBOS [124]. The matrix element of H_{mix} in Eq.(2-75) were then formed using wave functions of the two separate configurations and the resulting mixing Hamiltonian was diagonalized by the computer code NPMIX [112].

The calculated energy spectra, after mixing, are presented along with the experimental spectra in figures (3.32-40). The figures includes the $N_\pi = 4$ ground state rotational band up to $J^+ = 8$, and the levels up to 3 MeV.

The $N_\pi = 2$ 8^+ levels are we11 above the energy for which the IBM is expected to be valid, since the pairing assumption breaks down at about 3 MeV. Before mixing, the $N_\pi = 2$ and $N_\pi = 4$ spectra look like good quasi-vibrational and quasi-rotational spectra, respectively. After mixing, it can be seen that many of the states have been moved dramatically.

The figures show other states in the $N_\pi = 4$ configuration. The quasi-beta band heads 0^+ and the quasi-gamma band heads 2^+ for $^{64-82}$Ge mix strongly with the $N_\pi = 4$ ground state band (gsb) 0^+ and 2^+ states, respectively, as can be seen in figures (3.33-41). Similarly, the $^{64-72}$Ge 4_2^+ states mix with the $N_\pi = 4$ gsb 4^+ states. The $^{64-72}$Ge 3^+ states mix strongly with the corresponding $N_\pi = 4$ 3^+ states. These latter states are not shown in any of the figures, where, for simplicity, only the gsb, beta band and gamma band, are presented for the $N_\pi = 4$ configuration. Figures (3.33-41) also shows the lowest set of 2^+ states. The *Ge* experimental spectrum is rich in levels which have been assigned angular momentum 3 or 2 and positive (or no) parity.

A better fit to the quasi-gamma band head for each isotope could be obtained with appropriate changes in the parameter $C_{2\nu}^{2\pi}$. In the interest of a simple parameter trend, this has not been done. The experimental 2^+ states close to the calculated $^{64-82}$Ge 2^+ state at ~ 1.5 MeV. Curiously, there is an experimental 0^+ state at 0.961 MeV in ^{72}Ge. This state is included in figure (3-37), since it is thought to be outside the IBM model space.

At the time these calculations were performed, there were no published calculated data on ^{82}Ge levels. The IBM parameters for this isotope are based on trends from the other isotopes, and the assumption that the effective middle of the shell is at ^{80}Ge. The extreme case for the situation is the neutron closed-shell nucleus

$^{82}_{32}Ge_{50}$, that has $N_\nu = 0$, in configuration mixing excitation (p-h) across the major shell $N = 50$, therefore $N_\nu = 2$ and $N_\pi = 1$ in $^{82}_{32}Ge_{50}$.

All the calculated energy levels above 1.5 MeV are somewhat high. The calculated 3^+ levels are quite high, except for $^{64\text{-}72}$Ge. However, there is general agreement with experiment for all the isotopes concerned.

A few comments on the uncertainties involved in the calculated energies are, perhaps, appropriate, even though these uncertainties cannot be estimated in a rigorous way. For the most part, the estimates given represent a change in energy due to a change in one of the parameters by a given amount, usually one unit in the least significant place.

The fitting of the $N_\nu = 4$ configuration for A~ 78 is speculative. The dominant parameter is $\kappa^{4\pi}$. For ^{80}Ge, the determination of this parameter is based on one experimental number, a possible 2^+ state at 0.612 MeV. A change of 1 keV in $\kappa^{4\pi}$ changes the rotational states by 10-20 keV. For A > 80, the values of $\kappa^{4\pi}$ are based solely on extrapolation.

The choice of the ^{82}Ge parameters is based on extrapolation and the expectation that the parameters and energies should be roughly reflected about the middle of the shell. Since this nucleus is the only one of the isotopes studied to have neutron particle bosons, as opposed to hole bosons (e.g., the only nucleus below mid-shell), the ^{82}Ge levels are somewhat speculative.

A conservative estimate of the uncertainty in the calculated energies of the intruder (4π) states in $^{70\text{-}76}$Ge is 10-20 keV. The low-lying vibrational states also have an estimated uncertainty of 10-20 keV (considering a 5 or 10 keV change in ε or κ). The uncertainty in the higher levels is 40 keV or more. This is partly because the higher energy states are more sensitive to the parameters and partly because, for the most part, the parameters are not fitted to these states.

In many cases, the discrepancy between calculated and experimental energies is deliberately greater than the above uncertainties, in order to simplify the parameter trends. In other cases, especially for the higher energy levels, the discrepancy is probably partly due to the fact that the model is too simple.

Figure (3-32): Comparison between experimental and calculated energy levels for ^{64}Ge (N_π =4). The experimental data are taken from ref. [117].

Figure (3-33): Comparison between experimental and calculated energy levels for ^{66}Ge (N_π =4). The experimental data are taken from ref. [117].

Figure (3-34): Comparison between experimental and calculated energy levels for ^{68}Ge (N_π =4). The experimental data are taken from ref. [117].

Figure (3-35): Comparison between experimental and calculated energy levels for ^{70}Ge (N_π =4). The experimental data are taken from ref. [117].

Figure (3-36): Comparison between experimental and calculated energy levels for ^{72}Ge (N_π =4). The experimental data are taken from ref. [117].

Figure (3-37): Comparison between experimental and calculated energy levels for ^{74}Ge (N_π =4). The experimental data are taken from ref. [117].

Figure (3-38): Comparison between experimental and calculated energy levels for ^{76}Ge (N_π =4). The experimental data are taken from ref. [117].

Figure (3-39): Comparison between experimental and calculated energy levels for ^{78}Ge (N_π =4). The experimental data are taken from ref. [117].

Figure (3-40): Comparison between experimental and calculated energy levels for ^{80}Ge (N_π =4). The experimental data are taken from ref. [117].

Figure (3-41): Comparison between experimental and calculated energy levels for ^{82}Ge (N_π =4). The experimental data are taken from ref. [117].

3.4.3 Electric Transition Probability

The E2 transition operator, is given in Eq. (2.83). The effective boson charges e_π and e_ν were calculated by plotting [118] M_1 and M_2 which are given in Eqs. (3-2,3) against N_ν / N_π (see figure (3-42)). For a mathematical simplicity we use the values of the boson effective charges where $e_{2\pi} = e_{4\pi} = e_2$ and $e_{2\nu} = e_{4\nu} = e_4$, for all *Ge* isotopes. The best fit of effective charges to $^{64-80}$*Ge* isotopes was obtained $e_\pi = 0.11095$ *eb* and $e_\nu = 0.05$ *eb*. The results of the calculations are presented in table (3-28). Looking through the table, one can easily recognizes that our calculations reproduce the experimental data quite well.

(e^2b^2) , $M_{2(e^2b^2)} M_1$
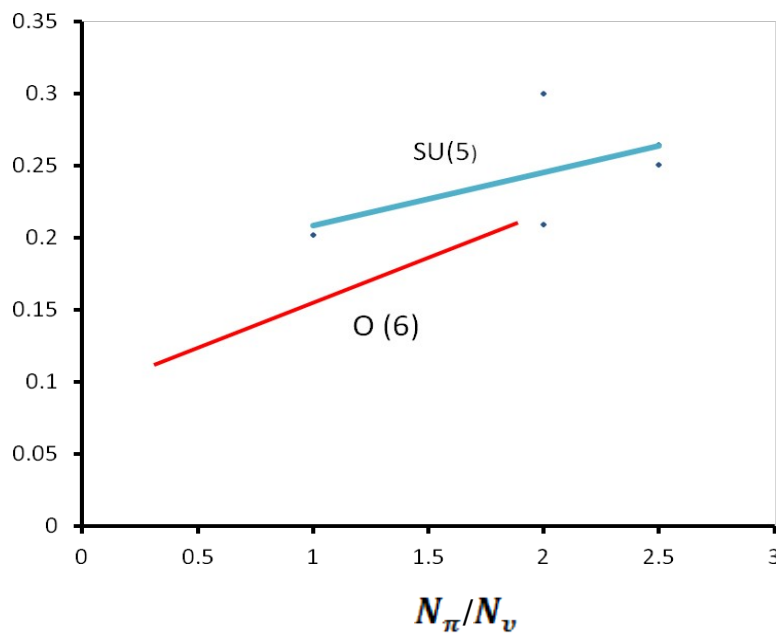
Figure (3-42): The plot of the quantity M_1 and M_2 versus $e_\pi + e_\nu N_\nu / N_\pi$ for $^{64-80}$*Ge* Isotopes.

114

Table (3-28): Electric Transition Probability for *Ge* isotopes in e^2b^2 units

Isotopes	$J_i^+ \rightarrow J_f^+$	Exp. [117]	Present Work	Subber [92]
Ge-64	$0_1 \rightarrow 2_1$	(60) 0.0410	0.0351	0.0125
	$0_1 \rightarrow 2_2$	(5)0.00015	0.0012	0.0028
	$2_1 \rightarrow 2_2$	(210) 0.0620	0.0523	0.0166
	$0_1 \rightarrow 2_3$	-	0.0033	0.0018
	$2_1 \rightarrow 2_3$	-	0.0027	0.0012
	$2_1 \rightarrow 4_1$	-	0.020	0.0121
	$4_1 \rightarrow 6_1$	-	0.119	-
	$4_1 \rightarrow 4_2$	-	0.059	-
	$Q(2_1^+)$	-	-0.182	-
Ge-66	$0_1 \rightarrow 2_1$	(362)0.01896	0.0129	0.0212
	$0_1 \rightarrow 2_2$	(6)0.00016	0.0014	0.0029
	$2_1 \rightarrow 2_2$	(1264)0.02686	0.0310	0.0283
	$0_1 \rightarrow 2_3$	-	0.0024	0.0018
	$2_1 \rightarrow 2_3$	-	0.0281	0.0225
	$2_1 \rightarrow 4_1$	-	0.0335	0.0325
	$4_1 \rightarrow 6_1$	-	0.127	-
	$4_1 \rightarrow 4_2$	-	0.052	-
	$Q(2_1^+)$	-	-0.170	-
Ge-68	$0_1 \rightarrow 2_1$	$0.01517 \leq$	0.0182	0.0273
	$0_1 \rightarrow 2_2$	(329)0.02912	0.0371	0.0048
	$2_1 \rightarrow 2_2$	(4)0.00023	0.0004	0.0406
	$0_1 \rightarrow 2_3$	(34)0.00086	0.00077	0.0038
	$2_1 \rightarrow 2_3$	-	0.0082	0.0076
	$2_1 \rightarrow 4_1$	-	0.0529	0.0446
	$4_1 \rightarrow 6_1$	-	0.129	-
	$4_1 \rightarrow 4_2$	-	0.050	-
	$Q(2_1^+)$	-	0.0012	-
Ge-70	$0_1 \rightarrow 2_1$	(29)0.02287	0.0321	0.0340
	$0_1 \rightarrow 2_2$	(68)0.03593	0.0301	0.0069
	$2_1 \rightarrow 2_2$	(85)0.00171	0.00232	0.0500
	$0_1 \rightarrow 2_3$	(189)0.0497	0.0618	0.0030
	$2_1 \rightarrow 2_3$	-	0.0015	0.0010
	$2_1 \rightarrow 4_1$	(11)0.04112	0.0681	0.0579
	$4_1 \rightarrow 6_1$	-	0.134	-
	$4_1 \rightarrow 4_2$	-	0.0481	-
	$Q(2_1^+)$	+0.04(3)	0.037	-
Ge-72	$0_1 \rightarrow 2_1$	(3)0.040	0.039	0.0330
	$0_1 \rightarrow 2_2$	-	0.0076	0.0099
	$2_1 \rightarrow 2_2$	(12)0.114	0.129	0.0478
	$0_1 \rightarrow 2_3$	-	0.0024	0.0017
	$2_1 \rightarrow 2_3$	-	0.018	0.0190
	$2_1 \rightarrow 4_1$	(71)0.0641	0.048	0.0565
	$4_1 \rightarrow 6_1$	-	0.141	-
	$4_1 \rightarrow 4_2$	-	0.0479	-
	$Q(2_1^+)$	-0.13(6)	-0.122	-
Ge-74	$0_1 \rightarrow 2_1$	(3)0.060	0.065	(5)0.028
	$0_1 \rightarrow 2_2$	$0.078 \geq$	0.0671	0.0055
	$2_1 \rightarrow 2_2$	(203)0.0997	0.0897	0.0470
	$0_1 \rightarrow 2_3$	-	0.0014	0.0017
	$2_1 \rightarrow 2_3$	-	0.0047	0.0056

	$2_1 \rightarrow 4_1$	(55)0.0664	0.0605	0.0464
	$4_1 \rightarrow 6_1$	-	0.147	-
	$4_1 \rightarrow 4_2$	-	0.0431	-
	$Q(2_1^+)$	-0.19(2)	-0.178	-
Ge-76	$0_1 \rightarrow 2_1$	(3)0.046	0.0498	0.026
	$0_1 \rightarrow 2_2$	-	0.0032	0.0041
	$2_1 \rightarrow 2_2$	(96)0.0746	0.0687	0.0308
	$0_1 \rightarrow 2_3$	-	0.0019	0.0011
	$2_1 \rightarrow 2_3$	-	0.0013	0.000
	$2_1 \rightarrow 4_1$	(13)0.073	0.0587	0.0373
	$4_1 \rightarrow 6_1$	-	0.152	-
	$4_1 \rightarrow 4_2$	-	0.374	-
	$Q(2_1^+)$	-0.19(6)	-0.1885	-
Ge-78	$0_1 \rightarrow 2_1$	(30)0.044	0.0402	0.0230
	$0_1 \rightarrow 2_2$	-	0.0041	0.0033
	$2_1 \rightarrow 2_2$	(238)0.0396	0.0298	0.0164
	$0_1 \rightarrow 2_3$	-	0.0037	0.0040
	$2_1 \rightarrow 2_3$	-	0.00066	0.0007
	$2_1 \rightarrow 4_1$	$0.0218 \leq$	0.029	0.0160
	$4_1 \rightarrow 6_1$	-	0.160	-
	$4_1 \rightarrow 4_2$	-	0.0341	-
	$Q(2_1^+)$	-	-0.178	-
Ge-80	$0_1 \rightarrow 2_1$	(5)0.028	0.021	0.034
	$0_1 \rightarrow 2_2$	-	0.0019	0.0012
	$2_1 \rightarrow 2_2$	-	0.0023	0.0019
	$0_1 \rightarrow 2_3$	-	0.00167	0.000
	$2_1 \rightarrow 2_3$	-	0.00023	0.000
	$2_1 \rightarrow 4_1$	-	0.0042	0.0036
	$4_1 \rightarrow 6_1$	-	0.163	-
	$4_1 \rightarrow 4_2$	-	0.0310	
	$Q(2_1^+)$	-	-0.168	
Ge-82	$0_1 \rightarrow 2_1$	9.467×10^{-3}	0.0008	-
	$0_1 \rightarrow 2_2$	-	0.0023	-
	$2_1 \rightarrow 2_2$	-	0.0025	-
	$0_1 \rightarrow 2_3$	-	0.0021	-
	$2_1 \rightarrow 2_3$	-	0.00034	-
	$2_1 \rightarrow 4_1$	-	0.0028	-
	$4_1 \rightarrow 6_1$	-	0.0135	-
	$4_1 \rightarrow 4_2$	-	0.0289	-
	$Q(2_1^+)$	-	0.12	-

Calculation of electric transition properties gives us a good test of the nuclear model prediction. The electromagnetic matrix elements between eigenstates were calculated using program NPBTRN for IBM-2 model.

The $B(E2;2_1^+ \rightarrow 0_1^+)$ decreased for $^{64-68}Ge$ as neutron number increased toward the middle of the shell for the $^{70-74}Ge$. While for the $^{76-82}Ge$ as the value is decreased toward the closed shell. The transition $B(E2;2_2^+ \rightarrow 2_1^+)$ has small value

because contains admixture of $M1$. As a consequence of possible $M1$ admixture, this quantity is rather difficult to measure.

The values of $B(E2;2_2^+ \to 0_1^+)$, $B(E2;2_3^+ \to 0_1^+)$ and $B(E2;2_3^+ \to 2_1^+)$ is small because this transition from quasi-beta band to ground state band (cross over transition).

The IBM-2 results are compared not only with experiment, but also with predictions from the following other work by *Subber* [92] .

The quadrupole moment for first excited state in *Ge* isotopes are very well described. The calculated values of $Q(2_1^+)$ indicated the $^{64\text{-}66}Ge$ has prolate shape in first excited states, while the $^{68\text{-}70}Ge$ has a oblate shape in first excited states. The $^{72\text{-}80}Ge$ has a protate shape in 2_1^+ states.

The signs of $Q(2_1^+)$ are correctly predicted for the isotopes for which experimental data are available. (These signs depend on χ_π and χ_ν). The calculated magnitudes are close to the experimental values.

The intention of the present work is to give a good overall characterization of a whole chain of isotopes with a simple set of parameters, rather than to give the best possible fit to any one nucleus. Hence, it is not surprising that some of the experimental results listed in table (3-28) are better fit with experimental data. On the whole, the IBM results for E2 transition rates and quadrupole moments compared well with the experimental results and with the predictions of other work for the *Ge* isotopes .

3.4.4-Magnetic Transition Probability

The magnetic transition operator $T(M1)$ were calculated using Eq.(2- 84), and the boson gyromagnetic factors were estimated using the fact that $g = Z/A$ and the relation (3-4), used to compute the 2_1^+ state g -factor. The value of the measured magnetic moment $\mu = 2g = 1.1(3)$ μ_N [117] for ^{68}Ge, and the experimental mixing ratio $\delta(2_2^+ \rightarrow 2_1^+) = -0.2(0.1)$ [100] were used to produce satiable estimation for the boson gyromagnetic factors. The values are ($g_{2\pi} = g_{4\pi} = g_\pi$) $g_\pi = 0.562$ μ_N and $g_{2v} = g_{4v} = g_v$) $g_v = 0.397$ μ_N . The results of the calculations are listed in table (3-29).

Table (3-29): Reduced transitions probability $B(M1)$ in μ_N^2 units for $^{64-82}$Ge isotopes

Transitions	B(M1)									
	^{64}Ge	^{66}Ge	^{68}Ge	^{70}Ge	^{72}Ge	^{74}Ge	^{76}Ge	^{78}Ge	^{80}Ge	^{82}Ge
$2_1 \rightarrow 2_2$	0.0662	0.0288	0.0132	0.00043	0.0043	0.000421	0.00987	0.00011	0.00003	0.00004
$2_1 \rightarrow 2_3$	0.0378	0.0191	0.0002	0.002	0.0052	0.00051	0.0057	0.00005	0.00262	0.0017
$2_2 \rightarrow 2_3$	0.0561	0.0442	0.0251	0.0045	0.00022	0.0020	0.0209	0.00012	0.00005	0.000033
$2_1 \rightarrow 3_1$	0.0662	0.0432	0.00145	0.0389	0.00081	0.000421	0.00987	0.00011	0.00003	0.000027
$2_2 \rightarrow 3_1$	5×4510^{-4}	5.67×10^{-4}	2×10^{-4}	1.39×10^{-4}	1.77×10^{-4}	2.15×10^{-4}	2.34×10^{-4}	2.451×10^{-4}	2.561×10^{-4}	2.7×10^{-4}
$3_2 \rightarrow 3_1$	2.5×10^{-5}	5.6×10^{-4}	1.02×10^{-3}	4.99×10^{-3}	2.43×10^{-3}	2.15×10^{-3}	6.53×10^{-3}	1.004×10^{-3}	1.28×10^{-3}	1.33×10^{-3}
$0_1 \rightarrow 1_1$	0.451	0.560	0.755	0.799	0.823	0.896	0.9022	0.910	0.943	0.975
$2_1 \rightarrow 1_1$	0.0632	0.0641	0.0655	0.0753	0.0762	0.0811	0.0892	0.0994	0.149	0.254
$\mu(2_1^+)$ (Exp.)	-	-	1.1 (3)	0.936(52)	0.77(5)	0.70(24)	0.56(12)	-	0.839(46)	-
$\mu(2_1^+)$ IBM-2	1.53	1.43	1.34	1.022	0.871	0.80	0.591	0.531	0.77	0.832

[Experimental data for magnetic dipole moment for first excited state are given from ref.[117

In phenomenological studies g_π and g_v are treated as parameters and kept constant for a whole isotopes chain. The total g factor is defined by Many relations could be obtained for a certain mass region and then the average g_π and g_v values for this region could be calculated, and one of the experimental B(M1) values. It is found that $g_\pi - g_v = 0.176$ μ_N . The estimated values of the parameter are $g_\pi = 0.562$ μ_N and $g_v = 0.397$ μ_N . These were used to calculate the   magnetic transition probability $B(M1)$. These values were then generalized for all Ge isotopes. They are different from those of the rare–earth nuclei, $(g_\pi - g_v = 0.65\mu_N)$, suggested by Van Isacker *et al.*, [108]. However they also used $g_\pi = 1\mu_N$ and $g_v = 0\mu_N$ to reduce the number of the model parameters in their calculation of M1 properties in deformed nuclei. The results of our calculations are listed in table (3-29). There is no experimental data to compare with the *IBM*-2 calculations. As can be seen from the table yields to a simple prediction that *M*1 matrix elements values for gamma to

ground and transitions should be equal for the same initial and final spin. Also the size of gamma to ground matrix elements seems to decrease as the mass number increases.

3.4.5-Mixing Ratio $\delta(E2/M1)$

The δ(E2/M1) mixing ratios for some selected transitions in *Ge* isotopes are calculated from the useful equations as above and with the help of $B(E2)$ and $B(MI)$ values which are obtained from NPBEM (computer code which is subroutine of *NPBOS* package program); the results are given in table (3-30). In general, the calculated electromagnetic properties of the *Ge* isotopes do not differ significantly from those calculated in experimental and theoretical work. However, there is a large disagreement in the mixing ratios of $\delta(2_2^+ \rightarrow 2_1^+)$, $\delta(3_1^+ \rightarrow 2_1^+)$ and $\delta(3_1^+ \rightarrow 2_2^+)$, due to the small value of M1 matrix elements.

Table (3-30): Mixing ratios δ(E2/M1) for *Ge*[64-80] in eb / μ_N units

Isotopes	$J_i^+ \rightarrow J_f^+$	Exp.[100,117]	$IBM - 2$	[Subber [92
Ge-64	$2_2 \rightarrow 2_1$	-	-4.450	-5.6
	$2_3 \rightarrow 2_1$	-	3.764	2.3
	$3_1 \rightarrow 2_1$	-	12	10.74
	$3_1 \rightarrow 2_2$	-	0.0921	-2.027
	$4_1 \rightarrow 2_1$	-		-
Ge-66	$2_2 \rightarrow 2_1$	-3.5^{+18}_{-26}	2.276	-1.591
	$2_3 \rightarrow 2_1$	-	-2.980	-1.56
	$3_1 \rightarrow 2_1$	-	17.98	20.9
	$3_1 \rightarrow 2_2$	-	3.220	2.61
	$4_1 \rightarrow 2_1$	-	-3.989	-
Ge-68	$2_2 \rightarrow 2_1$	(0.1)0.2-	-0.811	-1.934
	$2_3 \rightarrow 2_1$	-	-2.0	-1.734
	$3_1 \rightarrow 2_1$	(0.1)0.2-	-1.77	-36.78
	$3_1 \rightarrow 2_2$	(0.3)0.2-	-0.33	-0.31
	$4_1 \rightarrow 2_1$		-4.77	-
Ge-70	$2_2 \rightarrow 2_1$	(3.0)5.0-	-10.19	-1.76
	$2_3 \rightarrow 2_1$	-	0.011	-5.78
	$3_1 \rightarrow 2_1$	(5-3+)2.2-	-2.86	-0.35
	$3_1 \rightarrow 2_2$	(8)0.05-	-0.087	-3.45
	$4_1 \rightarrow 2_1$	-	7.188	-
Ge-72	$2_2 \rightarrow 2_1$	(13)10.3-	-13.4	-3.89
	$2_3 \rightarrow 2_1$	-	10.32	-7.88

	$3_1 \rightarrow 2_1$	-	11.6	3.92
	$3_1 \rightarrow 2_2$	4.0+ ≈	5.22	-3.67
	$4_1 \rightarrow 2_1$	-	9.66	-
Ge-74	$2_2 \rightarrow 2_1$	(4)3.4+	3.96	-1.222
	$2_3 \rightarrow 2_1$	(3)2.8-	-3.21	7.44
	$3_1 \rightarrow 2_1$	(5)0.34	0.661	3.02
	$3_1 \rightarrow 2_2$	(4)1.3+	2.4	-5.789
	$4_1 \rightarrow 2_1$	-	-0.9	-
Ge-76	$2_2 \rightarrow 2_1$	(15)3.5+	5.21	3.50
	$2_3 \rightarrow 2_1$	-	3.4	-11.58
	$3_1 \rightarrow 2_1$	-	17.2	2.44
	$3_1 \rightarrow 2_2$	-	-7.34	-6.87
	$4_1 \rightarrow 2_1$	-	-0.411	-
Ge-78	$2_2 \rightarrow 2_1$	-	1.456	0.98
	$2_3 \rightarrow 2_1$	-	21.90	29.5
	$3_1 \rightarrow 2_1$	-	2.11	1.96
	$3_1 \rightarrow 2_2$	-	-2.56	-1.2
	$4_1 \rightarrow 2_1$	-	5.108	-
Ge-80	$2_2 \rightarrow 2_1$	-	-2.64	-1.6
	$2_3 \rightarrow 2_1$	-	0.002	-1.37
	$3_1 \rightarrow 2_1$	-	-0.414	-0.511
	$3_1 \rightarrow 2_2$	-	0.0115	-
	$4_1 \rightarrow 2_1$	-	10	-
Ge-82	$2_2 \rightarrow 2_1$	-	-1.06	-
	$2_3 \rightarrow 2_1$	-	0.0019	-
	$3_1 \rightarrow 2_1$	-	-0.411	-
	$3_1 \rightarrow 2_2$	-	-2.25	-
	$4_1 \rightarrow 2_1$	-	8.318	-

3.4.6-Electric Monopole Matrix Element $\rho(E0)$

The expressions for $\rho(E0)$ matrix elements is given in Eq. (2-86). They involve five parameters. Four of them, $\overline{\beta_{02\pi}}$, $\overline{\beta_{02\nu}}$, $\overline{\beta_{04\pi}}$ and $\overline{\beta_{04\nu}}$, multiply the

matrix elements of $\hat{n}_{2d\pi}$, $\hat{n}_{2dv}$, $\hat{n}_{4d\pi}$ and $\hat{n}_{4dv}$, respectively. The last parameter, which occurs in the isotope shift expression only, is an additive constant, γ_{0v} . (It is the sum of $\gamma_{02\,v}$ and $\gamma_{04\,v}$). The quantity X -values defined in Eq. (2-61).

The values of the parameters $\beta_{02\,\pi}^{-}$, $\beta_{02\,v}^{-}$ and γ_{0v} are determined by fitting to the experimental ^{72}Ge isotope shifts, which are dominated by the 2π configuration. The values of the parameters $\beta_{04\,\pi}^{-}$ and $\beta_{04\,v}^{-}$ are subsequently determined to fit the X- values for ^{72}Ge . The parameter values are**:**

$\beta_{02\,\pi}^{-}= 0.832\,fm^2$, $\beta_{02\,v}^{-}=$-0.286 fm^2, $\beta_{04\,\pi}^{-}=$-0.500 fm^2, $\beta_{04\,v}^{-}= 0.182 fm^2$,

$\gamma_{0v} = $ -0.079   ………..(3- 5)

There is good agreement between the calculated value and the experimental result for both the $E0$ transition in ^{72}Ge isotope . However, rather different sets of the $E0$ parameters can be found which give similar isotope shifts but different isomer shifts. Therefore, in the absence of any experimental isomer shift data, it is not possible to tell whether or not Eq.(3-5) represents the "best" possible set of $E0$ parameters.

It appears that all five $T(E0)$ parameters are necessary to obtain reasonable results, unlike the $E2$ case, where $e_\pi = e_v$.

جدول

Mixed Symmetry States-3.4.7

Another probable indication for the need for an increased Majorana force for the germanium calculations is the presence of the mixed-symmetry 2_3^+ states in

figures (3.24-32) at about 2 MeV. There is no experimental evidence for such states, for $^{64\text{-}66}Ge$, where 2^+ states could be non-collective.

The calculations shown in figures were done with the Majarona parameters, to see what effect this larger Majorana force would have on the germanium 2π spectrum. The parameter $C_{0\nu}$ was also changed, as previously mentioned, and the parameters ε, $C_{2\nu}$, and $C_{4\nu}$ adjusted to fit the gsb. The parameter set is given in table (3-25). This calculation does not include configuration mixing.

The 1^+ and 2_3^+ levels have been shifted up out of the low energy spectrum, as desired. However, the calculated 3_γ^+ levels, which were already too high in figures (3.24-32), have also been pushed up. These 3_γ^+ levels, along with the 2^+ and 4^+ members of the quasi-gamma band, are shown on the figures. Recent microscopic calculations for *Ge* [92] find ξ_2 changed from -0.06 MeV to -0.013 MeV, and $\xi_1 = \xi_3$ changed from 0.061 MeV to -0.1 MeV, resulting in reasonable agreement with experiment for the 3^+ levels. The 2_3^+ levels of *Subber* [92] are around 2 MeV, however. It appears that an optimal set of Majorana parameters has yet to be found. Such a set will likely involve $\xi_1 \neq \xi_3$.

The newly found collective 1^+ state in ^{156}Gd [*Bohle et al.*, [106]] indirectly affects the germanium calculations because it suggests that the strengths of the Majorana terms used in most of the IBM-2 calculations to date have been too small. This 1^+ level was found at 3.1 MeV in an inelastic electron scattering experiment (e,e'), which selectively excites collective states. In the IBM, 1^+ states are clearly not totally symmetric; they cannot be obtained in IBM-1. Thus, they are quite sensitive to the strength of the Majorana force.

The M1 state (as it is called) in ^{156}Gd can be reproduced by IBM-2 with the Majorana strengths $\xi_2 = 0.2$ MeV and $\xi_1 = \xi_3 = -0.4$ MeV [106]. In comparison, the values of the parameters $\xi_1 = \xi_3$ used by this worker and *Subber* work [92] are also much smaller than those of *Bohle et al.*, [106].

Although some of the germanium isotopes have low-lying 1^+ states, there is no evidence that these states are collective. Therefore, the calculated 1^+ levels should be higher in energy than those shown in figures, indicating that one or more of the parameters $\xi_{1,2,3}$ need to be increased (in absolute value).

Chapter Three
Results and Discussion

Kr **Isotopes 3.1**

Hamiltonian Interaction Parameters 3.1.1

Since the Hamiltonian contains many parameters it is unpractical and not very meaningful to vary all parameters freely. Instead it is convenient to use the behavior of the parameters predicted by a microscopic point of view as a zeroth-order approximation. In a simple shell-model picture based upon degenerate single nucleon levels [114] the expected dependence of $\varepsilon, \kappa, \chi_\nu$ and χ_π on neutron (N_ν) and proton (N_π) boson numbers can be expressed as:

$$\varepsilon = \text{constant}, \quad \kappa = \kappa_\pi \kappa_\nu, \quad \kappa_\rho = \sqrt{\frac{\Omega_\rho - N_\rho}{\Omega_\rho - 1}} \kappa_\rho^{(0)}, \quad \chi_\rho = \frac{\Omega_\rho - 2N_\rho}{\sqrt{\Omega_\rho - N_\rho}} \chi_\rho^{(0)} \quad \rho = \pi, \nu. \quad (3\text{-}1)$$

Here $\kappa_\rho^{(0)}$ and $\chi_\rho^{(0)}$ are constants, and Ω_ρ is the pair degeneracy of the shell. We see that while κ_ρ has always the same sign, χ_ρ changes sign in the middle of the shell.

In realistic cases the estimates of eq.(3-1) are expected to be valid only approximately. In our approach we have imposed somewhat weaker constrains on the parameters: (**i**) it is assumed that within a series of isotones (isotopes) $\chi_\nu(\chi_\pi)$ does not vary at all; (**ii**) the parameters ε, κ and χ_ν are assumed to be smooth functions of (N_ν).

Concerning the sign of χ_ν and χ_π a complication arises. From very simple microscopic consideration it follows that the $\chi's$ (which also determined to a large extent the sign of the quadrupole moment of the first excited state 2_1^+ are negative in the region where the valence shell is less than half filled (particle-boson) and positive in the region where the valance shell is more than half filled (hole-boson). Quantitatively, such a behavior was confirmed in other phenomenological calculations with IBM-2. For example in a study of the *Ba* isotopes with $72 < N < 80$ good fit to the energy levels was obtained with $\chi_\nu \approx 0.90$ [115]. Since in the naïve shell-model picture in the *Kr* region both neutrons and protons are hole-like and therefore both $\chi's$ would be positive, there would be no way to obtain an SU(5) type spectrum, which requires opposite signs of χ_ν and χ_π. This indicates that the situation is not so simple and that more complicated effects play a role, such as a possible nonclosedness of the $Z = 50$ or the $N = 82$ core. Although the Hamiltonian invariant under simultaneous change in sign of both χ_ν and χ_π and thus equally good fits to energy spectra can be obtained for both combinations $\chi_\nu > 0$ and $\chi_\pi < 0$. Namely, only with this choice the observed sign of the mass quadrupole moment of the 2_1^+ state in *Kr* can be reproduced.

The remaining parameters play a less important role and are used mainly to improve the fit with experiment. In this work only $C_{0\nu}$ and $C_{2\nu}$ representing part of the d-boson conserving interaction between neutron bosons, were used as free parameters independent of N_π. Finally, the values of ξ_2 and ξ_3 were vary from

isotope to another, ξ kept constant. The parameters used for the various isotopes are shown in table (3-1) .

It is seen that parameters are constant or vary smoothly: within a series of isotopes χ_π does not vary, the variation in ε is very small and there is a slight decrease of the value of κ for the lighter Kr isotopes. The change in character of the spectra through a series of isotopes is essentially due to two effects: (**i**) the increase of the value of χ_ν for $^{76-84}Kr$ and decreases for $^{88-90}Kr$, and (**ii**) the decrease of the number of neutron bosons N_ν. We note that the behaviors of $\varepsilon, \kappa, \chi_\nu$ and χ_π is a qualitative agreement with microscopic considerations (see eq.(3-1)). It was found that both $C_{0\nu}$ and $C_{2\nu}$ vary for the isotopes. Such a behavior agree with the trend found in other regions [34]. The positive value of ξ_2 guarantees that no low-lying anti-symmetric multiplets occur for which there is no experimental evidence.

Table (3-1): IBM-2 Hamiltonian parameters for Kr isotopes, all parameters in MeV units except χ_π and χ_ν are dimensionless

Isotopes	N_π	N_ν	ε	κ	χ_ν	χ_π	$C_{0\nu}$	$C_{2\nu}$	$C_{4\nu}$	$C_{0\pi}$	$C_{2\pi}$	$C_{4\pi}$	ξ	ξ_2
$^{76}_{36}Kr_{40}$	4	5	0.701	-0.080	0.41	-0.60	-1.20	0.20	0.11	-1.2	0.30	0.30	0.051	0.032
$^{78}_{36}Kr_{42}$	4	4	0.722	-0.090	0.52	-0.60	-0.66	0.27	0.11	-1.2	0.31	0.30	0.102	0.130
$^{80}_{36}Kr_{44}$	4	3	0.890	-0.081	0.60	-0.60	-0.22	0.11	0.11	-0.48	-0.21	0.05	0.242	0.050
$^{82}_{36}Kr_{46}$	4	2	0.960	-0.081	0.70	-0.60	0.11	-0.82	-0.37	1.43	-0.18	0.07	0.182	0.050
$^{84}_{36}Kr_{48}$	4	1	0.949	-0.080	0.81	-0.60	0.0	0.0	0.0	0.14	0.25	0.38	0.601	0.440
$^{88}_{36}Kr_{52}$	4	1	0.920	-0.087	0.62	-0.60	0.12	0.12	0.12	-0.30	-0.18	0.0	0.601	0.450
$^{90}_{36}Kr_{54}$	4	2	0.862	-0.992	059	-0.60	0.11	0.11	0.11	0.17	0.17	0.17	0.632	0.510

$$\xi = 0.11 \text{ MeV}$$

3.1.2 Energy Spectra

The calculated excitation energies of positive parity levels to $^{76-90}Kr$ are given in table (3-1) and displayed in figures.(3-1,2,3,4,5,6,7). The agreement between the calculated and experimental values is satisfactory.

Using the parameters in table (3-1), the estimated energy levels are shown in the figures, along with experimental energy levels. As can be seen, the agreement between experiment and theory is quite good and the general features are reproduced well. We observe the discrepancy between theory and experiment for high spin states. But one must be careful in comparing theory with experiment, since all calculated states have a collective nature, whereas some of the experimental states may have a particle-like structure. Behavior of the ratio $R_{4/2} = E(4_1^+)/E(2_1^+)$ of the energies of the first 4_1^+ and 2_1^+ states are good criteria for the shape transition [116]. The value of $R_{4/2}$ ratio has the limiting value 2.0 for a quadrupole vibrator, 2.5 for a non-axial gamma-soft rotor and 3.33 for an ideally symmetric rotor. $R_{4/2}$ remain nearly constant at increase with neutron number. The estimated values change from isotope to another (see table 3-2)), this meaning that their structure seems to be varying from axial gamma soft to quadrupole vibrator $SU(5) \rightarrow O(6)$. Since *Kr* nucleus has a rather vibrational-like character, taking into account of the dynamic symmetry location of the even-even *Kr* nuclei at the IBM phase Casten triangle where their parameter sets

are at the $SU(5) \rightarrow O(6)$ transition region and closer to SU(5) character and we used the multiple expansion form of the Hamiltonian for our approximation.

The shape transition predicted by this study is consistent with the spectroscopic data for these nuclei. $^{88-90}Kr$ are typical examples of isotopes that exhibit a smooth phase transition from vibrational nuclei (SU(5)) to soft triaxial rotors (O(6)).

Table (3-2): Energy ratio $R_{4/2} = E(4_1^+)/E(2_1^+)$ for Kr isotopes

$E(4_1^+)/E(2_1^+)$	$^{76}_{36}Kr_{40}$	$^{78}_{36}Kr_{42}$	$^{80}_{36}Kr_{44}$	$^{82}_{36}Kr_{46}$	$^{84}_{36}Kr_{48}$	$^{88}_{36}Kr_{52}$	$^{90}_{36}Kr_{54}$
Exp. [117]	2.44	2.459	2.327	2.345	2.375	2.121	3.043
IBM-2	2.49	2.467	2.312	2.354	2.329	2.116	3.043

In the Figures we show the results of our calculations for the energies of the ground state band ($2_1^+, 4_1^+, 6_1^+, 8_1^+$ and 10_1^+) in the $^{76-90}Kr$ isotopes . We observe the discrepancy between theory and experiment for $J^\pi = 6^+, 8^+$ in Kr isotopes with neutron bosons ($N = 42, 44, 46, 48$). However, one must be careful in comparing theory with experiment, since all calculated low-lying states have a collective nature.

The order of the 0_2^+ and 3_1^+ is correctly predicted in $^{76-90}Kr$ isotopes and we remark that the energy of the 3_1^+ state is predicted systematically too high. This is a consequence of the presence of a Majarona term $M_{\pi\nu}$ in the Hamiltonian (eq. (2-43)). We have chosen the parameters of the Majarona force in such a way that it pushes up states which are not completely symmetric with respect to proton and neutron bosons, since there is no experimental evidence for such states. However, experimental information becomes available about these states with mixed symmetry, this situation could possibly be improved. In the present case it would have been possible to further higher its energy by constant the value of ξ_3 .

The position of the 2_3^+ state relative to the 0_2^+ state especially in ^{78}Kr, ^{82}Kr and ^{88}Kr isotopes. The moment of inertia of the ground state band increases, the quasi γ-band is pushed up, and also 0_2^+ state becomes a member of a $K = 0$ β-band.

The energy spectra show that the first criterion for identifying the intruder 0^+ states. For instance, in $^{76-82-84-88}Kr$ the experimental energies of the 0_2^+ states are lager than those of the calculated 0_2^+ states. As a consequence, we suspect that these states are intruder. On the contrary in $^{78-80}Kr$ the experimental data are close to the calculated states and thus they may be the collective 0_2^+ states. However, no final conclusion can be drawn from the energies alone, since it is very likely that both intruder and collective 0^+ states will occur in the same energy region.

Figure (3-1): Comparison between experimental and calculated energy levels for ^{76}Kr. The experimental data are taken from ref. [117].

Figure (3-2): Comparison between experimental and calculated energy levels for ^{78}Kr. The experimental data are taken from ref. [117].

Figure (3-3): Comparison between experimental and calculated energy levels for ^{80}Kr. The experimental data are taken from ref. [117].

Figure (3-4): Comparison between experimental and calculated energy levels for ^{82}Kr. The experimental data are taken from ref. [117].

Figure (3-5): Comparison between experimental and calculated energy levels for ^{84}Kr. The experimental data are taken from ref. [117].

Figure (3-6): Comparison between experimental and calculated energy levels for ^{88}Kr. The experimental data are taken from ref. [117].

Figure (3-7): Comparison between experimental and calculated energy levels for ^{90}Kr. The experimental data are taken from ref. [117].

3.1.3-Electric Transition Probability

The effective boson charges e_π and e_ν were calculated by plotting [118] M against N_ν / N_π where

$$M_1 = (1/N_\pi)\left[NB(E2;2_1^+ \to 0_1^+\right]^{1/2} e.b = e_\pi + e_\nu N_\nu / N_\pi \qquad \text{(for the SU(5) limit ....(3-2}$$

$$M_2 = (1/N_\pi)\left(\frac{5N}{N+4} B(E2;2_1^+ \to 0_1^+\right)^{1/2} e.b = e_\pi + e_\nu N_\nu / N_\pi \qquad \text{(for the O(6) limit......(3-3}$$

where $B(E2)$ is the reduced transition probability, N_π and N_ν are the boson numbers of proton and neutron respectively, $N = N_\pi + N_\nu$ is the total boson number. The difference between the effective charge and the charge of the single nucleon is referred to as the polarization charge. The value of effective charge may depend somewhat on the orbit of the nucleon. In particular, the polarization effect decreases when the binding energy of the nucleon becomes small.

Figure (3-8) represent the relation between $\left[NB(E2;2_1^+ \to 0_1^+ / N_\pi^2\right]^{1/2}$ and

$e_\pi + e_\nu N_\nu / N_\pi$ for the SU(5) limit, $\left(\frac{5N}{N+4} B(E2;2_1^+ \to 0_1^+ / N_\pi^2\right)^{1/2}$ and

$e_\pi + e_\nu N_\nu / N_\pi$

for O(6) limit. The linearity is indeed present giving $e_\pi = 0.0288$ eb and $e_\nu = 0.209$ eb in the SU(5) limit and $e_\pi = 0.0575$ eb and $e_\nu = 0.1047$ eb in the O(6) limit .The best fit of effective charges to $^{76-90}Kr$ isotopes was obtained $e_\pi = 0.04315$ eb and $e_\nu = 0.15685$ eb .This result gives a clear indication that the rotational contribution in nuclear motion in this region is very high.

We use used these results of effective charges to calculate the electric transition probabilities using the NPBEM code. The results are presented in table (3-3).
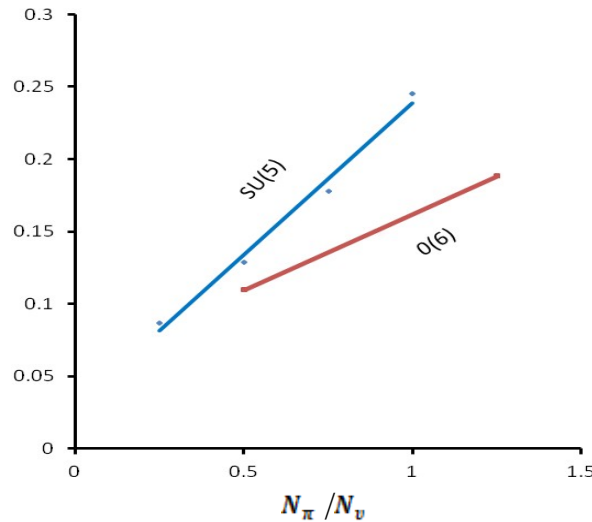
Figure (3-8): The plot of the quantities M_1 and M_2 versus $e_\pi + e_\nu N_\nu / N_\pi$ for $^{76-90}Kr$ Isotopes.

It is well known that absolute gamma ray transition probabilities offer the possibility of a very sensitive test of nuclear models and the majority of the information on the nature of the ground state has come from studies of the energy level spacing. The transition probability values of the exited state in the ground state

band constitute another source of nuclear information. Yrast levels of even-even nuclei ($J_i = 2,4,6,.....$) usually decay by *E2* transition to the lower lying yrast level with $J_f = J_i - 2$.

In table (3-3) we show the $B(E2;2_1^+ \rightarrow 0_1^+)$ and $B(E2;4_1^+ \rightarrow 2_1^+)$ values , which are of the same order of magnitude and display a typical decrease towards the middle of the shell.

As a consequence of possible *M1* admixture the $B(E2;2_2^+ \rightarrow 2_1^+)$ quantity is rather difficult to measure. For *Kr* isotopes, we give the different, conflicting experimental results and we see that no general feature be derived from them, from these values seems to increase for $^{76-78-80}Kr$ and decrease for $^{82-84}Kr$.

In the table we show $B(E2;2_2^+ \rightarrow 0_1^+)$ values. Experimentally the results are radically different for the *Kr* isotopes . In the some *Kr* isotopes the value seems to increased towards the middle of the shell, whereas in another *Kr* isotopes is decreased. Our calculations could not reproduce these contradictory features simultaneously.

The quantity $B(E2;0_2^+ \rightarrow 2_1^+)$, which is shown in table (3-3), provides a second clue for identifying intrude 0^+ states. If the experimental $B(E2;0_2^+ \rightarrow 2_1^+)$ value largely deviates from the results of our calculation, it is very likely the observed 0_2^+ states does not correspond to the collective state, but it is rather an intruder state. In ^{82}Kr isotope, there is a good agreement between experimental and calculated $B(E2;0_2^+ \rightarrow 2_1^+)$ value. This confirm our earlier statement about the nature of the lowest 0^+ state in this isotope.

The electric transition probabilities from the mixed-symmetry state $J = 1^+$ to the symmetric states $(2_1^+,2_2^+)$ is weak collective *E2* transition. The E2 transition between the 1^+ and the 2_1^+ ground state is small, whereas E2 transitions are large between fully-symmetric states and between mixed-symmetry states.

To conclude this section on the *E2* properties, we give the results for the quadrupole moments $Q(2_1^+)$ of the first excited 2^+ state in table (3-3) (see equation (2-41)). We show complication of theoretical results. The general features of these results is clear, namely an increased in the negative quadrupole moment with increasing neutron number.

جدول

3.1.4-Magnetic Transition Probability

The $B(M1)$ reduced transition probabilities were calculated using Eq.(2-54), and the boson gyromagnetic factors g_π, g_ν were estimated using the fact that $g = Z / A$ and the relation [119]

$$g = g_\pi \frac{N_\pi}{N_\pi + N_\nu} + g_\nu \frac{N_\nu}{N_\pi + N_\nu} \quad .... (3-4)$$

and one of the experimental $B\left(M1;2_2^+ \to 2_1^+\right) = 0.0429 \ \mu_N^2$ [24] for ^{76}Kr isotope, was used to produce a suitable estimation for the boson gyromagnetic factors. These values are $g_\pi = 0.782 \ \mu_N$ and $g_\nu = 0.328 \ \mu_N$. They are different from those of the rare–earth nuclei, $(g_\pi - g_\nu = 0.65 \mu_N)$, suggested by Van Isacker *et al.*, [120] also used $g_\pi = 1\mu_N$ and $g_\nu = 0\mu_N$ to reduce the number of the model parameters in their calculation of $M1$ properties in deformed nuclei. The results of our calculation are listed in table (3-4). A good agreement between the theory and the available experimental data is achieved. As can be seen from the table yields to a simple prediction that M1 matrix elements values for gamma to ground band and transitions should be equal for the same initial and final spin. Also the size of gamma to ground band matrix elements seems to decrease as the mass number increases.

The results shows that the transitions between low-lying collective states are relatively weak. This is because of the increase of the anti-symmetric component in the wave functions introduced by *F-spin* breaking in the Hamiltonian. The magnitude of M1 values increases with increasing spin for $\gamma \to g$ and $\gamma \to \gamma$ transitions and we see:

1- By fitting B(M1) from 2_γ to 2_g we always get small value for $g_\pi - g_\nu$ compared with the value basis on the microscopic calculations $g_\pi - g_\nu = 1$.

2- There are evidences that M1 small mode exists in all spectra.

3- one can not make decisive conclusions related to the agreement between theoretical and experimental data from the above table due to the lack of experimental data. However both experiments and theory predicts small M1 component which is due to symmetry and forbiddances of band crossing gamma transitions.

4- The $\gamma \to \gamma$ M1 matrix elements are larger than the $\gamma \to g$ M1 matrix elements by a factor of 2 to 3. Again, this agree qualitatively with the perturbation expressions derived in ref. [121] .

5-   The size of the $\gamma \rightarrow g$ M1 matrix elements seems to decrease with increasing mass. Specially, a change in $\gamma \rightarrow g$ M1 strengths occurs when the gamma band crosses the beta band.

The *M1* properties of collective nuclei are certainly very sensitive to various, even small, components in the wave functions either of collective or non-collective character. In the $^{88-90}Kr$ isotopes it was shown that the inclusion of excitations across the major shell and two quasi-particle states is important. One excepts that also for $^{88-90}Kr$ isotopes (which are near to closed shell for neutron) similar effects come into play. As above analysis suggests they can manifest in considerable renormalization of IBM-2 boson g-factors from their slandered values. The magnetic dipole moment for first excited state is given by

$$\mu(2_1^+) = g_\pi L_\pi + g_\nu L_\nu ....(3-5)$$

where $g_\pi(g_\nu)$ is the g-factor for the correlated proton (neutron) boson and $L_\pi(L_\nu)$ is the corresponding angular momentum operator. According to the microscopic foundation of the model, $g_\pi(g_\nu)$ is expected to depend, in first approximation on proton (neutron) number $N_\pi(N_\nu)$ only, $g_\pi = g_\pi(N_\pi)$ and $g_\nu = g_\nu(N_\nu)$. The IBM-2 calculations for $\mu(2_1^+)$ are listed in table 4, we see a good agreement with experimental data.

It is clear that the two effects contribute to the dependence of the magnetic moments on proton and neutron number: the dependence of g_π and g_ν on proton and neutron number and the variation of the matrix elements of the operator $L_\pi(L_\nu)$ with N_π and N_ν. As will be better shown below, the former effect is related to the shell structure of the orbits, while the latter is related to the average number of proton and neutron boson taking part in the collective motion.

جدول

3.1.5-Mixing Ratio $\delta(E2/M1)$

We evaluate the mixing ratio $\delta(E2/M1)$ for *Kr* isotopes, which depends on the equation (2-55). These are compared with experimental and theoretical results in table (3-5), where one can see good agreement with estimated and experimental

values. The variations in sign of the *E2/M1* mixing ratios from one isotope to another for the same class of transitions, and within a given nucleus for transitions from different spin states, suggest that a microscopic approach is needed to explain the data theoretically. For such reason, the sign of the mixing ratio is not taken into consideration. Sign convention of mixing ratios has been explained in detail by *Lang et al.*, [100] .

   These results exhibit disagreement in some cases, with one case showing disagreement in sign. However, it is a ratio between very small quantities and any change in the dominator that will have a great influence on the ratio. The large calculated value for $2_2^+ \rightarrow 2_1^+$ is not due to a dominant E2 transition, but may be under the effect of very small *M*1 component in the transition. Moreover, the large predicted value for transition $2_2^+ \rightarrow 2_1^+$ in ^{80}Kr compared with experimental value may be related to high predicted energy level value of the IBM-2; $E(2_2^+)$ =1.287 MeV, while the experimental value is 1.256 MeV. We are unable to bring the energy value of this state close to experimental value simply by changing the Majorana parameters.

جدول

3.1.6-Electric Monopole Matrix Element $\rho(E0)$

The $E0$ transition occurs between two states of the same spin and parity by transferring energy and zero units of angular momentum, and it has no competing gamma ray. The $E0$ transition is present when there is a change in the surface of the

nucleus. For example, in nuclear models where the surface is assumed fixed, $E0$ transitions are strictly forbidden, such as in shell and IBM models. Electric monopole transitions are completely under the penetration effect of atomic electrons on the nucleus, and can occur not only in $0^+ \rightarrow 0^+$ transition but also, in competition with gamma multipole transition, and depending on transition selection rules that may compete in any $\Delta J = 0$ decay such as a $2^+ \rightarrow 2^+$ or any $J_i = J_f$ states in the scheme. When the transition energy greater than $2m_oc^2$, monopole pair production is also possible.

The $E0$ reduced transition probability is given in equation (2-60). The parameters in equation (2-57) can be predicted from the isotope shift [117] (see table (3-7)), since such data are not available for Kr isotopes, we calculate these parameters by fitting procedure into two experimental values of isotopic shifts (equation (2-62)). The parameters which were subsequently used to evaluate the $\rho(E0)$ -values were; $\beta_{0\pi} = 0.062$ fm^2 , $\beta_{0v} = -0.021$ fm^2 and $\gamma_{0v}=0.032$ fm^2 . From the table (3-6), in general there is no experimental data to compare with the IBM-2 calculations**.**

The monopole matrix element is important for nuclear structure and the model predictions due to their sensitivity for the nuclear shape. We conclude that more experimental work is needed to clarify the band structure and investigate an acceptable degree of agreement between the predictions of the models and the experimental data.

We also find good agreement between the calculated and experimental values for isotopic shifts for all krypton isotopes (table 3-7).

Table (3-6): Monopole matrix elements ρ(E0) for *Kr* isotopes in e.b

$J_i^+ \rightarrow J_f^+$	^{76}Kr	^{78}Kr	^{80}Kr	^{82}Kr	^{84}Kr	^{88}Kr	^{90}Kr
$0_2 \rightarrow 0_1$	0.0431	0.0551	0.070	0.0750	0.0082	0.0094	0.075
$0_3 \rightarrow 0_1$	0.0067	0.00073	0.00080	0.00083	0.00089	0.00092	0.0009
$0_3 \rightarrow 0_2$	3.18*10-3	0.0045	0.00034	0.00089	0.00094	0.0099	0.0102
$2_2 \rightarrow 2_1$	0.0002	0.0034	0.0056	0.0076	0.0096	0.0099	0.013
$2_3 \rightarrow 2_1$	0.00034	0.0041	0.00046	0.00052	0.00065	0.00067	0.00070
$2_3 \rightarrow 2_2$	0.0021	0.0027	0.00351	0.00395	0.00519	0.00531	0.00872

Table(3-7): Isotopic Shifts for *Kr* Isotopes

Nucleus	$\Delta \langle r^2 \rangle$ fm^2	
	Exp .[117]	*IBM-2*
$^{76}_{36}Kr_{40} - ^{78}_{36}Kr_{42}$	-	-0.009
$^{78}_{36}Kr_{42} - ^{80}_{36}Kr_{44}$	-	-0.0148

$^{80}_{36}Kr_{44} \rightarrow ^{82}_{36}Kr_{46}$	-0.028(5)	-0.0298
$^{82}_{36}Kr_{46} \rightarrow ^{84}_{36}Kr_{48}$	-0.040(4)	-0.055
$^{84}_{36}Kr_{48} \rightarrow ^{86}_{36}Kr_{46}$	0.071(3)	0.0810
$^{86}_{36}Kr_{50} \rightarrow ^{88}_{36}Kr_{52}$	0.379(7)	0.431
$^{88}_{36}Kr_{52} \rightarrow ^{90}_{36}Kr_{54}$	0.751	0.655

Mixed Symmetry States-3.1.7

One of the advantage of the IBM-2 is ability of reproducing the mixed symmetry states. These states are created by a mixture of the wave function of protons and neutrons that are observed in most even-even-even nuclei. This mixed symmetry states (*MSSs*) has been observed in many nuclei. In more vibrational and $\gamma-soft$ nuclei this mixed symmetry states (*MSSs*) have been observed in many nuclei. In more vibrational and gamma soft nuclei. We expect the lowest MSS with $J = 2^+$ state, while in rotational nuclei observed as the $J^\pi = 1^+$ state. In $^{76\text{-}90}Kr$ isotopes we see that when the states $J^\pi = 2^+_2, 2^+_4$ and 3^+_1 are strongly dominated by the $F=F_{max}$, the strongest contribution to the $J^\pi = 2^+_3, 3^+_2$ states is the one with $F=F_{max}$-1. We can see the $J^\pi = 2^+_3, 3^+_2$ states as a mixed symmetry states in $^{76\text{-}90}Kr$ isotopes.

In this work, we proposed that the 2^+_3 state decays to the first excited state with an energy 1.598 MeV in ^{76}Kr with a mixing ratio $\delta(E2/M1) = 1.189$ which means it is dominated by the M1 transition, with $B(M1)$ equal to 0.0031 μ^2_N . In ^{78}Kr isotope, for the third $J = 2^+$ state at energy 1.685 MeV excitation is close to the experimental data for 1.755 MeV . The energy is well reproduced by the calculation, where the choice of the Majarona parameters plays a crucial role. This state is quite pure F_{max}-1 with $R \propto J|F^2|J > / F_{max}(F_{max}+1) = 50\%$, . The excitation energy of 3^+_2 state is 2.399 MeV with mixing ratio $\delta(E2/M1; 3^+_2 \rightarrow 2^+_1) = 2.565$, $B(M1; 3^+_2 \rightarrow 2^+_1) = 0.00301 \mu^2_N$. In the ^{80}Kr , the calculation predicted the 2^+_3 state at 2.251 MeV with $R = 83\%$.

In other $^{82\text{-}84\text{-}88\text{-}90}Kr$ isotopes the states 2^+_3 and 3^+_2 are mixed symmetry states their excitation energies are close to available experimental data and the values of $R = 73\%, 75\%, 72\%$ and 80% respectively .

In all $^{76\text{-}90}Kr$ isotopes that the second 3^+ states to be the lowest $J^\pi = 3^+$ mixed symmetry states with two phonon excitation. The low-lying levels with angular momentum greater than 3^+ with a large mixed symmetry states component are predicted in this work.

The energy fit to several levels is very sensitive to the parameters in the Majorana term which also strongly influence the magnitude and sign of the multipole mixing ratios of many transitions. In particular we find that the calculated energies of a number of states are affected in a very similar way and these might be considered to

have a mixed-symmetry origin, or contain substantial mixed-symmetry components. Those with a mixed-symmetry origin have no counterpart in *IBM*-1. The energy dependence of the 2_2^+ and 2_4^+ levels is consistent with the mixed-symmetry character of the 2_3^+ level being shared with neighboring states.

        The influence of the parameters on these states is shown in table (3-1). The ξ_2 term strongly affects the energies of all of the levels considered to have a mixed-symmetry character or to contain mixed-symmetry components . In obtaining this value of the ξ_1 and ξ_3 terms were maintained at their best-fit values. The mixing ratio data, discussed in the above section have a strong dependence on ξ_2 and show that ξ_2 cannot be zero in our fit.

        The 1^+ level is strongly affected by changing ξ_1, while the 3_1^+ level energy depends on the ξ_3 value. The 2_3^+ mixed-symmetry state and the predominantly symmetric 2_2^+ and 2_4^+ levels are largely unaffected by changing ξ_1, or ξ_3 in contrast to their dependence on ξ_2.

        Most experimentally observed low-spin levels, apart from 1^+ states below 2.5 MeV; have their counterpart in the *IBM*-2 level spectrum although the energy match is not good in every case. It also appears that we may identify the members of the family of mixed-symmetry states corresponding to the [*N*-1,1] representation [122,123]. The small *E2/M1* mixing ratios are consistent with this interpretation but level lifetimes are required for a firmer identification.

        In *Kr* isotopes, all hitherto discovered *MSS*s have been reviewed in [123]. It has been shown that the lowest lying *MSSs* is the one quadrupole phonon *MSS* labeled as $2_{1,MS}^+$, $3_{1,MS}^+$ and characterized by a weakly-collective *E2* transition probability to the ground state and a large *M*1 transition to the 2_1^+ state.

        Table (3-6) contains the calculated $\rho(E0)$ values. In general there is no experimental data to compare with the IBM-2 results. It must also be remarked that the comparatively large $\rho(E0)$ values for transitions from the 2_3^+ mixed-symmetry state and from the 2_1^+ and 2_2^+ states indicate that substantial *E0* components occur in these decays from mixed-symmetry states. The *E0* matrix element describing such decay is proportional to β_π and β_ν, although the β values are small, their sign difference results in the *E0* matrix being greatest.

Nd Isotopes 3.3

Hamiltonian Interaction Parameters 3.3.1

The isotopes chosen in this work are A=144, 146, 148, 150, 152, 154 due to the presence of available experimental data for energy levels, the electromagnetic transition probability, the mixing ratios and monopole transition values. We have $N_\pi = 5$, (10 protons outside the closed shell 50), and N_ν varies from 1 for Nd[144] to 6 for Nd[154], measured from the closed shell at 82. While the parameters ε, κ and χ_ν, as well as the Majorana parameters ξ_k, with k =1,2,3, were treated as free parameters and their values were estimated by fitting with the experimental values. The procedure was made by selecting the traditional value of the parameters and allowing one parameter to vary while keeping the others constant until the best fit with the experimental obtained. This was carried out until one overall fit was obtained. The best values for the Hamiltonian parameters are given in table (3-17).

This parameters was carried out iteratively until an overall fit was achieved. Having obtained wavefunctions for the states in [144–154]Nd after fitting the experimental energy levels in IBM-2, we can calculate the electromagnetic transition rates between states using the program NPBOS [124]. The Hamiltonian sets of parameters which have been varied along the isotopic chain are shown as a function of the neutron number for Nd isotopes in table (3-17).

Table (3-17): IBM-2 Hamiltonian parameters for [144-154]*Nd* isotopes, all parameters in MeV units except χ_π and χ_ν are dimensionless.

Isotopes	N_π	N_ν	N	ε	κ	χ_ν	χ_π	$\xi_1 = \xi_3$	ξ_2
$^{144}_{60}Nd_{84}$	5	1	6	0.86	-0.093	-1.19	-1.18	0.012	-0.09
$^{146}_{60}Nd_{86}$	5	2	7	0.82	-0.096	-1.11	-1.18	0.012	-0.09
$^{148}_{60}Nd_{88}$	5	3	8	0.70	-0.082	-1.11	-1.18	0.012	-0.09
$^{150}_{60}Nd_{90}$	5	4	9	0.51	-0.080	-1.11	-1.18	0.012	-0.09
$^{152}_{60}Nd_{92}$	5	5	10	0.42	-0.070	-1.11	-1.18	0.012	-0.09
$^{154}_{60}Nd_{94}$	5	6	11	0.44	-0.069	-1.11	-1.18	0.012	-0.09

$$C_{0\nu} = C_{2\nu} = C_{4\nu} = 0.0, \quad C_{0\pi} = C_{2\pi} = C_{4\pi} = 0.0$$

Energy Spectra 3.3.2

Concentration was made on the 2_1^+ to make a reasonable fit to experimental data. A sample of experimental and theoretical decay scheme is presented in figures (3-16,17,18,19,20,21). As one can see an overall a good agreement was obtained for the gamma and beta bands for [144-154]Nd isotopes. The results in the figures show a comparison between experimental and theoretical energy levels in [144-154]Nd isotopes, the agreement is very good for the 2_1 and 4_1, but the model does not able to predict the 8_1 and this may be due to the high spin of this state. Actually this has slim effects on calculations of transitions probability.

The behavior of the ratio of the energies $E(4_1^+)/E(2_1^+)$ are good criterion for the shape transition (see table(3-18)). From the table (3-18), the systematic of basic observables in $^{144\text{-}54}$Nd isotopes showing $E(4_1^+)/E(2_1^+)$ values increased gradually with increasing neutron numbers, and the agreement between the experimental values and the calculated ones. The calculated values change from about 1.885 to about 3.281. It means that their structure seems to be varying from very near-harmonic vibrator (HV) SU(5) limit to rotation nuclei (SU(3) characters) .

Table (3-18): Energy ratio $R_{4/2} = E(4_1^+)/E(2_1^+)$ for $^{144\text{-}154}Nd$ isotopes

$(E(4_1/2_1$	$_{84}{}^{144}_{60}Nd$	$^{146}_{60}Nd_{86}$	$^{148}_{60}Nd_{88}$	$^{150}_{60}Nd_{90}$	$^{152}_{60}Nd_{92}$	$^{154}_{60}Nd_{94}$
Exp. [117]	1.887	2.297	2.493	2.930	3.263	3.230
IBM-2	1.885	2.300	2.490	2.930	3.255	3.281
X(5)	2.91	2.91	2.91	2.91	2.91	2.91

From the table (3-18), the $^{144\text{-}146}$Nd shows a nuclear structure is spherical (near harmonic vibrator), ^{148}Nd being a transitional nucleus (O(6) limit)). As it is seen from the table (3-18) the calculated and experimental energy values for ^{150}Nd are very close to X(5) predictions. Around $N = 90$, the positions of the excited 0^+ states are also close to the X(5) prediction and we note that the spacings in the excited sequence follow the expected behavior. It is regarded as a transitional nucleus, since it exhibits both the features of vibrational nuclei, like a two phonon triplet at approximately twice the excitation energy of 2_1^+ as well as the features of rotational nuclei, like an intrinsic quadrupole moment and an enhanced $B(E2)$ value of the 2_1^+ state.
:[For $X(5)$ critical point symmetry these signatures are listed below [93
 . The energy ratio $E(4_1^+)/E(2_1^+)$ should be approximately 2.91 -1

The position of the first excited collective 0_2^+ state is approximately 5.67 times -2 the
.energy of the 2_1^+ state
Clearly there are many examples of nuclei with yrast energies that closely follow the $X(5)$ prediction. However, most of these can be excluded on the basis of their deduced yrast B(E2;J→J-2) values. Indeed, from the available data, the only nuclei that remain candidate is the ^{150}Nd. For this subset of isotope, the properties of the excited states, and the transitions from them, can be   examined in more detail. For ^{150}Nd the position of the 0_2^+ level is significantly lower than the X(5) prediction and little further information is known about states in the relevant excited sequences. For the $N = 90$ isotones, the positions of the 0_2^+ levels are close to the X(5) prediction of E(0_2^+) ~ 5.67 E(2_1^+) but the energy spacing of sates in the excited sequence are much lower than predicted. However, the X(5) picture can be applied to a limited number of transitional nuclei, where it is able to reproduce properties of the yrast .states

The nucleus ^{150}Nd have been very well studied and are quite close to X(5), and the existing data for the others suggest they are good candidates. Further data in these cases would be very useful. The $^{152\text{-}154}$Nd taken the rotational shape to deformed rotor shape .

75

Figure (3-16): Comparison between experimental and calculated energy levels for [144]Nd. The experimental data are taken from ref. [117].

Figure (3-17): Comparison between experimental and calculated energy levels for [146]Nd. The experimental data are taken from ref. [117].

Figure (3-18): Comparison between experimental and calculated energy levels for ^{148}Nd. The experimental data are taken from ref. [117].

Figure (3-19): Comparison between experimental and calculated energy levels for ¹⁵⁰Nd. The experimental data are taken from ref. [117].

Figure (3-20): Comparison between experimental and calculated energy levels for ¹⁵²Nd. The experimental data are taken from ref. [117].

Figure (3-21): Comparison between experimental and calculated energy levels for ^{154}Nd. The experimental data are taken from ref. [117].

3.3.3 Electric Transition Probability

The effective boson charges e_π and e_ν were calculated by plotting [118] M_1 (SU(5) limit) in Eqs. (3-1) and M_3 (for SU(3) limit) is given by the equation:

$$M_3 = (1/N_\pi)\left(\frac{5N}{2N+3} B(E2;2_1^+ \to 0_1^+)\right)^{1/2} e.b = e_\pi + e_\nu N_\nu / N_\pi \quad \text{(For SU(3) limit}.........(3-5$$

against N_ν / N_π. The linearity is indeed present giving $e_\pi = 0.3778$ eb and $e_\nu = 0.0946$ eb in the SU(5) limit and $e_\pi = 0.33$ eb , and $e_\nu = 0.075$ eb in the SU(3) limit. The best fit to $^{144-154}Nd$ isotopes was obtained $e_\pi = 0.3538$ eb and $e_\nu = 0.0848$ eb . We use used these results of effective charges to calculate the electric transition probabilities B(E2)'s using the NPBEM code. The results are presented in table (3-19).

M_1 (e²b²) , M_3 (e²b²)
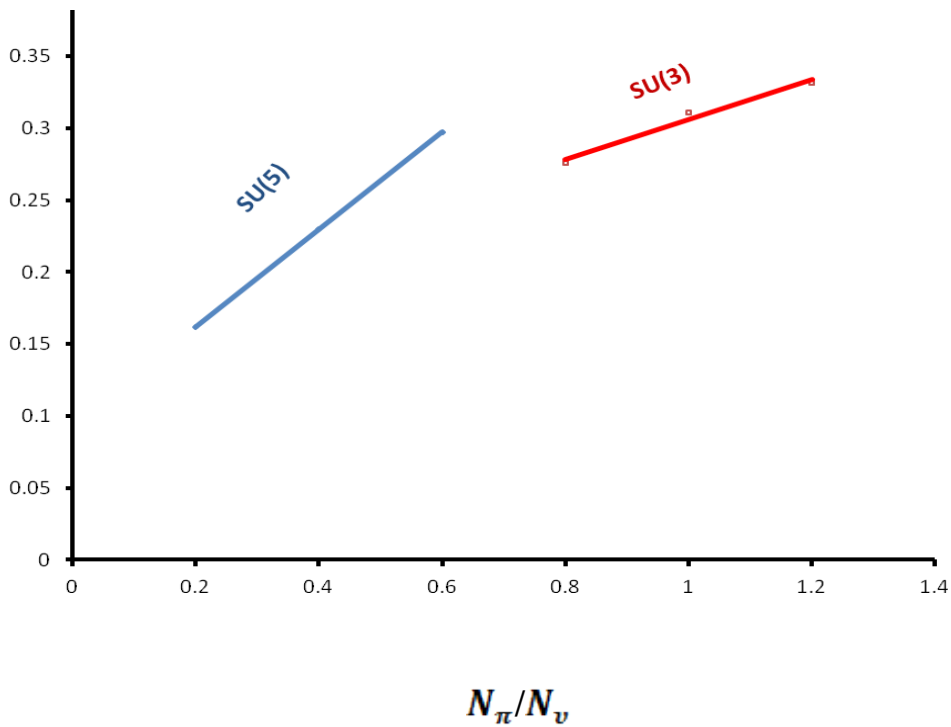
Figure (3-22): The plot of the quantity M_1 and M_3 versus $e_\pi + e_\nu N_\nu / N_\pi$ for [144-154]Nd isotopes.

In table (3-19), shows some $B(E2)$ electric transition probabilities of levels for even–even $^{144-154}$Nd isotopes. The results of the present study were compared with

experimental values and it was seen that they are in good agreement. We have calculated $E2$ transition properties of $^{144-154}$Nd in the framework of IBM-2.

The calculated and theoretical $B(E;2_1^+ \rightarrow 0_1^+)$, $B(E;4_1^+ \rightarrow 2_1^+)$ and $B(E;6_1^+ \rightarrow 4_1^+)$ values are mostly in good agreement and increased with increasing neutron number and they show similar distribution and display a typical increase towards the middle of the shell. The enhancement of B(E2) values towards the middle of the shell should be noted.

The large electric transition probability values in neodymium isotopes is the main indicator of the vibrational behaviour of these isotopes.

In table (3-19), we show the results for $B(E;2_2^+ \rightarrow 0_1^+)$ and $B(E;2_3^+ \rightarrow 0_1^+)$ values. This quantity is rather small since this transition is forbidden in all three limits of IBM [27]. The results for the $B(E;2_2^+ \rightarrow 2_1^+)$ values are shown. The experimental .information of this quantity is very limited, and this transition contain M1 admixture

For ^{150}Nd (X(5) model) the strength of transitions between yrast states as reflected in the B(E2;J→J-2) values should increase with angular momentum J at a .rate intermediate between the values for a vibrator and a rotor

The quadrupole moment for first excited state in $^{144-154}Nd$ isotopes are very well described. As mentioned above, the calculated values of $Q(2_1^+)$ indicated this nucleus has prolate shape in first excited states.

الجدول

(3-19)

3.3.4-Magnetic Transition Probability

The M1 transition operator is given in Eq.(2-49), where the gyromagnetic factors for bosons g_π and g_ν are estimated. The reduced E2 and M1 matrix elements were combined in a calculation of mixing ratio $\delta(E2/M1)$ using the relation which is given by Eq. (2-55).

Sambatora *et al.*, [119] suggested a total g-factor which is given in Eq. (3-4), used to compute the 2_1^+ state g-factor. The value of the measured magnetic moment $\mu = 2g = 0.35(3)\ \mu_N$ [117], and the experimental mixing ratio $\delta(2_2^+ \rightarrow 2_1^+) = -1.6(5)$ [100] were used to produce sutable estimation for the boson gyromagnetic factors. The values are $g_\pi = 0.413\ \mu_N$ and $g_\nu = 0.322\ \mu_N$. The results of the calculations are listed in table (3-20).

Table (3-20): Reduced transitions probability $B(M1)$ in μ_N^2 units for $^{144-154}Nd$ isotopes

$J_i^+ \rightarrow J_f^+$	$B(M1; J_i^+ \rightarrow J_f^+)\mu_N^2$						
	^{144}Nd	^{146}Nd	^{148}Nd	^{150}Nd	^{152}Nd	^{152}Nd	^{154}Nd
$2_1 \rightarrow 2_2$	0.0006	0.00075	0.000871	0.00053	0.000412	0.000522	0.000631
$2_1 \rightarrow 2_3$	0.00011	0.00015	0.00021	0.00029	0.00033	0.000412	0.000520
$2_2 \rightarrow 2_3$	0.00045	0.00056	0.00061	0.00062	0.00083	0.00088	0.000892
$2_1 \rightarrow 3_1$	0.00231	0.00439	0.00521	0.00431	0.0051	0.00530	0.0067
$2_2 \rightarrow 3_1$	0.0047	0.0031	0.0081	0.009	0.018	0.0194	0.0210
$3_2 \rightarrow 3_1$	$10^{-5}*2$	0.0006	0.0010	0.0054	0.0057	0.00602	0.0073
$0_1 \rightarrow 1_1$	0.732	0.747	0.824	0.902	0.932	0.986	1.340
$\mu(2_1^+)$ (Exp.)	0.35(3)	0.58(2)	0.64(8)	0.644(18)	-	-	-
$\mu(2_1^+)$ IBM-2	0.297	0.432	0.542	0.589	0.621	0.763	0.872

[Experimental data are taken from refs.[117

From the results of $B(M1)$, the transitions between low-lying collective states in IBM-2 vanish is not necessarily a consequence of F-spin symmetry, but may be related to the existence of other symmetries, like O(5) or SU(3).

The M1 excitation strength for the $B(M1; 1_1^+ \rightarrow 0_1^+)$ transition is proportional to the factor g_ν^2 and depends only weakly on the strength of Majarona force.

The magnetic dipole moment for first excited state in even-even $^{144-154}$Nd isotopes provide a sensitive test of the effective boson number in the IBM-2 framework, in Nd isotopes with N = 84-90, confirm the validity of assuming a drastic change in number of proton boson when the number of neutron boson is increased from 88 to 90.

3.3.5-Mixing Ratio $\delta(E2/M1)$

The E2/M1 multipole mixing ratios for $^{144\text{-}154}$Nd isotopes, $\delta(E2/M1)$, were calculated for some selected transitions between states. The sign of the mixing ratio must be chosen according to the sign of the reduced matrix elements. The equations used are (2-52) for M1 transitions and (2-55) for the mixing ratios. The results are listed in table (3-21). The agreement with available experimental data [100,117] is more than good especially in the sign of the mixing ratio. However, there is a large disagreement in the mixing ratios of some transitions, is not due to a dominate E2 transition, but may be under the effect of very small value of M1 matrix element. However, it is a ratio between very small quantities and may change in the dominator that will have a great influence on the ratio.

86

الجدول (3-21)

3.3.6-Electric Monopole Matrix Element $\rho(E0)$

Electric monopole (E0) transitions between nuclear levels proceed mainly by internal conversion with no transfer of angular momentum to the ejected electron. For transition energies greater than $2m_0c^2$, electron- positron pair creation is also possible; two-photon emission is possible at all energies but extremely improbable. The E0 transition also occurs in cases where the levels have the same spin and parity ($I_i = I_f \neq 0$). This means that the E0 transition competes with E2 and M1 components in these transitions.

The reduced matrix monopole transition is given in Eq.(2-60), the necessary parameters of the monopole matrix element $\rho(E0)$ are derived from the values of $\rho(E0; 0_2^+ \to 0_1^+) = 1.8(2)$ [100] for ^{144}Nd and the value of the isomer shift for the same isotopes $\delta < r^2 \gg 1.62 \, fm^2$ [131]. We obtain $\beta_{0\pi} = 0.0426 \, fm^2$, $\beta_{0\nu} = 0.0206 \, fm^2$ and $\gamma_{0\nu} = -45 * 10^{-3} \, fm^2$. Table (3-22) contain the calculated $\rho(E0)$ values . In general there is no experimental data to compare with IBM-2 calculations.

Table (3-22): Monopole matrix element ρ(E0) for *$^{144-154}$Nd* isotopes in e.b

$J_i^+ \to J_f^+$	^{144}Nd		^{146}Nd		^{148}Nd		^{150}Nd		^{152}Nd		^{154}Nd	
	Exp.	IBM-2	Exp.	IBM-2	Exp.	IBM-2	Exp.	IBM-2	Exp.	IBM-2	Exp.	IBM-2
$0_2 \to 0_1$	1.82(6)	1.976	-	0.072	-	0.078	-	0.083	-	0.086	-	0.098
$0_3 \to 0_1$	-	3.18*10⁻³	-	0.0074	-	0.0077	-	0.0079	-	0.0084	-	0.0089
$0_3 \to 0_2$	-	0.070	-	0.00034	-	0.00089	-	0.00093	-	0.00096	-	0.0010
$2_2 \to 2_1$	-	0.0034	-	0.0055	-	0.0076	-	0.0079	-	0.0085	-	0.0089

Experimental data are taken from ref. [100]

We notice that the theoretical values for the $X(E0/E2)$ ratio are small, for some transitions (see table (3-23)) which means that there is a small contribution of E0 transition on the life time of the 0^+ states. There are two high values of $X(E0/E2)$ in transitions from 0_2^+ to 0_1^+ in $^{144-154}$Nd isotopes means that this state decay mostly by the E0 and according to this one could say that the study of this state give information about the shape of the nucleus, because the E0 transitions matrix elements connected strongly with the penetration of the atomic electron to the nucleus. So combination of the wavefunction of atomic electron, which is well known, and the nuclear surface give good information of the nuclear shape.

Table(3-23): *X(E0/E2)* values for *$^{144-154}$Nd* Isotopes

$J_i^+ \rightarrow J_f^+$	^{144}Nd	^{146}Nd	^{148}Nd	^{150}Nd	^{152}Nd	^{154}Nd
	IBM-2	IBM-2	IBM-2	IBM-2	IBM-2	IBM-2
$0_2 \rightarrow 0_1$	4.560	6.980	10.672	13.0	18.0	16
$0_3 \rightarrow 0_1$	$10^{-2}*3.33$	0.0046	0.0054	0.0075	0.0089	0.00076
$0_3 \rightarrow 0_2$	3.230	4.189	10.342	10.650	15.0	12.55
$2_2 \rightarrow 2_1$	4.220	8.620	9.451	11.0	23	27.870

To evaluate the isomer shifts for $^{144-154}$Nd isotopes, we depend on Eq.(2- 63). The results of isomer shifts are listed in table (3-24). We notice the values of IBM-2 and the available experimental data are increased with increasing neutron number.

Table (3-24) : The isomer shifts δ <r^2> fm^2 for $^{144-154}$*Nd* isotopes

isotopes	^{144}*Nd*	^{146}*Nd*	^{148}*Nd*	^{150}Nd	^{152}Nd	^{154}Nd
Exp.[117]	0.162	0.164	-	0.167	-	-
IBM-2	0.155	0.176	0.181	0.188	0.194	0.218

3.3.7-Mixed-Symmetry States

Collective excitations are a common phenomena in atomic nuclei. These excitations arise from the coherent movement of many particles in the nucleus. A special class of collective excitations, called mixed-symmetry states, which are defined in the IBM-2, have been found in atomic nuclei and are interpreted geometrically as an out of phase motion of protons and neutrons. Together with collective excitations in which the protons and neutrons move in phase, these states can be used as building blocks for a general description of collective phenomena in nuclei. Mixed symmetry states are also sensitive to the strength of the residual proton-neutron quadrupole interaction in the valence shell and thus their properties are important in constraining the strength of this interaction. A number of one-quadrupole phonon mixed symmetry (2_3^+) states have been found in vibrational nuclei in the *A*= 140-150 and 1_1^+ in the A=152-154 mass region. To better understand the evolution of mixed-symmetry states in this mass region, experiments were done to identify the 2_3^+ state in the isotopes $^{144-150}$Nd and 1_1^+ state in $^{152-154}$Nd isotopes.

The evolution of the energy of the 2_3^+ state in the *N* = 84 isotope shows in increase in the proton-neutron interaction in the valence shell. The energy of these states were fitted by performing an IBM-2 calculation, which shows that the evolution in energy can be modelled with an appropriate set of terms in the IBM-2 Hamiltonian. The 2_3^+ state in the *N* = 86 isotope shows a similar behavior to the corresponding states in the *N* = 88 isotope and show that the mixed-symmetry states are sensitive to the residual proton-neutron interaction in this mass region.

The M1 transitions strengths for $^{144-145}$Nd are given in table (3-22). They are increased with increasing neutron number, each corresponding to the large or small values of mixing ratio δ. The larger M1 transition of
$B(M1;2_3^+ \rightarrow 2_1^+) = 0.000520 \ \mu_N^2$ for ^{154}Nd corresponding to δ = 12.0 is favored due to the fact that the other possible value of the B(M1) results in a
$B(E2;2_3^+ \rightarrow 2_1^+) = 0.0018 \ e^2b^2$, which is much larger than can be accounted for from any standard description of collective nuclei. Taking the values of the larger M1 transitions for the $1_1^+ \rightarrow 0_1^+$ transition for all $^{144-154}$Nd isotopes as can be seen in table (3-22) we find the 1_1^{+} state is the dominant fragment of the 0_1 mixed-symmetry state.

The small values of the mixing ratio δ suggest that there may be a strong M1 transition between 2_3^+ and 2_1^+. This would be consistent with transition from mixed symmetry state to fully symmetry although, as we shall see, the boson number enhancement factor is not present in the vibrational limit [130].

In the vibrational limit the ground state contains no *d* bosons and there are two 2^+ states with one *d* boson, corresponding to full symmetry and mixed symmetry [130]. We shall associate these two states with the 2_3^+ and 2_1^+ states, respectively. They are given in terms of the ground state $\left| 0^+ \right\rangle$

$$\left| 2_1^+ \right\rangle = \frac{1}{\sqrt{N}} \left(d_\nu^+ s_\nu + d_\pi^+ s_\pi \right) \left| 0^+ \right\rangle$$

$$\left| 2_3^+ \right\rangle = \left\{ \left(N_\pi / NN_\nu \right)^{1/2} d_\nu^+ s_\nu - \left(N_\pi / NN_\pi \right)^{1/2} d_\pi^+ s_\pi \right\} \left| 0^+ \right\rangle$$

Xe Isotopes 3.2

Hamiltonian Interaction Parameters 3.2.1

The computer program NPBOS [124] was used to make the Hamiltonian diagonal. In principle, all parameters can be varied independently in fitting the energy spectrum of one nucleus. However, in order to reduce the number of free parameters and in agreement with microscopic calculations of Turkan *et al*., [66], only ε and κ are vary as a function to both of N_π and N_ν *i.e.* $\varepsilon = \varepsilon(N_\pi, N_\nu)$ and $\kappa = \kappa(N_\pi, N_\nu)$ are allowed. The other parameters depend only on N_π or N_ν, *i.e.* $\chi_\pi = \chi_\pi(N_\pi)$, $\chi_\nu = \chi_\nu (N_\nu)$, $C_{L\pi} = C_{L\pi}(N_\pi)$ and $C_{L\nu} = C_{L\nu} (N_\nu)$. Thus, in isotopes chain, χ_π is kept constant, $C_{L\pi}$ and $C_{4\nu}$, $\xi_1 = \xi_3$, ξ_2 are kept constant for all isotopes (see table (3-8)).

The isotopes $^{124-134}Xe$ have $N_\pi = 2$ and N_ν varies from 6 to 1, while the parameters ε , κ and χ_ν were treated as free parameters and their values were estimated by fitting to the measured level energies. This procedure was made by selecting the "traditional" values of the parameters and then allowing one parameter to vary while keeping the others constant until a best fit was obtained. This was carried out iteratively until an overall fit was achieved. The best fit values for the Hamiltonian parameters are given in table (3-8).

Table (3-8): IBM-2 Hamiltonian parameters for $^{124-134}Xe$ isotopes, all parameters in MeV units except χ_π and χ_ν are dimensionless

Isotopes	N_π	N_ν	N	ε	κ	χ_ν	χ_π	$C_{0\nu}$	$C_{2\nu}$	$C_{4\nu}$	$\xi_1 = \xi_3$	ξ_2
$^{124}_{54}Xe_{70}$	2	6	8	0.70	-0.145	0.0	-0.80	0.10	-0.10	0.0	0.12	-0.4
$^{126}_{54}Xe_{72}$	2	5	7	0.70	-0.155	0.20	-0.80	0.30	0.0	0.0	0.12	0.4-
$^{128}_{54}Xe_{74}$	2	4	6	0.76	-0.170	0.33	-0.80	0.30	0.10	0.0	0.12	0.4-
$^{130}_{54}Xe_{67}$	2	3	5	0.76	-0.190	0.50	-0.80	0.30	0.10	0.0	0.12	-0.4
$^{132}_{54}Xe_{78}$	2	2	4	0.90	-2.10	0.90	-0.80	0.30	0.10	0.0	0.12	0.4-
$^{134}_{54}Xe_{80}$	2	1	3	0.93	-0.080	0.2	-0.80	0.0	0.0	0.0	0.12	0.4-

$$C_{0\pi} = C_{2\pi} = C_{4\pi} = 0.0$$

3.2.2 Energy Spectra

The calculated and experimental energy levels are shown in figures (3-9,10,11,12,13,14). The experimental data are taken from [117]. The IBM-2 parameters employed in the calculation are shown in table (3-8). Overall, the evaluation of the parameters follows a smooth trend, according to the gradual changes in nuclear structure of the isotopes.

The agreement between the theoretical and the experimental levels is, in general, good except for some cases in high spin states, we believe that is due to the change of the projection of the angular momentum which may be due to band crossing and change in angular momentum.

The calculated results show that $R_{4/2} > 2$ for all $^{124\text{-}134}Xe$ isotopes (see table (3-9)) and it means that their structure seems to be varying from gamma-soft rotor O(6) to along near-harmonic vibrator (HV) SU(5).

The energy levels of $^{124\text{-}126}Xe$ appear to form a pattern typical for O(6) symmetry (IBM-1 limits). Similarly to Refs [125,126], for each eigenstate with O(6) quantum number $\sigma = N$ a corresponding nuclear state can be found up to O(5) quantum number $\tau = 5$ and angular momentum $10\,\square$, while the 0_3^+ state seems to be the band-head of the excited O(6) family with $\sigma = N - 2$.

Using this approach, we have quantitatively show that, in $^{124,126}Xe$, the O(6) symmetry is completely dissolved while the O(5) symmetry is only slightly perturbed. It is therefore important the issue to be investigated further which requires more *E2* transition rates for high-lying off-yrast states of nuclei that are currently being viewed as close to the O(6) symmetry be measured and analyzed with the method we have proposed here.

The most basic structural signature of the E(5) symmetry is a value of the ratio $R_{4/2} = E(4_1^+)/E(2_1^+)$ of 2.20. This value is intermediate between the values for spherical nuclei (2.00) and gamma -soft rotor (2.50). However there are large number of nuclei in the mass region A~130 having the value for this ratio in the desired range. Thus, an interpretation based only on the $R_{4/2}$ can be ambiguous and additional signatures need to be considered. Often, the decay properties of the lowest excited 0^+ states are used as an additional signature of the E(5) structure.

In the case of $^{128\text{-}130\text{-}132}Xe$, the $R_{4/2}$ value 2.271, 2.270 and 2.163 respectively, (see table (3-9)) lies very close to the ideal value for the E(5) symmetry indicating that it lies more towards the SU(5) side.

A comparison of the key signatures for E(5) critical point symmetry is done for the *Xe* isotopes obtained from the present work with the calculated E(5) values and the values obtained as given in table (3-9). The values shown in the table, suggest that the $^{128\text{-}130\text{-}132}Xe$ isotopes has many evidences of lying near the E(5) critical point symmetry. The value of $E(0_3^+)/E(2_1^+)$ for ^{132}Xe is 3.73 lies very near to the ideal value 3.59; also the value for the ratio $E(0_3^+)/E(0_2^+)$ 1.33 shows good resemblance with the theoretical value for E(5) symmetry 1.18.

It has been observed that the positioning of the 0^+ states plays a crucial role in determining the behavior of the nucleus near the critical symmetry. This can be seen from the figures. These figures show the changes in positioning of the levels as the neutron number changes for *Xe* isotopes respectively. It is clear from the figures that the variation of the levels other than the 0_2^+ levels is smooth, where as there are abrupt changes in the positioning of these two levels.

Our data and our analysis have emphasized the significance of the ordering of the excited 0_3^+ and 0_2^+ configurations for assigning the structure of a nucleus near

the E(5) critical point. Therefore, it is interesting to examine the behavior of the observable $\Delta_{0+} = [E(O_2^+)-E(O_3^+)]/E(2_1^+)$. It takes the values -1 (harmonic vibrator), -0.56 (E(5)), 0 at the crossing point of the $O_{3,2}^+$ configurations and becomes positive towards the O(6) limit. Along the chain of *Xe* isotopes we consider the experimental energies of the first and the second excited 0^+ states with dominant O_3^+ or O_2^+ assignment. The assignments of their dominant character have been done for ^{124}Xe ([125,126]), ^{126}Xe ([127]), ^{128}Xe , ^{130}Xe [128], and this work, already in the literature. The $R_{4/2}$ ratios shown on top decrease monotonically as a function of neutron number from 2.48 for ^{124}Xe to 2.04 for ^{134}Xe. The value of 2.20 expected for E(5) is crossed between ^{130}Xe and ^{132}Xe. The 0^+ configurations cross between ^{128}Xe and ^{130}Xe . The Δ_{0+} value for ^{128}Xe is positive. This rules out ^{128}Xe as a candidate for a realization of E(5) symmetry. We observe, however, that $\Delta_{0+} = -0.42$ for ^{130}Xe making that nucleus a promising candidate for a close match of E(5) predictions.

In general, the ground bands are fitted very well, The fitting in the gamma bands are slightly worse but are still better than those for the beta bands. The fitting in beta bands are not so good as those in the ground bands and gamma bands. Also it is in the beta bands that IBM-2 show the most distinct improvements become smaller as we go to lighter isotopes. This suggest that the interactions between unlike bosons are relatively more important in system which are closer to the closed shells.

Table (3-9): Energy ratios for *124-134Xe* isotopes

Isotopes	$E(4_1^+)/E(2_1^+)$			$E(0_2^+)/E(2_1^+)$			$E(0_3^+)/E(2_1^+)$			$E(0_3^+)/E(0_2^+)$		
	E(5)	IBM-2	Exp.	E(5)	IBM-2	Exp.	E(5)	IBM-2	Exp.	E(5)	IBM-2	Exp.
$^{124}_{54}$ *Xe* $_{70}$	2.2	2.486	2.482	3.03	3.412	3.584	3.59	5.008	4.773	1.18	1.467	1.33
$^{126}_{54}$ *Xe* $_{72}$	2.2	2.484	2.424	3.03	2.670	3.378	3.59	4.853	4.530	1.18	1.817	1.340
$^{128}_{54}$ *Xe* $_{74}$	2.2	2.272	2.332	3.03	3.649	3.573	3.59	3.9233	4.238	1.18	1.075	1.185
$^{130}_{54}$ *Xe* $_{76}$	2.2	2.272	2.247	3.03	3.346	3.080	3.59	3.582	3.759	1.18	1.124	1.217
$^{132}_{54}$ *Xe* $_{78}$	2.2	2.163	2.157	3.03	2.696	2.796	3.59	3.471	3.372	1.18	1.340	1.33
$^{134}_{54}$ *Xe* $_{80}$	2.2	2.0523	2.043	3.03	–	1.931	3.59	–	–	1.18	–	–

[Experimental data are taken from ref.[65,100,117

Figure (3-9): Comparison between experimental and calculated energy levels for ^{124}Xe. The experimental data are taken from ref. [117].

Figure (3-10): Comparison between experimental and calculated energy levels for ^{126}Xe. The experimental data are taken from ref. [117].

Figure (3-11): Comparison between experimental and calculated energy levels for ^{128}Xe. The experimental data are taken from ref. [117].

Figure (3-12): Comparison between experimental and calculated energy levels for ^{130}Xe. The experimental data are taken from ref. [117].

Figure (3-13): Comparison between experimental and calculated energy levels for ¹³²Xe. The experimental data are taken from ref. [117].

Figure (3-14): Comparison between experimental and calculated energy levels for ^{134}Xe. The experimental data are taken from ref. [117].

3.2.3 Electric Transition Probability

The effective boson charges e_π and e_ν were calculated by plotting [118] M_1 and M_2 which are given in eq. (3-2,3) against N_ν / N_π (see figure (3-16)) . The two effective charges are taken to be $e_\pi = 0.13435 \ eb$ and $e_\nu = 0.1379 \ eb$. The results of the calculations are presented in table (3-10). Looking through the table, one can easily recognize that our calculations reproduce the experimental data quite well.

The $B(E2;2_1^+ \rightarrow 0_1^+)$ and $B(E2;4_1^+ \rightarrow 2_1^+)$ values decreased as neutron number increases toward the middle of the shell as the value of $B(E2;2_2^+ \rightarrow 2_1^+)$ has small value because contains admixture of M1. As a consequence of possible M1 admixture, this quantity is rather difficult to measure. The value of $B(E2;2_2^+ \rightarrow 0_1^+)$ is small because this transition from quasi-beta band to ground state band (cross over transition).

In table (3-10) the B(E2)'s we obtained between ground state band agree almost perfectly with experiment. The agreement of the IBM-2 B(E2)'s with experiment, for transitions from beta and gamma bands states to the ground band states are also rather good, though no as good as they are for transitions within the ground band states.

The $^{128-130-132}$Xe isotopes has many evidences of lying near the E(5) critical point symmetry, the theoretical and experimental signatures are listed below [75]:

1- $B(E2;4_1^+ \rightarrow 2_1^+)$ value should be approximately 1.5 times the $B(E2;2_1^+ \rightarrow 0_1^+)$ value.

2- There should be excited 0_2^+ states lying at approximately 3–4 times the energy of the 2_1^+ state.

3-The decay of the 0_2^+ should reflect its multiphonon structure. There is an allowed E2 transition to the 2_2^+ level, but no allowed transition to the 2_1^+ level.

4- The decay of the 0_3^+ state should also be characteristic of E(5). There is an allowed transition to the 2_1^+ level with strength of approximately 0.5 the $B(E2;2_1^+ \rightarrow 0_1^+)$ value.

What one finds, therefore, is the $0^+ - 2^+ - 2^+$ sequence characteristic of an O(6)→SU(5) nuclei identified several times in Xe isotopes. The agreement between the IBM-2 calculations and experimental transition probabilities is remarkable. For

the levels of in figures (3-9,10,11,12,13,14) all transitions which are calculated to be intense are the strongest observed, all forbidden transitions are weak or unobserved, but usually <<10 percent of the strongest transition.

$_{(e^2b^2)}$, $M_{2(e^2b^2)}M_1$
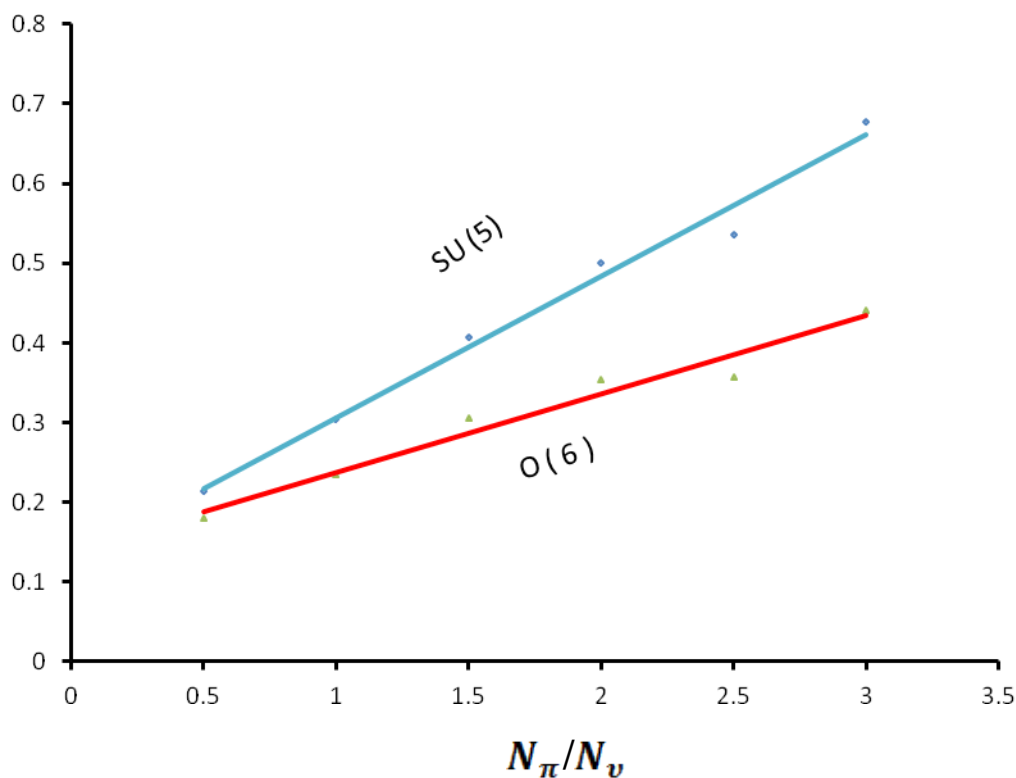
Figure (3-15): The plot of the quantity M_1 and M_2 versus $e_\pi + e_\nu N_\nu / N_\pi$ for $^{124\text{-}134}Xe$ Isotopes.

جدول

3.2.4-Magnetic Transition Probability

We also investigated M1 transition rates and the magnetic moment of the first excited 2^+ state, using the boson M1 operator which is given in Eq.(2- 52),

indicating that the M1 transition properties are exclusively determined by the gyromagnetic factors g_π and g_ν. The boson gyromagnetic factors were estimated using the fact that $g = Z/A$ and the relation (3-4). Taking the number of bosons for ^{126}Xe as $N_\pi = 2$ and $N_\nu = 5$, and experimental value $B(M1;2^+_2 \rightarrow 2^+_1) = 4.35 \times 10^{-4} \mu_N^2$ [65], we obtained $0.428 = 0.285\,g_\pi + 0.714\,g_\nu$, which places limits on the gyromagnetic factors. We used the value $g_\pi = 0.810\,\mu_N$ and $g_\nu = 0.342\,\mu_N$ in equation (2-49) to calculate the M1 matrix elements.

The resulting IBM-2 calculation for B(M1), together with experimental values are shown in table (3-11). The results for the transitions feature for gamma band to ground band are claimed to have a collective origin. Several trends are apparent from the data in table (3-11): (**i**) the magnitude of the M1 matrix elements increased with spin both gamma band to ground band transitions, in agreement with spin dependence. (**ii**) the size of gamma band to ground band matrix element seems to decrease with increasing mass number. (**iii**) The gamma-beta band M1 transitions are larger than gamma band to beta band transition by a factor of 2 to 3.

These three aspects of M1 data shown in table (3-11) are reproduced by the calculation through a smooth variation of the parameters ε and χ with a few exceptions good agreement between the theory and experimental data is achieved.

Magnetic dipole moment for first excited state is given in table (3-11), it has been shown that data on $\mu(2^+_1)$ in $^{124-134}Xe$ isotopes provide a sensitive test of the effective proton boson number in the IBM-2 framework, in $^{124-134}Xe$ isotopes, conform the validity of assuming a drastic change in N_ν when the number of neutron increased.

جدول

3.2.5-Mixing Ratio $\delta(E2/M1)$

We evaluate the mixing ratio $\delta(E2/M1)$ for $^{124\text{-}134}Xe$ isotopes, depends on the equation (2-55). The resulting of IBM-2 calculation for $\delta(E2/M1)$ together with experimental values are shown in table (3-12).

The results for the $\gamma \rightarrow g$ and $\gamma \rightarrow \gamma$ mixing ratios , the sign of the mixing ratios is not arbitrary . For large majority of the $\gamma \rightarrow g$ transitions considered in table (3-12) to the experimentally known δs are negative ; the sign are not known for $\gamma \rightarrow \gamma$. According we have assumed that all $\delta(\gamma \rightarrow g)$ values are negative and used it as a constraint on the parameters χ_ν and χ_π. Specially, it implies that $\chi_\nu - \chi_\pi > 0$.

The experimental $\gamma \rightarrow g$ M1 transition probability in table (3-11) have been obtained by recourse to the IBM-2: the $\delta(E2/M1)$ mixing ratios from the complication of Lang *et al*., [100] from this work are combined with the $B(E2; 2_3^+ \rightarrow 0_1^+)$ values and the conventional band mixing parameters. Note that in a few cases the asymmetric errors on the measured mixing ratio values have been incorporated in the M1 matrix elements by shifting the central value slightly to ensure that the overall error range denoted is correct .

For $\gamma \rightarrow \gamma$ transitions the intraband B(E2) values have been estimated by assuming that the intrinsic E2 matrix elements in the ground and gamma bands are equal. Then combining these B(E2) values with the E2/M1 mixing ratios to the tabulated M1 transitions shown in table (3-11). We note that in the IBM-2 the intrinsic E2 matrix element of the gamma band is smaller than that of the ground band due to the finite-dimensionality of the boson space.

جدول

3.2.6-Electric Monopole Matrix Element $\rho(E0)$

      Monopole transitions are known to be pure penetration effect where the transition is caused by an electromagnetic interaction between the nuclear charge and atomic electrons penetrating the nucleus. E0 transition could to pure for $\Delta J = J_i - J_f = 0 \Rightarrow J_i = J_f = 0$, when J is the total angular momentum of the nuclear state.

69

Monopole matrix element is not easy to measure so in order to get information about the nuclear structure, one can measure B(E2) and the state X(E2/E0), then could be calculated which is found for SU(5) nuclei very small. The $E0$ reduced transition probability is given in equation (2-60). The parameters in equation (2-60) can be predicted from the isotope shift [117] (see table (3-13)), since such data are not available for *Xe* isotopes, we calculate these parameters by fitting procedure into two experimental values of isomeric shifts (equation (2-63)). The parameters which were subsequently used to evaluate the $\rho(E0)$ -values were; $\beta_{0\pi} = 0.063$ *eb* , $\beta_{0v} = 0.235$ *eb* and γ_{0v}=0.032 fm². From the table (3-13), in general there is no experimental data to be compared with the IBM-2 calculations.

Table (3-13): The Monopole matrix element ρ(E0) for $^{124-134}Xe$ isotopes

$J_i^+ \rightarrow J_f^+$	^{124}Xe	^{126}Xe	^{128}Xe	^{130}Xe	^{132}Xe	^{134}Xe
$0_2 \rightarrow 0_1$	-10.3x10⁻³	-0.432x10⁻³	2.25x10⁻³	2.631x10⁻³	2.744x10⁻³	2.871x10⁻³
$0_3 \rightarrow 0_1$	0.743x10⁻³	1.240x10⁻³	4.220x10⁻³	3.981x10⁻³	4.761x10⁻³	4.992x10⁻³
$0_3 \rightarrow 0_2$	0.872x10⁻³	-0.543x10⁻³	6.155x10⁻³	6.213x10⁻³	12.2x10⁻³	12.624x10⁻³
$2_2 \rightarrow 2_1$	-0.876x10⁻³	0.439x10⁻³	3.987x10⁻³	9.431x10⁻³	11.43x10⁻³	13.289x10⁻³

As pointed out previously [128], a large $X(E0/E2)$ value is not necessarily a signature of a β-vibrational state. For instance our calculated $X(E0/E2)$ value for $2_2^+ \rightarrow 2_1^+$ transition. However, it be kept in mind that a large results from the vanishing B(E2) values, specially in the case of higher bands whose structure may be quite different from that of the lower bands. Because of the possibility of accidental cancellations in the calculation of a sum of terms with different signs, only the correct order of magnitude can be expected from present calculation of a large number of states and matrix element.

In the present $X(E0/E2)$ branching ratios are used to extract the $B(E2;0_2^+ \rightarrow 0_1^+)$ and $\rho^2(0_2^+ \rightarrow 0_1^+)$ values associated with 0_2^+ states. Our results are shown in table (3-14). In to complete the monopole values of $^{124-134}Xe$ isotopes, the measurements of E0 matrix elements of excited 0_3^+ states in these isotopes are in progress. The ratio of the reduced transition probabilities, $X = B(E0;0_2^+ \rightarrow 0_1^+)/B(E2;0_2^+ \rightarrow 0_1^+)$ is in the range from 0.000125 to 0.034 which is close to transitional rotor value. However, the assumed two-phonon 0_2^+ state is strongly pushed to high in energy, which is explained as being due to gamma-soft.

The most conspicuous features of the 0_3^+ states in $^{124-134}Xe$ is strongly enhanced *E2* decay to the 0_1^+ state. This may be connected with intriguing question of the possible deformation of the excited 0^+ state: the large $B(E2)$ values could alternatively be interoperated to imply a vibrational structure associated e.g., with mixed bands.

Table (3-14) : The branching ratio X(E0/E2) for $^{124-134}Xe$ isotopes

$J_i^+ \rightarrow J_f^+$	^{124}Xe	^{126}Xe	^{128}Xe	^{130}Xe	^{132}Xe	^{134}Xe
$0_2 \rightarrow 0_1$	3.4×10^{-2}	2.45×10^{-2}	2.81×10^{-2}	8.33×10^{-4}	1.25×10^{-4}	1.77×10^{-4}
$0_3 \rightarrow 0_1$	8.77×10^{-4}	5.05×10^{-2}	4.31×10^{-3}	8.96×10^{-3}	5.35×10^{-4}	5.35×10^{-4}
$0_3 \rightarrow 0_2$	1.86×10^{-3}	2.83×10^{-2}	1.94×10^{-2}	1.53×10^{-3}	1.4×10^{-4}	1.38×10^{-4}
$2_2 \rightarrow 2_1$	2.45×10^{-4}	9.5×10^{-3}	1.17×10^{-4}	4.6×10^{-5}	1.23×10^{-3}	1.1×10^{-4}

The isomeric shift, which is the difference between the mean square radius $\delta \langle r^2 \rangle$ of an excited state and the ground state in a given nucleus [102]. In table (3-15), we compared the calculated isotopic shifts with experimental data. [117].

Table (3-15) : The isomer shifts δ<r²> fm² for $^{124-134}Xe$ isotopes

isotopes	^{124}Xe	^{126}Xe	^{128}Xe	^{130}Xe	^{132}Xe	^{134}Xe
Exp.[117]	-0.25	-0.22	-0.20	-0.15	-0.10	–
IBM-2	-0.23	-0.19	-0.18	-0.13	-0.11	-0.8

Mixed Symmetry States-3.2.7

The existence of the mixed symmetry states is recognized as a manifestation of a new nuclear mode consisting of oscillations of the angle between symmetry axes of the deformed valance neutron and valance proton. The occurrence of the mixed symmetry state in even-even nuclei is a well established fact [130], and they lie usually high in energy. In even-even nuclei, the identification is based on the measurement of $M1$ and $E2$ transitions to symmetry states, and strong from these states, weakly collective E2 transitions to symmetric states, and strong $M1$ transitions can take place via the bosons.

At this point, the following issue arises: Does the fundamental isovector quadrupole collective mode (2_{Ms}) fragment along the path from vibrational nuclei towards γ-unstable rotors in such a way that associated strength gradually escapes detection or does it slowly dissolve and finally completely disappear in $^{124,126}Xe$? Both hypotheses could explain the observed experimental behavior. In the first case, it is possible we only observe the lowest fragment of the MSS, which does not necessarily carry the largest part of the total $M1$ strength, because the experimental technique we used was limited to a certain excitation energy. In the second case, the states with mixed-symmetry character at the $U(5)$ limit gradually lose their isovector character toward mid-shell and the $M1$ strength finally disappears. This scenario would require an yet as unknown mechanism. The former case can be discussed in the framework of a simple two-state mixing model.

According to the two-state mixing scheme outlined in Refs. [90,143], the observed 2_1^+ and 2_M^+ states arise through the mixing of the unperturbed proton and neutron 2^+ configurations (their energies are labeled here as ε_π and ε_ν, respectively) in which the proton-neutron coupling matrix element increases as a function of the product $N_\pi N_\nu$.

In the figures (3-9,10,11,12,13,14) we show the mixed symmetry states $J_i^\pi = 1_M^+$ and 2_M^+. These results are obtained with a Majorona force $\xi_1 = \xi_3 = 0.12$ MeV and $\xi_2 = -0.4$ MeV, which was determined so as to obtain the mixed symmetry $J_i^\pi = 1^+, 2^+$ levels with a pronounced mixed proton-neutron symmetric wavefunction. In the ^{124}Xe there is no mixed symmetry states below 2.3 MeV and in the ^{126}Xe no mixed symmetry state below 2.1 MeV. The levels $J_i^\pi = 1_M^+$ and 2_M^+ in $^{128\text{-}134}$Xe isotopes are close in excitation energy ($\Delta E \sim 150$ MeV). In the table (3-16) the energy and the magnetic transition probability from the mixed symmetry state 2_M^+ to 2_1^+ in $^{124\text{-}134}Xe$ isotopes

Table (3-16): Energy levels and $B(M1; 2_M^+ \rightarrow 2_1^+)$ for $^{128\text{-}134}Xe$

isotopes	MSS	Energy		$B(M1; 2_M^+ \rightarrow 2_1^+)$	
		Exp. (MeV)	IBM-2 (MeV)	Exp. (μ_N^2)	IBM-2 (μ_N^2)
^{128} Xe	2_4^+	2.127	2.276	0.042(12)	0.033
^{130} Xe	2_4^+	2.150	3.141	0.15(4)	0.20
^{132} Xe	2_3^+	1.986	1.896	0.020(6)	0.033
^{134} Xe	2_3^+	2.262	2.577	0.020(5)	0.056

In summary, low lying excited states of ^{130,132}Xe have been investigated with IBM-2. The 2_M^+ levels have been identified. This allowed us to trace its evolution along the Xe isotopic chain from close to the $N = 82$ neutron shell closure out towards mid- shell. We observe the energy of the 2_M^+ state increases and the $2_M^+ \rightarrow 2_1^+$ $M1$ strength decreases as the number of valence neutron hole pairs (N_v) increases. The decrease and disappearance of the $M1$ strength can be explained by two different mechanisms: either the 2_M^+ state fragments on the path from vibrators to γ-unstable rotors or the 2_M^+ state loses slowly its isovector character and finally completely disappears towards mid-shell. It remains to be determined by future measurements searching for higher-lying $M1$ transitions in these Xe isotopes which of the two mechanisms is responsible for our observations. We have discussed the former case by using a two-state mixing scheme, which suggests fragments of the 2_M^+ state may exist at energies higher than 2.5 MeV in ^{124,126,128,130,132}Xe. This fragmentation is also supported by the upper limit of the 2^+ state at 2.718 MeV in ^{128}Xe. Thus we also call for the measurement of the multipole mixing ratio of the 2.275 MeV γ-transition in the nucleus ^{128}Xe.

Chapter Two
Nuclear Collective Models

2.1 Collective Models - General nuclear deformation

The collective model starts essentially with the idea that in order to explain the extremely large static electric quadrupole moments of nuclei lying between closed shell some co-operative motion of nuclear matter, resulting in a permanent nuclear deformation, is necessary. It is supposed that this deformation (which vanishes for closed-shell nuclei), is produced by a polarizing effect of the individual or intrinsic motion of the nucleons outside closed shells. It is vital to the detailed development of the collective model that it should be possible to envisage a clear separation between the individual motion of the loose nucleons and the collective motion of the core. This means that the single-particle energies associated with the shell-model states of the nucleons should be large compared with the rotational and vibrational energies of the core. It is then possible, by allowing some interaction between the two types of motion, to present a unified picture of nuclear motion in which both shell-model and collective features appear. This approach is a combination of the individual particle type of model with the strong interaction type; it not only explains the large quadrupole moments but also predicts a fine structure of the nuclear level spectrum owing to energies associated with the vibrational and rotational motion of the core.

The most simplified model of the description of the nucleus would consider that the distribution of nucleons is homogeneous and has no preferred direction in space. The nucleus is then spherical. However, in order to minimize its potential energy, the shape of the nucleus can deviate from its spherical shape and find a "new" equilibrium with a deformed shape. For the magic numbers (8, 20, 28, 50, 82, 126), the shape of a nucleus is in general spherical. Between these numbers most nuclei are deformed. The electrical potential V created by the distribution of charges in the nucleus at a distance R from the origin O can be expanded in multipoles [65]:

$$V(R) \propto \frac{1}{R} \int \rho(r) dr + \frac{1}{R^2} \int z\rho(r) dr + \frac{1}{R^3} \int \left(3z^2 - r^2\right)\rho(r) dr \dots\dots\dots ..(2-1)$$

where r denotes the distance from one point in the nucleus to the origin of the axis O and $\rho(r)$ is the charge density. The first term corresponds to the total charge of the nucleus. The second and third terms are the dipole and quadrupole terms respectively. Most of the nuclei are ellipsoidal and therefore have an axial symmetry. In this case the dipole term is zero which leaves the deformed nucleus as a quadrupole distortion only. There can also be octupole and hexadecapole shapes. The shape of the nucleus can then be parametrized from a spherical shape corrected by the spherical harmonics $Y_{\lambda\mu}$ [65]:

$$R(\theta, \Phi) = R_0 \left[1 + \sum_{\lambda=0} \sum_{\mu=-\lambda}^{\lambda} \alpha_{\lambda\mu} Y_{\lambda\mu}(\theta, \Phi) \right] \dots\dots \dots\dots.(2-2)$$

where R_0 is the radius of a sphere of the same volume. The term $\lambda = 0$ describes volume variations, $\lambda = 1$ the translation of the system. The term with $\lambda = 2$ corresponds to quadrupole deformation and $\lambda = 3$ to octupole deformation. Using the transformation from the laboratory frame to the intrinsic frame, the five $\alpha_{\lambda=2,\mu}$ parameters are reduced

to three real parameters $\alpha_{2,0}$, $\alpha_{2,2} = \alpha_{2,-2}$ and $\alpha_{2,1} = \alpha_{2,-1} = 0$. These variables can be parametrized following the conventions of Hill and Wheeler [94]:

$$\alpha_{2,0} = \beta \cos \gamma \dots \dots \dots \dots ..(2-3)$$

$$\alpha_{2,2} = \alpha_{2,-2} = \frac{1}{\sqrt{2}} \beta \sin \gamma \dots \dots \dots ..(2-4)$$

where β represents the extent of the quadrupole deformation, while γ gives the degree of axial asymmetry. Most nuclei are axially symmetric, or close to it, at least in their ground states. For an axially symmetric nucleus, the potential has a minimum at $\gamma = 0°$. A common convention (Lund convention) for the ranges of the β and γ variables is that $\beta > 0$, $\gamma = 0°$ for an axially symmetric prolate nucleus and that $\beta > 0$, $\gamma = 60°$ gives an axially symmetric oblate nucleus as it is shown in figure (2-1). Note that for $\beta < 0$, $\gamma = 0°$, the nucleus is oblate. If γ is not a multiple of $60°$, one says that the nucleus is triaxial.
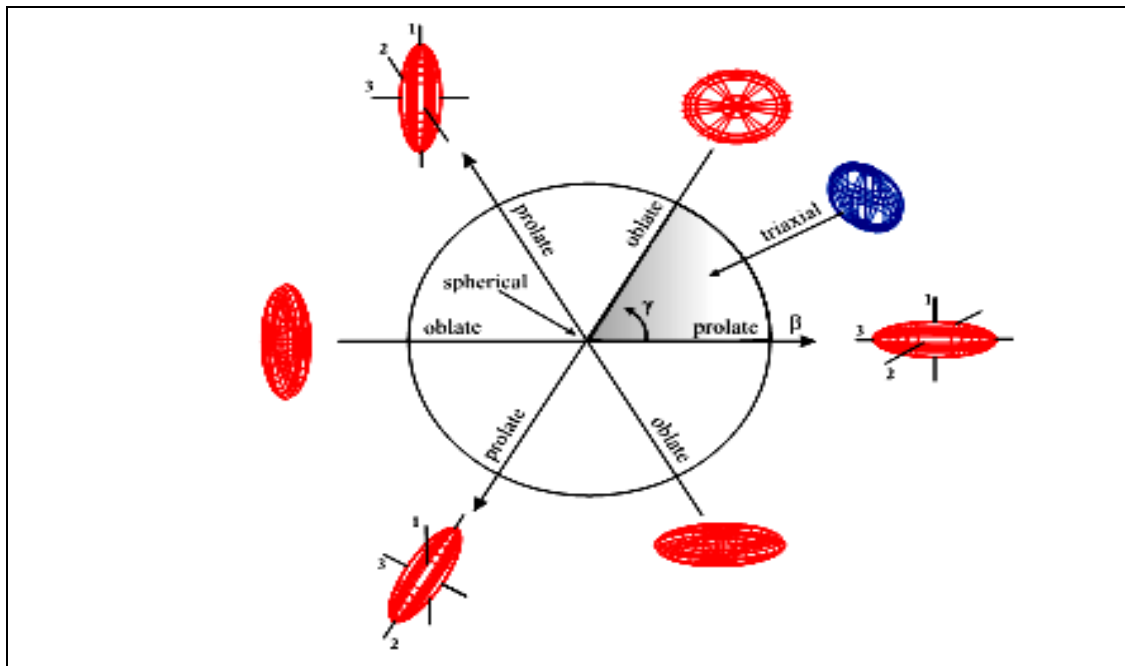
Figure (2-1): Nuclear deformation in the (β,γ) plane. The Lund conventions are used . The four cases $(\gamma=120°,180°, 240°, 300°)$ correspond to the cases with $\gamma=0°$ and $60°$ but with different orientations of their axis. The area $0°<\gamma<60°$ (in grey) is then sufficient to describe the nuclear deformation.[65].

2.2 The Vibrational Model (VM)

Nuclei with relatively few particle outside closed shells have spherical equilibrium form , and the collective motion takes the form of an oscillation of the loose particle about the spherical surface .In this type of motion the nucleus possesses a certain number of vibrational quanta or phonons of energy $\hbar\omega$ and angular momentum $\hbar l$ in accordance with the quantum mechanical picture of the harmonic oscillator. Since there is no stable deformation for these nuclei the static motion is not in enhanced , as in the case of nuclei far from closed shell .

The simplest vibrational spectra are found for even– even nuclei in which there is no contribution to the nuclear spin from the intrinsic motion. The basic vibrational spectrum is due to quadrupole phonons and is given in the figure (2.2),

together with permitted spin values ; in practice the degeneracy between the different levels is resolved and the expectation is a 0^+ ground state, a 2^+ first excited state (single phonon) and then a triplet of states 0^+ 2^+ 4^+ formed by coupling two phonons. Classically an octupole phonon has about the same energy as two quadrupole phonons and this may produce a 3^- state near to the triplet . The energies of these states vary regularly according to the distance of the nucleus concerned from closed shell. The

vibration of permanently deformed nuclei include oscillations of the parameter β and

of a further parameter γ which determines the relative deformation of the three axes of

the ellipsoid. The β – vibrations preserve an axis of symmetry, but γ vibrations do

not . Rotational bands may be built upon each vibrational state.

Vibrations are one example of the collective behavior of the nucleons. In the vibrational model, the $\lambda = 2$ excitation (Eq. (2-2)) is seen as a one phonon excitation (or quadrupole phonon) carrying two units of angular momentum (units $\hbar$). In even-even nuclei, adding a quadrupole phonon to the 0^+ ground state leads to the first excited 2_1^+ state. A two-phonon coupling results in three states with angular momenta: 0^+, 2^+, 4^+ while a three phonon excitation results in a quintuplet of states with angular momenta: 0^+, 2^+, 3^+, 4^+, 6^+. This is shown in figure (2-2). The pure harmonic vibrational model predicts that the two-phonon triplet states lies at twice the energy of the 2_1^+ state while the three-phonon quintuplet states at three times the energy of the 2_1^+ state. Consequently, one fingerprint of the vibrational model is the energy ratio $R_{4/2} = E(4_1^+)/E(2_1^+) = 2.0$. In realistic situations this ratio is typically 2-2.5. Such nuclei often called "vibrators" are situated near closed shells (or magic nuclei 8, 20, 28, 50, 82, 126). In the IBM framework, they correspond to the $U(5)$ dynamical symmetry.
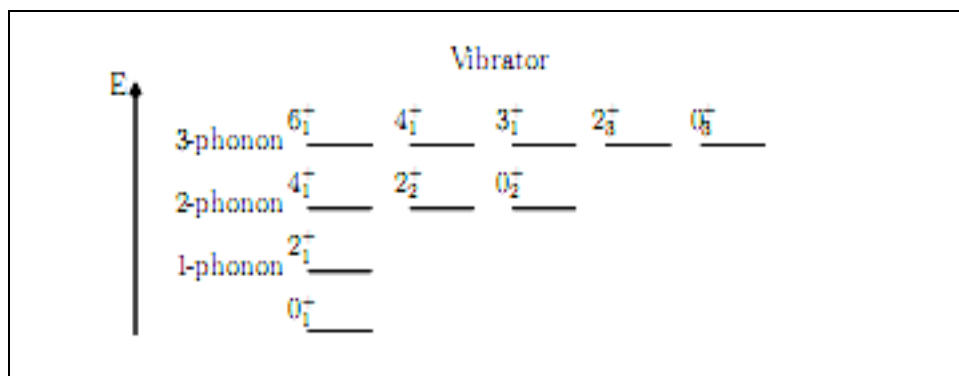
Figure (2-2): Low-lying levels in the pure harmonic vibrational model in even-even nuclei. .[65].

2.3 The Rotational Model (RM)

A more nucleons are added outside the closed shell, the deformation of the nucleus increases and eventually it gets permantly deformed. This implies a stability of orientation, and such a nucleus in space can be described by a set of angles. The rotational spectrum is characterized by:
(i) same parity for levels .
(ii) increase in angular momentum by $2\hbar$.
(iii) spacing between adjacent levels increases with increasing spin.

In the discussion above we had assumed a nucleus without any intrinsic angular momentum. In any text book of quantum mechanics it is shown that a particle with spin $J < 1$ cannot have an observable quadrupole moment. However, in the figure (2-1) we have taken a nucleus without any spin, and have shown a permanent deformation resulting into a quadrupole moment. This contradiction can be removed by noting that a nucleus can have an intrinsic quadrupole moment due to the permanent deformation, which gives rise to the rotational spectrum. However, the observable quadrupole moment is zero since for spineless nucleus we cannot talk about any particular (preferred) axis and so the quadrupole moment is averaged over all directions resulting into a zero value.

Another collective approach is to view the nucleus as an axially symmetric rigid rotating system along an axis perpendicular to the symmetry axis. Rotational motion can be observed only in nuclei with non-spherical equilibrium shapes. These nuclei are often called *deformed* nuclei. The rotational energy of such a rotating system with total angular momentum $\vec{J}$ is given by:

$$E_{rot}(J) = \frac{\hbar^2}{2I} J(J+1)\text{.........}\quad\text{...........}\quad\text{.......}(\ 2-5)$$

where I is the moment of inertia (here for a rigid object) and only even J are allowed in the ground state band. Increasing the quantum number J corresponds to adding rotational energy to the nucleus, and the nuclear states form a sequence known as a *rotational band*. Considering the low-lying excitation spectrum in even-even nuclei, the low lying rotational energy levels are labeled by $J^{\pi}=0^+, 2^+, 4^+, 6^+,...$ and $E(2_1^+) = 6\hbar^2/2I, E(4_1^+) = 20\hbar^2/2I,...$. The structure of a rotational band is shown in   figure(2-3). An important result here is the signature for rotational behavior with $R_{4/2} = E(4_1^+)/E(2_1^+) = 3.33$. Such nuclei are often called "rotors" and they are found in the mass ranges $150 < A < 190$ and $A > 220$ (rare earths and actinides). In the IBM framework, they correspond to the $SU(3)$ dynamical symmetry.
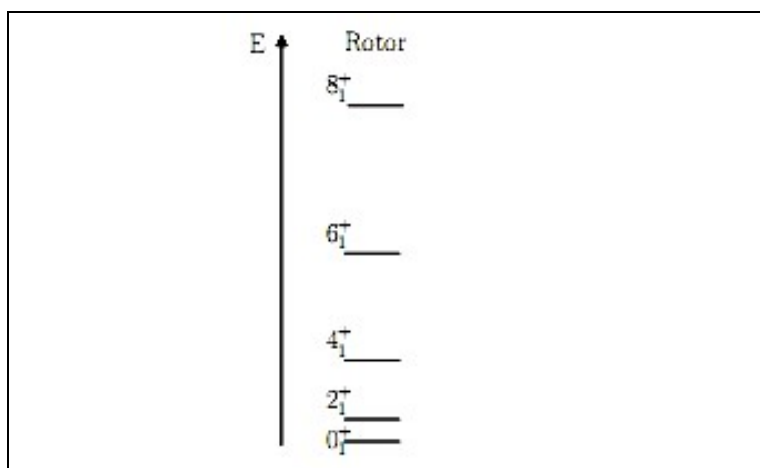
Figure (2-3): Low-lying levels in the rotational model in even-even nuclei. .[65].

2.4 The Interacting Boson Model

The Interacting Boson Model (IBM) is a model for describing collective excitations in atomic nuclei. It has been introduced by Iachello and Arima in 1975 [15] and has been used to model a wide variety of nuclear properties and phenomena. One of the advantages of the model is its use of the symmetries of the boson operators introduced in the model, which allows for analytic expressions of the states and expectation values for three different ideal limits of nuclei. In this chapter a brief introduction and some background to the model will be presented. Most of the presentation of this chapter follows the book of Iachello and Arima [36].

2.4.1 Interacting Boson Model-1 (IBM-1)

In this section, the Interacting Boson Model-1 (IBM-1) will be introduced. Although the IBM-1 is not used explicitly in the analysis or direct interpretation of the present work, it is helpful to use it to formulate the basic ideas and expressions in the IBM and then extend it to the Interacting Boson Model-2 (IBM-2). In the IBM-1, the number of bosons is given by the number of pairs of protons and pairs of neutrons outside of closed shells. No distinction is made between proton type and neutron type bosons.

The basic foundation of the Interacting Boson Model is that collective excitations can be described with bosons. These bosons can be of two types, *s* and *d* having and angular momentum of either $L = 0$ or $L = 2$ units of $\Box$, respectively. Both bosons have positive parity. The number of bosons is determined by the number of nucleon pairs or hole pairs that are outside of a closed shell. The reason for this comes from the interpretation of the bosons as correlated nucleon pairs. The total number of bosons *N* in the IBM is a conserved quantity. In the IBM-1, the nucleon or hole pairs must be the same type of nucleon, meaning pairs consisting of a proton and neutron are not included. The IBM-1 is applicable only to even-even nuclei.

The nuclear states are represented in the framework of second quantization. The boson creation operators are given by $s^{\dagger}$ and d^{+}_{μ} and the boson annihilation operators by *s* and d_{μ}, where $\mu=-2,-1,0,1,2$. They satisfy the following commutation relations:

$$[s, s] = [s^{\dagger}, s^{\dagger}] = 0,$$
$$[s, d_{\mu}] = [s^{\dagger}, d] = [s, d^{\dagger}] = [s^{\dagger}, d^{\dagger}] = 0,$$
$$[d_{\mu}, d_{\mu'}] = [d^{\dagger}_{\mu}, d^{\dagger}_{\mu'}] = 0,$$
$$[d_{\mu}, d^{\dagger}_{\mu'}] = \delta_{\mu\mu'} \text{........(2-6)}$$

Since nuclear states studied in the laboratory almost always have a definite angular momentum, which results from the Hamiltonian being rotationally invariant, it is useful to use spherical tensors. These tensors transform as irreducible representations of the rotation group. The boson creation operators transform as a spherical tensors while the spherical tensor for the annihilation operator needs to be defined as

$$b_{\tilde{l}m} = (-1)^{l+m} b_{l,-m} \cdots\cdots \cdots(2-7)$$

Two spherical tensors operators can be coupled as

$$T_m^{(l)} = \left[T^{(l_1)} \times T^{(l_2)} \right]_m^{(l)} \ldots\ldots\ldots\ldots(2-8)$$

to form a new spherical tensor operator, where the product is defined as

$$T_M^{(l)} = \left[T^{(l_1)} \times T^{(l_2)} \right]_m^{(l)} = \sum_{m_1,m_2} \langle l_1 m_1 l_2 m_2 | lm \rangle T_{m_1}^{(l_1)} T_{m_2}^{(l_2)} \ldots\ldots(2-9)$$

where the symbol represents the $\sum_{m_1,m_2} \langle l_1 m_1 l_2 m_2 | lm \rangle$ Clebsch-Gordan coefficients.

For example, to form a state with two bosons one would express it as

$$\left[b_{l,m}^+ \times b_{l',m'}^+ \right]_M^{(L)} | 0 \rangle \ldots\ldots\ldots\ldots(2-10)$$

where *L* and *M* are the angular momentum and magnetic quantum number of the state, respectively, whose values are restricted by the angular momentum addition rules.

Operators in the IBM are constructed from the creation and annihilation operators. Since the total number of bosons is conserved, all the terms in an operator have the same number of creation and annihilation operators with the exception of pair transfer operators.

The Hamiltonian operator is given by the expression:

$$H = E_0 + \sum_{\alpha,\beta} \varepsilon_{\alpha\beta} b_\alpha^+ b_\beta^+ + \sum_{\alpha,\beta,\delta,\gamma} \frac{1}{2} u_{\alpha\beta\delta\gamma} b_\alpha^+ b_\beta^+ b_\delta b_\gamma \ldots\ldots (2-11)$$

One can then see that the Hamiltonian is invariant under rotations. Since the Hamiltonian must be a scalar and Hermitian operator, it can be limited to the following form:

$$H = \varepsilon_s s^+ s + \varepsilon_d \sum_m d^+ \tilde{d}_m + \sum_{J=0,2,4} \frac{1}{2}(2J+1)^{1/2} c_J \left[(d^+ d)^{(J)} \left(\tilde{d}\tilde{d} \right)^{(J)} \right]^{(0)}$$

$$+v_2 \left[(d^+ d^+)^{(2)} \left(\tilde{d}\tilde{s} \right)^{(2)} + (s^+ d^+)^{(2)} \left(\tilde{d}\tilde{d} \right)^{(2)} + \left(\frac{1}{2} \right)^{1/2} v_0 \left[(d^+ d^+)^{(0)} \left(\tilde{s}\tilde{s} \right)^{(0)} + (s^+ s^+)^{(0)} \left(\tilde{d}\tilde{d} \right)^{(0)} \right]^{(0)} \right]$$

$$+u_2 \left[(d^+ d^+)^{(2)} \left(\tilde{d}\tilde{s} \right)^{(2)} \right]^{(0)} + \left(\frac{1}{2} \right) u_0 \left[(s^+ s^+)^{(0)} \left(\tilde{s}\tilde{s} \right)^{(0)} \right]^{(0)} \ldots\ldots\ldots(2-12)$$

where $s^+(s)$ is the creation (annihilation) operator for s-boson, $d^+(\tilde{d})$ is the creation (annihilation) operator for *d*-boson, and the parentheses denote angular momentum couplings. The parameters c_J, v_J, u_J, are related to the two-body matrix element by [27] :

$$c_J = \langle d^2 J | V | d^2 J \rangle$$

$$v_2 = \langle ds\, 2 | V | d^2\, 2 \rangle [5/2]^{\frac{1}{2}}$$

$$v_0 = \langle d^2\, 0 | V | s^2\, 0 \rangle (1/2)^{1/2} \qquad \dots\dots\dots\dots(2\text{-}13)$$

$$u_2 = \langle ds\, 2 | V | ds\, 2 \rangle (5)^{\frac{1}{2}}$$

$$u_0 = \langle s^2\, 0 | V | s^2\, 0 \rangle$$

        Another useful way to express the Hamiltonian that is used in many practical applications of the IBM-1 is by using the multipole expansion:
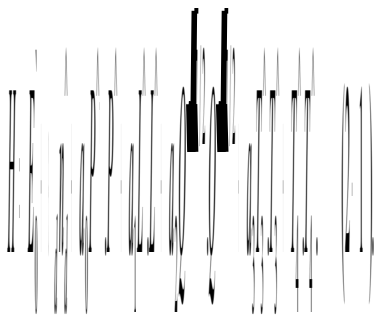
where the multipole operators are given by:

$$\hat{n_d} = d^\dagger . \tilde{d}$$

$$\hat{P} = \frac{1}{2}(\tilde{d}.\tilde{d} - \tilde{s}.\tilde{s})$$

$$\hat{L} = \sqrt{1}\left[d^\dagger \times \tilde{d} \right]^{(1)}$$

$$\hat{Q} = \left[d^\dagger \times \tilde{s} + s^\dagger \times \tilde{d} \right]^{(2)} - \frac{\sqrt{7}}{2}\left[d^\dagger \times \tilde{d} \right]^{(2)}$$

$$\hat{T_3} = \left[d^\dagger \times \tilde{d} \right]^{(3)}$$

$$\hat{T_4} = \left[d^\dagger \times \tilde{d} \right]^{(4)} \qquad\dots\dots\dots\dots\dots(2\text{-}15)$$

With such a Hamiltonian, one is able to see more easily what the effect each multipole degree of freedom has on the nuclear states and determine which ones are the most important for a given set of nuclei.

        Once the IBM-1 Hamiltonian is chosen, a basis of states needs to be chosen

to find the corresponding energy eigenvalues and eigenstates. A basis may be constructed from states created by applying the boson creation operators to the vacuum state. This basis is represented as

$$B: b_\alpha^+ b_\beta^+ |0\rangle \text{.......... ....} (\; 2-16)$$

To have states with definite angular momentum, the appropriate tensor product of boson creation operators can be used to give the set

$$B: \left[b_\alpha^+ \times b_\beta^+ \times ...\right]_m^{(l)} |0\rangle \text{.......... ....} (\; 2-17)$$

It turns out that the angular momentum and magnetic quantum numbers are not sufficient to label all the states of a basis. Additional quantum numbers are needed to uniquely label the states. These additional quantum numbers can be found from the representations of a _Lie_ algebra and its subalgebras that are formed from the bilinear products of creation and annihilation operators.

The _Lie_ algebra _U(6)_

After having defined the boson operators and the tensor product, one introduces now the transformation generators

$G_0^{(0)}(s,s) = \left[s^+ \times \tilde{s}\right]_0^{(0)}$	1
$G_\mu^{(2)}(d,s) = \left[d^+ \times \tilde{s}\right]_2^{(\mu)}$	5
$G_\mu^{(2)}(s,d) = \left[s^+ \times \tilde{d}\right]_2^{(\mu)}$	5
$G_\mu^{(0)}(d,d) = \left[d^+ \times \tilde{d}\right]_0^{(0)}$	1
$G_\mu^{(1)}(d,d) = \left[d^+ \times \tilde{d}\right]_1^{(\mu)}$	3
$G_\mu^{(3)}(d,d) = \left[d^+ \times \tilde{d}\right]_2^{(\mu)}$	5
$G_\mu^{(2)}(d,d) = \left[d^+ \times \tilde{d}\right]_3^{(\mu)}$	7
$G_\mu^{(4)}(d,d) = \left[d^+ \times \tilde{d}\right]_4^{(\mu)}$	9
total	**36**

The commutation relations of these operators among themselves are the same as the commutation relation of the _Lie_ algebra of the group _U(6)_ of unitary transformations in 6 dimensions (hence _U(6)_). Definitions of group, algebra, _Lie_ algebra, unitary group, orthogonal group are given in [95]. These operators _G_ (in total $36 = 6^2$) are thus identified as the generators of the algebra _U(6)_. Thus one says that the Hamiltonian has the group structure of _U(6)_. We will see later that one can decompose this "parent" group _U(6)_ into "smaller" imbricated subgroups. This imbrication of groups is not always unique and reflects the symmetry of the Hamiltonian.

The Three Dynamical Symmetries: _U(5), SU(3), O(6)_

Now, one wishes to diagonalize the Hamiltonian. A clever way to do so, is to know the states, which have "good" quantum numbers. The technique used is to decompose the "parent" algebra *U(6)* into chain of subalgebras, each of them characterized by different quantum numbers. A subalgebra is generated by a subset of the generators of the full algebra *U(6)*. For example, from the 36 generators *G* of *U(6)* one considers only the generators using the *d*-bosons: $G_\mu^{(L)}(d,d)$ with $L =0, 1, 2, 3, 4$. This new set of generators happens to close under commutation (*i.e* the commutator of any two generators belonging to the subalgebra is expressible in terms of generators belonging to the same subalgebra only). These 25 operators happen to be the generators of the algebra *U(5)*, the group of unitary transformation in 5 dimensions. It turns out that there are only three possible chains of subalgebra decomposing the "parent" algebra *U(6)* and containing the required *O(3)* subalgebra:

$$U(6) \quad \supset \quad U(5) \quad \supset \quad O(5) \quad \supset \quad O(3) \quad \supset \quad O(2) \qquad (I) \dots\dots\dots\dots(2\text{-}18\ )$$
$$\quad N \qquad\qquad n_d \qquad\qquad v \qquad\qquad L \qquad\qquad M$$

$$U(6) \quad \supset \quad SU(3) \quad \supset \quad O(3) \quad \supset \quad O(2) \qquad\qquad (II)\dots\dots\dots\dots(2\text{-}19\ )$$
$$N(\lambda,\mu) \qquad K \qquad\qquad L \qquad\qquad M$$

$$U(6) \quad \supset \quad O(6) \quad \supset \quad O(5) \quad \supset \quad O(3) \quad \supset \quad O(2) \qquad (III) \dots\dots\dots. (2\text{-}20\ )$$
$$\sigma \qquad\qquad \tau \qquad\qquad n_\Delta \qquad\qquad L \qquad\qquad M$$

For each subalgebra, one can find operators which commute with all generators of this subalgebra. Such operators are called Casimir operators and are usually labeled by *C*. The general Hamiltonian from Eq.(2-9) can then be rewritten in terms of *Casimir operators:*

$$H = e_0 + e_1 C_1[U(6)] + e_2 C_2[U(6)] + \eta C_2[O(6)] + \tilde\varepsilon\, C_1[U(5)] + \alpha C_2[U(5)] + \beta C_2[O(5)]$$
$$+ \delta C_2[SU(3)] + \gamma C_2[O(3)] + \rho C_1[O(2)] \dots\dots\ \dots\dots(2-21)$$

The Vibrational limit *U(5)* symmetry

The *U(5)* symmetry corresponds to the chain (I) (Eq.2-13) where the general Hamiltonian from Eq.(2-9) can be simplified by considering only the Casimir perators of the subalgebras involved in this chain (*i.e* $\eta = \delta = 0$). The basis states of this symmetry are defined by $|N, n_d, v, v_\Delta, L, M\rangle$ with

$$N_d \in 0,1,\dots,\ N \qquad\qquad\qquad\qquad\qquad\qquad\qquad (2\text{-}22)$$
$$v \in n_d, n_d - 2,\dots, 0 \qquad (n_d = \text{even}) \text{ or } 1\ (n_d = \text{odd}) \qquad (2\text{-}23)$$
$$v_\Delta \in 0,1,\dots, [v/3] \qquad\qquad\qquad\qquad\qquad\qquad (2\text{-}24)$$
$$L \in \lambda, \lambda+1, \dots, 2\lambda-2, 2\lambda \qquad \text{with} \qquad\qquad (2\text{-}25)$$
$$\lambda = v - 3v_\Delta, \qquad\qquad\qquad\qquad\qquad\qquad\qquad (2\text{-}26)$$

where *N* is the total number of bosons, n_d the number of *d* bosons, *v* is called the seniority and is defined as the number of boson pairs not coupled to zero angular momentum, v_Δ is chosen as the number of *d*-boson triplets coupled to zero angular momentum, *L* is the total angular momentum and *M* is its projection. By construction, the *U(5)* Hamiltonian is diagonal in the *U(5)* basis with eigenvalues

$$E^{(I)}(N, n_d, v, n_\Delta, L, M) = E_B + \tilde\varepsilon\, n_d + \alpha n_d(n_d+4) + 2\beta v(v+3) + 2\gamma L(L+1) + 2\rho M \dots\dots(2-27)$$

with $E_B = e_0 + e_1 N + e_2 N(N+5)$. One can then "construct" an energy spectrum reflecting the *U(5)* symmetry for a given boson number *N*. Note that the ratio $R_{4/2} = E(4_1^+)/E(2_1^+)$ is about 2 if the parameter $\tilde\varepsilon \geq \alpha, \beta, \gamma$. The energy level

pattern of the *U(5)* symmetry is similar to the one from a vibrational nucleus and when $N \to \infty$, the *U(5)* limit corresponds to the anharmonic quadrupole vibrator of the geometrical model [96].

The Rotational Limit *SU(3)* Symmetry

The *SU(3)* symmetry corresponds to the chain (II) (Eq.2-14) where the general Hamiltonian from Eq.(2-9) can be simplified by considering only the Casimir operators of the subalgebras involved in this chain (*i.e* $\eta = \tilde{\varepsilon} = \alpha = \beta = 0$). The basis states of this symmetry are defined by $|N, (\lambda, \mu), K, L, M\rangle$ with

$$(\lambda, \mu) \in (2n,0), (2n-4,2),..., [(0,n) \quad n-even \text{ or } (2,n\text{-}1)\ n\ odd].......(2\text{-}28)$$
$$K \in 0,2,..., \min(\lambda, \mu)..(2-29)$$
$$L \in K, K+1,..., K+\max(\lambda, \mu)...(2-30)$$

where only the even values of L allowed for $K=0$. For the magnetic substates M, one has $M \in -L,..., L-1, L$. By construction, the *SU(3)* Hamiltonian is diagonal in *SU(3)* basis with eigenvalues :

$$E^{(II)}(N, n_d, \nu, \nu_\Delta, L, M) = E_B + \frac{2}{3}\delta[\lambda^2 + \mu^2 + \lambda\mu + 3(\lambda + \mu)] + \gamma 2L(L+1) + 2\rho M .....(2-31)$$

A typical energy spectrum reflecting the *SU(3)* symmetry is shown in ref. [36] (figure (2-2)). Note that, the ratio $R_{4/2} = E(4_1^+)/E(2_1^+)$ is exactly $\frac{10}{3} \approx 3.33$. In the case $N \to \infty$, the *SU(3)* limit corresponds to the axial symmetric rotor in the framework of the geometrical model [96].

The $\gamma -$ Unstable Limit *O(6)* Symmetry

The *O(6)* symmetry corresponds to the chain (III) (Eq. 2-15) where the general Hamiltonian from Eq.(2-9) can be simplified by considering only the Casimir operators of the subalgebras involved in this chain (*i.e* $\tilde{\varepsilon} = \alpha = \delta = 0$). The basis states of the *O(6)* symmetry are defined by the quantum numbers $|N, \sigma, \tau, n_\Delta, L, M\rangle$ whose values are given by:

$$\sigma \in N, N-2,..., 0 \quad 0 \text{ (N=even) or } 1 \text{ (N=odd)} \qquad (2\text{-}32)$$
$$\tau \in 0,1,..., \sigma \qquad (2.33)$$
$$n_\Delta \in 0,1,..., [\tau/3] \qquad (2.34)$$
$$L \in \lambda, \lambda+1, ..., 2\lambda-2, 2\lambda \quad \text{with} \qquad (2.35)$$
$$\lambda = \tau - 3n_\Delta, \qquad (2.36)$$

where τ is the boson seniority, *i.e,* the number of boson pairs not coupled to zero angular momentum and ν_Δ is the number of *d*-boson triplets coupled to zero angular

momentum. The physical meaning of σ is more complex and is not discussed here. By construction, the *O(6)* Hamiltonian is diagonal in the *O(6)* basis with eigenvalues:

$$E^{(III)} (\sigma, \tau, n_\Delta, L, M) = E_B + 2\eta\sigma(\sigma + 4) + 2\beta\tau(\tau + 3) + 2\gamma L(L + 1) + 2\rho M. \qquad (2.37)$$

A typical energy spectrum reflecting the *O(6)* symmetry is shown in ref. [36] (figure (2-3)). Note that the ratio $R_{4/2} = E(4_1^+)/E(2_1^+)$ is about 2.5 if $\gamma \ll \beta$. For $N \to \infty$, the *O(6)* limit corresponds in the geometrical model to the γ-soft (or γ-unstable) rotors of Wilets and Jean [97].

Electromagnetic transition operators

Besides excitation energy spectra, the IBM is also able to describe electromagnetic transition rates as well. To do so, one needs to define the transition operators in terms of boson operators. The general form for the electromagnetic transition operator is given by

$$T^{(L)} = t_0^{(0)} \delta_{L0} + \sum_{\alpha,\beta} t_{\alpha\beta}^{(L)} b_\alpha^+ b_\beta + ... \qquad ....(2-38)$$

where *L* is the multipole of the transition. Since all of the boson operators have positive parity, the all the transition operators also have positive parity. States of nuclei have definite angular momentum and it is useful to use the spherical tensors coupled to definite angular momentum to construct the transition operators. The transition operators then become:

$$T_\mu^{(L)} = t_0^{(0)} \delta_{L0} + \sum_{ll'} t_{ll'}^{(L)} [b_l^+ \times b_{l'}] + ... \qquad ....(2-39)$$

The transitions operator defined as

$$T(E0) = \alpha_0 + \beta_0 \hat{n}_d,$$

$$T(M1) = \beta_1 \hat{L}$$

$$T(E2) = |\hat{Q} + |_1' \hat{Q}$$

$$T(M3) = \beta_3 \hat{U}$$

$$T(E4) = \beta_4 \hat{V} \qquad ....(2-40)$$

where α_0 and β_L are the effective charges and $\hat{Q}'$ is given by

$$Q^{\wedge} = [d^{\dagger} \times d^{\dagger}]^{(2)} \ldots \ldots \ldots 2\text{-}.4.)($$

Critical Point Symmetry in Shape Transitions

   Nuclear shapes have always been a point of discussion. In general, an atomic nucleus is believed to have an ellipsoidal shape. The shape of the nucleus is determined by five independent quantities, the two shape parameters (β and γ) and the three Euler angles (Θ, Φ, Ψ). It is believed to have perfect spherical shape when the neutron number or the proton number of the nucleus is one of the magic number as predicted by the shell model (for e.g. ^{40}Ca, ^{208}Pb). However as the number of these nucleons changes the shape of the nucleus also changes and it no longer remains spherical. Thus shape transitions are to be seen in nuclei. These shape transitions in atomic nuclei were studied extensively in the early 80"s in the framework of the IBM.

   Dynamical symmetries of nuclear Hamiltonian are an inherent feature of Interacting Boson Model (IBM), whose *U(6)* group structure leads to subgroup chains denoted by *U*(5), *SO*(6) and *SU*(3), which describe vibrational, γ-soft rotational and axially symmetric rotational, respectively. These three symmetries are depicted as the three vertices of a (symmetry) triangle, shown in figure (2-4) [98]. Typical partial level schemes of these symmetries are shown at their respective vertex. Most nuclei do not directly manifest these symmetries exactly; however these symmetries provide a sort of bench mark of structure and allow for a simple mapping procedure to locate any collective nucleus in the triangle.
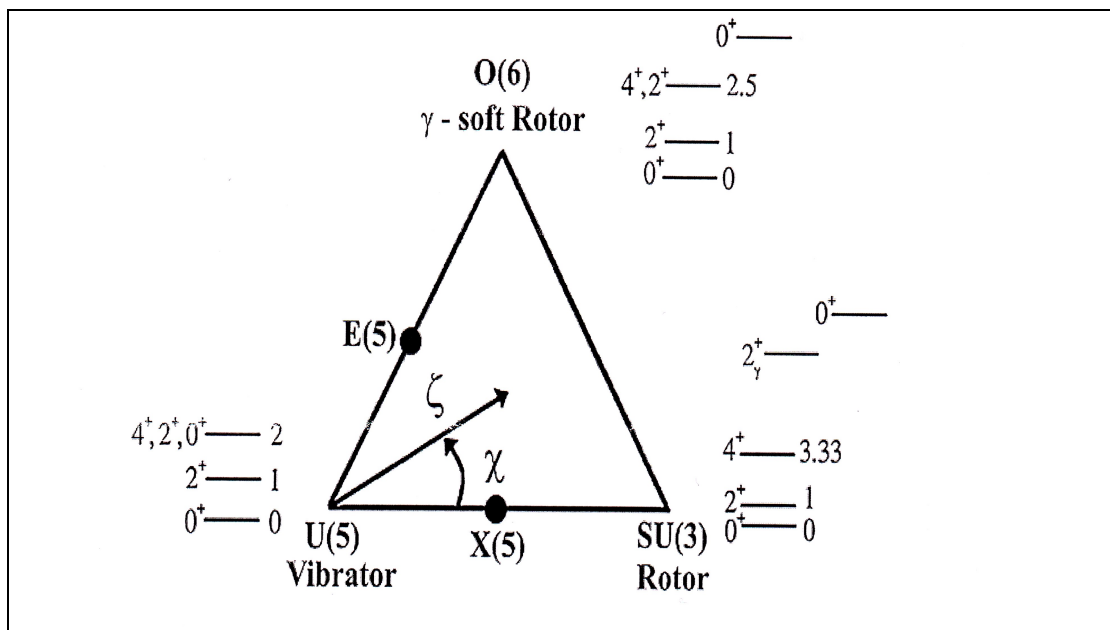
.[Figure (2-4): Casten symmetry triangle along with the partial level schemes of the various limits. [98

:The basic idea is embodied in the Ising-like Hamiltonian

$$H = H_{sph} + \kappa H_{def}.$$

where H_{sph} denotes the Hamiltonian of a higher symmetry (e.g. a spherical vibrator) with the coupling constant ε, whereas H_{def} has a lower symmetry of the deformed field with coupling constant κ. The resultant structure of the system is determined solely by the ratio ε/κ. If this ratio is large, the spherical solution dominates and if this ratio is small then the nucleus is said to be deformed. The transition in shapes takes place at a critical value $(\varepsilon/\kappa)_{crti}$. The IBM Hamiltonian in case of consistent Quantum formulation (*CQF*) can be written as:

$$H = n_d - Q.Q$$

the Hamiltonians described above has variation with respect to only one parameter ε/κ, thus only giving two extremes. The third dynamical symmetry is incorporated as the quadruple operator Q is dependent on an internal parameter χ, which determines the axial symmetry and its stiffness. With these two parameters any point in the symmetry triangle can be labeled. This is done in terms of polar coordinate, where ς which is related to ε/κ represents the radial coordinate and χ represents the angular coordinate. Table (2-1) lists the values for these parameters for each of the dynamical symmetries in IBM [99]. The Hamiltonian, described in the above equation, along with the dependence on these parameters also depends on the boson number N_B, defined as half the number of valence nucleons.

Observables such as $R_{4/2}$, defined as the ratio of level energy for the 2^+ and 4^+ levels, vary systematically across the triangle. The sudden change in the value for $R_{4/2}$ has been described in terms of phase transitional behavior, leading to a new class of critical point symmetries that describe nucleus at the phase transitional point. These are denoted by E(5) [for a second order vibrator to γ-soft rotor transition] and X(5) (for a first order vibrator to axial rotor phase transition).

Table (2-1): The values of the parameters ε, κ, and χ for the three dynamical symmetries proposed by IBM, β_e represents the equilibrium value of shape parameter β when the potential energy surface has a minimum Limit.

limit	ε	κ	χ	β_e
(U(5	ε	0	-	0
(SO(6	ε	κ	0	± 1
(SU(3	0	κ	$(-1/2)\sqrt{7}$	$\sqrt{2}$
	0	κ	$(+1/2)\sqrt{7}$	$\sqrt{2}$

2.4.2 Interacting Boson Model-2 (IBM-2)

In the IBM-2 model the neutrons and protons degrees of freedom are taken into account explicitly. Thus the Hamiltonian [34,36] can be written as,

$$H = H_\pi + H_\nu + V_{\pi\nu} \qquad \dots\dots\dots\dots\dots\dots\dots\dots\dots\dots\dots\dots..(2\text{-}42)$$

$$H = \varepsilon_\pi d_\pi^+ d_\pi^\sim + \varepsilon_\nu d_\nu^+ d_\nu^+ + V_{\pi\pi} + V_{\nu\nu} + \kappa Q_\pi . Q_\nu + M_{\pi\nu} \quad \ldots\ldots\ldots\ldots\text{(2-43)}$$

Here ε is the d-boson energy, κ is the strength of the quadrupole interaction between neutron and proton bosons.

In the IBM-2 model, the quadrupole moment operator is given by:

$$Q_{\rho\rho} = \left(s^+ d^\sim + d^+ s^\sim\right)_\rho^{(2)} + \chi_\rho \left(d^+ d^\sim\right)_\rho^{(2)}, \quad \text{(2-44)}\ldots\ldots\ldots\ldots\ldots$$

where $\rho = \pi$ or ν, $Q_{\rho\rho}$ is the quadrupole deformation parameter for neutrons $(\rho = \nu)$ and protons $(\rho = \pi)$. The terms $V_{\nu\nu}$ and $V_{\pi\pi}$ are the neutron-neutron and proton-proton d-boson interactions only and given by;.

$$V_{\rho\rho} = \sum_{J=0,2,4} \frac{1}{2} C_{L\rho} (2J+1)^{1/2} \left[\left(d^+ d^+\right)_\rho^{(2)} \left(\tilde{d}\,\tilde{d}\right)_\rho^{(2)}\right]^{(0)} \ldots\ldots\ldots\ldots\ldots\text{(2-45)}$$

The last term $M_{\pi\nu}$ is the Majorana interaction, shfits the states with mixed proton-neutron symmetry with respect to the totally symmetric ones. Since little experimental information is known about such states with mixed symmetry, which has the form:

$$M_{\pi\nu} = -\sum_{k=1,3} 2\xi_k \left(d_\pi^+ d_\pi^+\right)^{(k)} \left(d_\pi^\sim d_\pi^\sim\right)^{(k)} + \xi_2 \left(d_\pi^+ s_\nu^+ - s_\pi^\sim d_\nu^\sim\right)^{(2)} \left(d_\pi^\sim s_\nu^\sim - s_\pi^\sim d_\nu^\sim\right)^{(2)} \ldots\ldots\ldots \text{(2-46)}$$

Electromagnetic Transitions and Quadrupole Moments in IBM-2

The general one-body E2 transition operator in the IBM-2 is

$$T(l) = T_\pi(l) + T_\nu(l) \ldots\ldots\ldots\ldots\ldots\ldots\ldots\ldots\ldots\ldots..\ldots\ldots\ldots\text{(2-47)}$$

$$T(E2) = e_\pi \left[\left(s^+ d^\sim + d^+ s^\sim\right)_\pi^{(2)} + \chi_\pi \left(d^+ d^\sim\right)_\pi^{(2)}\right]^{(2)} + e_\nu \left[\left(s^+ d^\sim + d^+ s^\sim\right)_\nu^{(2)} + \chi_\nu \left(d^+ d^\sim\right)_\nu^{(2)}\right]^{(2)}$$

$$T(E2) = e_\pi Q_\pi + e_\nu Q_\nu \ldots\ldots\ldots \quad \ldots\ldots\ldots \quad \ldots\ldots\ldots \quad \ldots\ldots\text{(2-44)}$$

where Q_ρ is in the form of Eq.(2-40). For simplicity, the χ_ρ has the same value as in the Hamiltonian. This is also suggested by the single j-shell microscopy. In general, the E2 transition results are not sensitive to the choice of e_ν and e_π, whether $e_\pi = e_\nu$ or not. Thus, the reduced electric quadrupole transition rates between $I_i \rightarrow I_f$ states are given by:

$$B(E2; I_i^+ \rightarrow I_f^+) = \frac{1}{2I_i + 1} \left|< I_f^+ \| T(E2) \| I_i^+ >\right|^2 \ldots\ldots\text{(2-48)}$$

The static quadrupole moment Q_0 is given by the equation:

$$Q_0 = \frac{12}{10} ZR^2 \left(\frac{5}{4\pi}\right)^{1/2} \beta \ldots\ldots \quad \ldots\ldots\text{(2-49)}$$

where Z is the atomic number, R is radius of the nucleus and β is the deformation parameter. The electric quadrupole moment is given:

$$Q_{I_i} = \sqrt{\frac{1}{5}} \begin{pmatrix} I_i & 2 & I_i \\ -I_i & 0 & I_i \end{pmatrix} \langle I_i \| T(E2) \| I_i \rangle \qquad \ldots\ldots(2\text{-}50)$$

In the IBM-2, the M1 transition operator up to the one-body term ($l = 1$) is

$$T(M1) = \left[\frac{3}{4\pi}\right]^{\frac{1}{2}} \left(g_\pi L_\pi^{(1)} + g_\nu L_\pi^{(2)}\right) \qquad \ldots\ldots\ldots\ldots\ldots\ldots\ldots\ldots\ldots(2\text{-}51)$$

where $L_\rho^{(1)} = \sqrt{10}\,(d^+\tilde{d})_\rho$ and $L^{(1)} = L_\pi^{(1)} + L_\nu^{(1)}$. The g_π and g_ν are the boson g-factors (gyromagnetic factors(in unit μ_n (nuclear magneton) that depends on the nuclear configuration. They should be different for different nuclei.

$$T(M1) = \left[\frac{3}{4\pi}\right]^{\frac{1}{2}} \left[\frac{1}{2}(g_\pi + g_\nu)\left(L_\pi^{(1)} + L_\nu^{(1)}\right) + \frac{1}{2}(g_\pi - g_\nu)\left(L_\pi^{(1)} + L_\nu^{(1)}\right)\right] \ldots\ldots(2\text{-}52)$$

The magnetic dipole moment operator is given by:

$$T(M1) = 0.77\left[\left(d^+d^\sim\right)_\pi - \left(d^+d^\sim\right)_\nu\right]^{(1)} (g_\pi - g_\nu) \ldots\ldots\ldots\ldots(2\text{-}53)$$

the reduced magnetic dipole transition rates between $I_i \rightarrow I_f$ states are given by:

$$B\left(M1, I_i^+ \rightarrow I_f^+\right) = \frac{1}{2I_i + 1}\left|\langle I_f^+ \| T(M1) \| I_i^+ \rangle\right|^2 \qquad \ldots\ldots\ldots\ldots\ldots\ldots(2\text{-}54)$$

The reduced E2 and M1 matrix elements were combined in the calculation of the mixing ratio $\delta(E2/M1)$ using the relation [100]:

$$\delta\left(E2/M1; I_i^+ \rightarrow I_f^+\right) = 0.835\, E_\gamma\,(M\,eV)\frac{\langle I_f^+ \| T(E2) \| I_i^+ \rangle}{\langle I_f^+ \| T(M1) \| I_i^+ \rangle} \ldots\ldots\ldots (2\text{-}55)$$

The *E*0 (electric monopole transition) transition occurs between two states of the same spin and parity by transferring the energy and zero units of angular momentum, and it has no competing gamma ray. The *E*0 transition is present when there is a change in the surface of the nucleus. For example, in nuclear models where the surface is assumed fixed, *E*0 transitions are strictly forbidden, such as in shell and

IBM-1 models. Electric monopole transitions are completely under the penetration effect of atomic electrons on the nucleus, and can occur not only in $0^+ \rightarrow 0^+$ transition but also, in competition with gamma multipole transition, and depending on transition selection rules that may compete in any $\Delta I = 0$ decay such as a $2^+ \rightarrow 2^+$ or any $I_i = I_f$ states in the scheme. When the transition energy greater than $2m_o c^2$, monopole pair production is also possible. The $E0$ reduced transition probability is written [101]

$$B(E0; I_i \rightarrow I_f) = e^2 R_0^4 \rho^2(E0) \quad I_i = I_f \,......... \,....(2-56)$$

where e is the electron effective charge, $R_0 = 1.25 A^{1/3} \, fm$ is the nuclear radius and $\rho(E0)$ is the monopole transition matrix elements. There are only limited cases of $\rho(E0)$ that can be measured directly.

The electric monopole transition operator is

$$T(E0) = \beta_{0\rho}(d^+ \times d^\sim)^{(0)}_\rho + \gamma_{\varphi\rho}(s^+ \times s^\sim)^{(0)}_\rho .... \,....(2-57)$$

$$N_\rho = \sqrt{5}(d^+ \times d^\sim)^{(0)}_\rho + (s^+ \times s^\sim)^{(0)}_\rho .... \,........... \,.........(2-58)$$

$$T(E0) = \beta_{0\rho}(d^+ \times d^\sim)^{(0)}_\rho + \gamma_{\varphi\rho} N_{\varphi\rho} .... \,........... \,.....(2-59)$$

$$\beta'_{0\rho} = \beta_{0\rho} / \sqrt{5} - \gamma_{0\rho}$$

The monopole matrix element is given by:

$$\rho_{if}(E0) = \frac{Z}{R^2} \sum \beta'_{0\rho} < f | d^+_\rho \times d^\sim_\rho | i > .... \,(2-60)$$

The two parameters $\beta_{0\pi}$, β_{0v} in equation (2-56) must be estimated.

In most cases we have to determine the intensity ratio of $E0$ to the competing $E2$ transition, *X(E0/E2)* [101]

$$X(E0 / E2; I_i^+ \rightarrow I_f^+) = e^2 R^4 \rho^2(E0; I_i^+ \rightarrow I_f^+) / B(E2; I_i^+ \rightarrow I_i^+) .... \,........(2-61)$$

where $I_f = I_f'$ for $I_i = I_f' = 0$, and $I_f' = 2$ for $I_i = I_f = 0$. The two parameters $\beta_{0\pi}$ and β_{0v} in equation (2-57) may be estimated by fitting the isotope shift, which is different in the mean square radius $\Delta \langle r^2 \rangle$ between neighboring isotopes in their ground state. They are given by *Bijker et al.*, [102]:

$$\Delta \langle r^2 \rangle = \langle 0_1 | r^2 | 0_1 \rangle_A - \langle 0_1 | r^2 | 0_1 \rangle_{A+1}$$

$$\Delta < r^2 >= \beta^\sim_{0\pi}[< 0_1 | d^+_\pi d^\sim_\pi | 0_1 >_{N_v} - < 0_1 | d^+_\pi d^\sim_\pi | 0_1 >_{N_v}] + \beta^\sim_{0v}[< 0_1 | d^+_v d^\sim_v | 0_1 >_{N_v}$$

$$- < 0_1 | d^+_v d^\sim_v | 0_1 >_{N_v}] - \gamma_{0v} .... \,........... \,........... \,.....(2-62)$$

The isomer shift, which is the difference between the mean square radius $\delta \langle r^2 \rangle$ of an excited state and the ground state in a given nucleus [102]:

$$\delta < r^2 >= < r^2 >_{e.s} - < r^2 >_{g.s}$$

$$\delta < r^2 > \ = 2\langle 2_1 \big| r^2 \big| 2_1 > - < 0_1 \big| r^2 \big| 0_1 >$$

$$\delta <r^2 \succ = \beta^-_{0\pi}[<2_1 \big| d^+_\pi d^-_\pi \big| 2_1 > - <0_1 \big| d^+_\pi d^-_\pi \big| 0_1 >] + \beta^-_{0\nu}[<2_1 \big| d^+_\nu d^-_\nu \big| 2_1 > - <0_1 \big| d^+_\nu d^-_\nu \big| 0_1 >] \ldots \ldots (\ 2-63)$$

The *IBM-2* Basis States

The calculation of *IBM-2* energy eigenvalues and eigenfunctions is usually done numerically using the computer code NPBOS [103]. The resulting eigenvectors can then be used to calculate transition rates and related properties using the computer code NPBEM [103]. The relationship between the parameters of Eq. (2-39).

The basis states used in the calculations are products of neutron and proton basis states. The latter are *U(5)* basis states for neutron bosons and proton bosons, as given in expression (2-20).

The complete *IBM-2* basis state can be as .

$$| \Psi JM \rangle = |[N = N_\nu + N_\pi] n_{d\nu}, \nu_\nu, n_{\Delta\nu}, L_\nu, M_\nu; n_{d\pi}, \nu_\pi, n_{\Delta\pi}, L_\pi, M_\pi; JM \rangle$$

$$= \Big[|[N] n_d, \nu, n_\Delta, L, M \rangle_\nu |[N] n_d, \nu, n_\Delta, L, M \rangle_\pi \Big]^J_M$$

The basis states can be found by choosing states that transform as the representations of the chain of algebras that can be derived from the *U(6)* algebra formed by the bilinear pair of boson creation and annihilation operators. In the *IBM-2*, the bilinear pairs of proton and neutron creation and annihilation operators respectively form the algebras $U_\pi(6)$ and $U_\nu(6)$. There are several ways to decompose and combine the two algebras into a chain of subalgebras and each way will determine the basis. As in the IBM-1, the requirement for the chain is the inclusion of the $SO_{\pi+\nu}(3)$ algebra as it is related to a good total angular momentum quantum number. The algebra $SO_{\pi+\nu}(3)$ is created from the sum of generators of the algebras $SO_\pi(3)$ and $SO_\nu(3)$.

As an example, one may take the two chains of algebras for protons and neutron,
$$U_\pi(6) \supset U_\pi(5) \supset SO_\pi(5) \supset SO_\pi(3) \supset SO_\pi(2)$$
$$U_\nu(6) \supset U_\nu(5) \supset SO_\nu(5) \supset SO_\nu(3) \supset SO_\nu(2)$$
These two chains can be combined at any point up except at $SO_{\pi+\nu}(2)$ since the combined algebra $SO_{\pi+\nu}(3)$ is needed. One of the possibilities is

$$U_\pi(6) \supset U_\pi(5) \supset SO_\pi(5) \supset SO_\pi(3)$$
$$N_\pi \qquad n_{d\pi} \qquad v_\pi, n_{\pi\triangle} \qquad L_\pi$$

$$SO_{\pi+\nu}(3) \supset SO_{\pi+\nu}(2)$$

$$U_\nu(6) \supset U_\nu(5) \supset SO_\nu(5) \supset SO_\nu(3) \qquad L \qquad M$$
$$N_\nu \qquad n_{d\nu} \qquad v_\nu, n_{\nu\triangle} \qquad L_\nu$$

where the quantum numbers are labelled beneath the corresponding algebra. This is the basis that is used in the *IBM-2* program NPBOS.

Another set of bases can be obtained if one combines the algebras at a different point such as

$$U_\pi(6)$$
$$U_{\pi+\nu}(6) \supset U_{\pi+\nu}(5) \supset SO_{\pi+\nu}(5) \supset SO_{\pi+\nu}(3) \supset SO_{\pi+\nu}(2)$$
$$U_\nu(6)$$

In general there are three chains that can be combined at $U_{\pi+\nu}(6)$ to give three different bases. In these chains, the proton and neutron bosons exhibit a symmetry and this is the subject of the following section.

2.4.2.1 Mixed-Symmetry States (*MSS' s*)

The low-energy spectrum of even-even nuclei is dominated by simple collective excitation modes [96]. These correlations in the nucleon motion are induced by the long-range quadrupole component of the nuclear force. In spherical nuclei with few valence nucleons, surface vibrations evolve which can be described as bosons, so-called phonons. In an ideal case the excitation spectrum of a vibrator nucleus is a harmonic oscillator with equidistant level spacings $\hbar\omega$, where phonons can couple to multiphonon states with different angular momenta and parities. For large numbers of the valence nucleons an elliptically deformed equilibrium state becomes energetically more favorable. Its vibrational modes can be divided into vibrations of the deformation parameter β (β-vibrations) and the form parameter γ (γ-vibrations).

Multiphonon excitations of atomic nuclei are interesting collective structures of the nuclear many-body system. Their existence enables us to judge the capability of the corresponding phonon modes to act as building blocks of nuclear structure. Possible deviations from harmonic phonon coupling occur due to the microscopic structure of the underlying phonon modes and serve as a sensitive source of information on the formation of collectivity in the nuclear many-body system. The proton-neutron interaction in the nuclear valence shell has been known for a long time as the driving force for the evolution of the low-energy nuclear structure. This has been discussed in many ways, e.g., in terms of the evolution of collectivity in heavy nuclei as a function of the product of valence proton and neutron numbers $N_\pi N_\nu$ [104]. Otsuka *et al*., have identified the proton-neutron interaction as being responsible for the evolution of shell structure [105]. Therefore, it is interesting to

study those nuclear excitations that are most sensitive to the proton-neutron interaction in the valence shell. One class of states are collective isovector valence shell excitations that are frequently called mixed-symmetry states (*MSSs*) in the terminology of the interacting boson model.

The first observation of a nuclear *MSS* was made in electron scattering experiments [106] on the deformed nucleus ^{156}Gd. A strong *M1* excitation to a 1^+ state close to 3 MeV excitation energy, the scissors mode, was observed. The scissors mode has subsequently been studied mainly in electron and photon scattering experiments on deformed nuclei. Data are available for many nuclei in the rare-earth mass region and interpretations of the systematics of the centroid and the total strength as a function of deformation have been put forward [107].

F-spin

The *F*-spin formalism is analogous to the isospin formalism of nucleons. Proton bosons and neutron bosons have $F = 1/2$ and the *z*-projection is $F_z = +1/2$ for protons and $F_z = -1/2$ for neutrons. For a system of N_π proton bosons and N_ν neutron bosons, the maximum *F*-spin is $F = F_{max} = (N_\pi + N_\nu)/2$ and

$$F_z = \frac{|N_\pi - N_\nu|}{2} \leq F_{max} \leq \frac{N_\pi + N_\nu}{2} \quad \ldots\ldots\ldots(2\text{-}64)$$

In the *F*-spin space, one can also define the creation and annihilation operators F_+ and F_- by

$$F_+ = s_\pi^+ s_\nu + \sum_\mu d_{\pi,\mu}^+ d_{\nu,\mu} \cdots\cdots\cdots \quad (2-65)$$

$$F_- = s_\nu^+ s_\pi + \sum_\mu d_{\nu,\mu}^+ d_{\pi,\mu} \cdots\cdots\cdots \quad (2-66)$$

The projection operator F_z is given by

$$F_z = \frac{1}{2}\left[s_\pi^+ s_\nu + \sum_\mu d_{\pi,\mu}^+ d_{\nu,\mu} + s_\nu^+ s_\pi + \sum_\mu d_{\nu,\mu}^+ d_{\pi,\mu} \right]\ldots\ldots(2-67)$$

A state composed by N_π proton bosons and N_ν neutron bosons with *F*-spin quantum number $F = F_{max}$ can be transformed by the successive action of the *F*-spin raising operator F_+ into a state that consists of proton bosons only. This state has still a total *F*-spin quantum number $F = F_{max}$ since the raising operator does not change the total *F*-spin quantum number. This new state has only proton bosons and obviously stays unchanged under a pairwise exchange of proton and neutron labels. Therefore, *IBM-2* states with $F=F_{max}$ are called *Full Symmetry States* (*FSSs*). These states corresponds actually to the IBM-1 states which are all symmetric. All others states with *F*-spin quantum numbers $F < F_{max}$ contain pairs (at least one) of proton and neutron bosons that are antisymmetric under a pairwise exchange of protons and neutrons labels. They are called *Mixed-Symmetry States* (*MSSs*).

A comprehensive review of the *F*-spin symmetry of the IBM-2 has been given by Van Isacker *et al.,* [108]. One important result of the *F*-spin formalism is given by the proton-neutron contribution to the matrix elements of any one-body operator between FSSs:

$$< F_{\text{max}}, \alpha \| b_{\rho,\beta}^{+} b_{\rho,\beta} \| F_{\text{max}}, \alpha' \succ = N_{\rho} c_{\alpha\alpha',\beta\beta'} \dots\dots(2-68)$$

where $\alpha, \alpha', \beta, \beta'$ are additional quantum numbers and $c_{\alpha\alpha',\beta\beta'}$ is independent of ρ. This major result tells us that there are no $M1$ transition between FSSs.

Both operators $E2$ and $M1$ can be divided into F-scalar (denoted by s) and F-vector (denoted by v) parts

$$T(M1)_s = \frac{g_\pi + g_\nu}{2}\left(L_\pi + L_\nu\right)\dots\dots.(2-69)$$

$$T(M1)_v = \frac{g_\pi - g_\nu}{2}\left(L_\pi - L_\nu\right)\dots\dots.(2-70)$$

$$T(E2)_s = \frac{e_\pi + e_\nu}{2}\left(Q_\pi^{\chi_s} + Q_\nu^{\chi_s}\right)\dots\dots.(2-71)$$

$$T(E2)_v = \frac{e_\pi - e_\nu}{2}\left(Q_\pi^{\chi_v} - Q_\nu^{\chi_v}\right)\dots\dots.(2-72)$$

with

$$\chi^s = \frac{e_\pi \chi_\pi + e_\nu \chi_\nu}{e_\pi + e_\nu}\dots\dots\quad\dots\dots\quad\dots\dots(2-73)$$

$$\chi^v = \frac{e_\pi \chi_\pi - e_\nu \chi_\nu}{e_\pi - e_\nu}\dots\dots\quad\dots\dots\quad\dots\dots(2-74)$$

From the previous discussion concerning the $E2$ and $M1$ decays of full symmetric states and the mixed-symmetry states (here discussed in near vibrational nuclei), we expect following signatures for mixed-symmetry one-phonon and two phonon excitations for vibrational and transitional nuclei:

• The one-quadrupole-phonon $2_{1,Ms}^{+}$, state is the lowest-lying *MSS* in vibrational nuclei.

• The $2_{1,Ms}^{+}$ state decays to the 2_1^{+} state by a strong $M1$ transition

$$\left| \langle 2_{1,M}^{\cdot} \| T(M1) \| 2_1^{\cdot} \rangle \right|^2 \approx 1_\mu^2 \frac{}{N}$$

• A weakly collective $E2$ transition strength of a few $e^2 b^2$ for the $2_{1,Ms}^{+} \rightarrow 0_1^{+}$ transition.

In the IBM-1, geometrical shapes can be assigned to the algebras of the three possible chains, which correspond directly to the description of nuclear shapes by Bohr and Mottleson's shape variables [11,12]. In the *IBM-2*, the mixed-symmetry states correspond to a quadrupole vibration where the protons and neutrons oscillate out of phase as shown in part (a) of figure (2-5). For deformed nuclei, the protons and neutrons oscillate with respect to one another as the nucleus as a whole rotates as shown in part (b) of figure (2-5). Because of this type of motion, the mixed-symmetry states for deformed nuclei are also known as the scissors mode.

Mixed-symmetry states can be identified by their unique signature, namely a collective M1 decay to a fully-symmetric state. $M1$ transitions are forbidden between fully-symmetric states and between mixed-symmetry states in the *F*-spin basis.
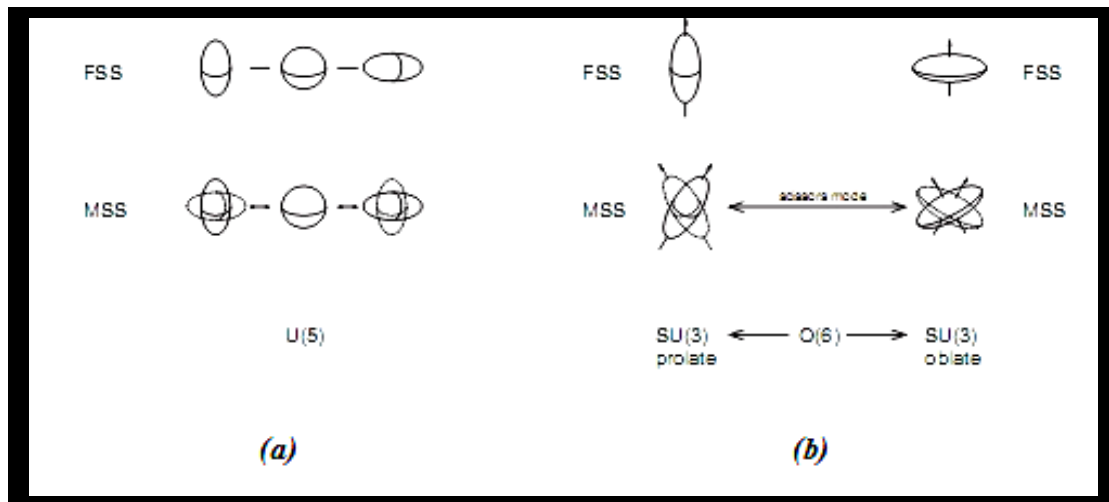
Figure: (2-5): Geometric interpretation of mixed-symmetry states are shown. The figure represents a snapshot of the nucleus in time. Part (a) represents the out of phase vibration for spherical nuclei and (b) represents the vibration of protons and neutrons with respect to each other for prolate or oblate deformed nuclei [65].

2.4.2.2 Configuration Mixing of Bosons

Some nuclei near" closed shells appear to have both the vibrational structure expected for a near-spherical shape, and rotational structure, which is typical of deformed nuclei [109]. This phenomenon of shape coexistence involves two configurations of the nucleus which have different numbers of active nucleons. In an IBM description, the two configurations have different boson numbers; N_ν being the same but N_π different, or vice versa. The most common situation involves a difference in $N_\nu(N_\pi)$ of two bosons between the normal configuration and the so-called intruder configuration, corresponding to a pair excitation across a shell or sub-shell gap [109,110]. There is often evidence of mixing between the two configurations, as shown in Chapter 3, for the *Ge* isotopes.

Configuration mixing can be treated in the IBM-2 using a technique developed by Duval and Barrett [111]. Separate IBM-2 calculations are done for the two configurations and the results are then mixed using the interaction:

$$V_{mix} = \alpha\left(s_\pi^+ \times s_\pi^+\right)^{(0)} + \beta\left(d_\pi^+ \times d_\pi^+\right)^{(0)} + hc \ldots\ldots\ldots(2-75)$$

where the intruder configuration is assumed to involve the proton shell. There are three parameters in the mixing calculation, the mixing strengths α and β in Eq.(2-72), and the pair excitation energy, Δ, which gives the relative energies of the two unperturbed configurations.

We first explain the essential ingredients of the model with specific reference to the lead isotopes. The model space for three configurations is built from N, $N+2$, and $N+4$ bosons and constitutes a boson representation of the shell-model configurations that are dominant in the low-energy region of the Ge isotopes. The N-boson states correspond to excitations of neutrons only, for which the proton shell $Z = 82$ remains closed; they can be characterized as the *0p-0h* configuration. The states with $N+2$ and $N+4$ bosons correspond to *2p-2h* and *4p-4h* excitations of the protons across the $Z = 82$ shell gap coupled the valence neutrons in the $N = 82\text{-}126$ shell.

The total mixing Hamiltonian is then given by

$$H = H_1 + H_2 + V_{mix} \ldots\ldots\ldots\ldots\ldots\ldots(2-76)$$

where H_1, (H_2) is the *IBM*-2 Hamiltonian for the first (second) configuration, as given by Eq.(2-39), and an amount Δ has been added to the energies of the second configuration.

The mixing Hamiltonian matrix, for a given angular momentum, is shown schematically in the equation:

$$H = \begin{pmatrix} H_1 & V_{mix} \\ V_{mix} & H_2 \end{pmatrix} \quad \ldots(2-77)$$
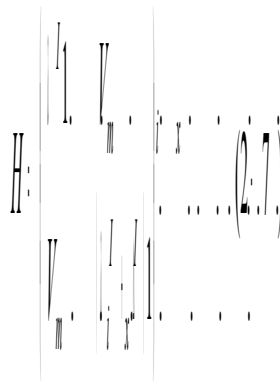
The non-diagonal matrix elements are

$$V_{ij} = \langle I_i L | V_{mix} | II_j L \rangle \ldots\ldots\ldots\ldots\ldots(2-78)$$

where $\left| I_i L \right>$ is the *ith* eigenfunction of angular momentum *L* for the

configuration *I*, $\left| II_j L \right>$ is the *jth* eigenfunction of angular momentum *L* for the

configuration *II*, and V_{mix} is given by Eq.(2.72). The diagonal parts are

$$\lambda_i^I = E_i^I + \lambda_o^I ....(2-79)$$

and

$$\lambda_j^{II} + \Delta = E_j^{II} + \lambda_o^{II} ....(2-80)$$

where λ_n is the actual energy eigenvalue, as determined by the computer code
NPBOS, *E* is the energy relative to the *n* ground state of the configuration in question,
λ_o is the ground state eigenvalue, and Δ is the pair-excitation energy. Note that
λ_o is the binding energy or deformation energy. It is intrinsically negative.

The unperturbed energies for the second configuration, relative to the ground
state of the first configuration, are given by

$$E_n^{II} = E_n^{II} + \Delta + \left| \lambda_o^I \right| - \left| \lambda_o^{II} \right| ....(2-81)$$

where E^{II} is the energy as given in the NPBOS output; the absolute value of the
ground state eigenvalue, λ_o is called the "binding energy" and is listed with the
energies in the NPBOS output; and the value of Δ is the NPMIX input parameter
EFIX.

The configuration mixing calculations are done using the computer code
NPMIX [112], which calculates the energy eigenvalues and eigenfunctions. The
computer codes NPBEMX and BEMIX [112] are subsequently used to calculate
matrix elements for transition rates and other properties.

Electromagnetic Transition Probability within configuration mixing

The E2 transition operator in configuration mixing, which is given in Eq.(2-47) can be
rewritten

$$T^{(l)} = T_{2\pi}^{(l)} + T_{2\nu}^{(l)} + T_{4\pi}^{(l)} + T_{4\nu}^{(l)} ....(2-82)$$

$$T(E2) = e_2 (Q_{2\pi} + Q_{2\nu}) + e_4 (Q_{4\pi} + Q_{4\nu}) ....(2-83)$$

being Q_{ρ}, the quadrupole operator defined in Eq.(2-40) for the normal $(j = 2)$ and
intruder $(j = 4)$ configurations. The values of the boson effective charges where
$e_{2\pi} = e_{4\pi} = e_2$ and $e_{1\nu} = e_{4\nu} = e_4$, for a mathematical simplicity we put $e_2 = e_4 = e$. for
all isotopes, following the work of Sambataro and Molnar [113] on the Mo isotopes)
were determined by the experimental electric transition probability $B(E2; 2_1^+ \rightarrow 0_1^+)$
values. The reduced transition *B(E2)* probability is given by the   Eq. (2-48).

The M1 transition operator in configuration mixing is given

$$T(M1)_{i\rho} = \left[\frac{3}{4\pi}\right]^{1/2}\left[\left(g_{2\pi}L^{(1)}_{2\pi} + g_{2\nu}L^{(1)}_{2\nu}\right) + \left(g_{4\pi}L^{(1)}_{4\pi} + g_{4\nu}L^{(1)}_{4\nu}\right)\right]\ldots\ldots\ldots(2-84)$$

and $g_{2\pi} = g_{4\pi} = g_{\pi} = 1\mu_n$ for a simplicity $g_{2\nu} = g_{4\nu} = g_{\nu} = 0\mu_n$

.(The reduced transition *B(M1)* probability is given by the Eq.(2-54

The expressions for $\rho(E0)$ matrix elements and isotope shifts are given in Eqs.(2-60) and (2-62). They involve five parameters. Four of them, $\beta_{02\pi}, \beta_{02\nu}, \beta_{04\pi}$ and $\beta_{04\nu}$ multiply the matrix elements of $n_{d2\pi}, n_{d2\nu}, n_{d4\pi}$ and $n_{d4\nu}$,respectively. The last parameter, which occurs in the isotope shift expression only, is an additive constant, $\gamma_{0\nu}$ (It is the sum of $\gamma_{02\nu}$ and $\gamma_{04\nu}$ in Eq.(2-62.)

The electric monopole transition in configuration mixing is given by the equation

$$T(E0) = \beta_{02\pi}\hat{n}_{d2\pi} + \beta_{02\nu}^{\wedge}\hat{n}_{d2\nu} + \beta_{04\pi}^{\wedge}\hat{n}_{d4\pi} + \beta_{04\nu}^{\wedge}\hat{n}_{d4\nu} + \gamma_{02\pi}\hat{N}_{2\pi}$$
$$+ \gamma_{02\nu}\hat{N}_{2\nu} + \gamma_{04\pi}\hat{N}_{4\pi} + \gamma_{04\nu}\hat{N}_{4\nu}\ldots\ldots\ldots\ldots\ldots(2-85)$$

The electric monopole transition matrix element is given by:

$$\rho(E0; J_i^+ \rightarrow J_f^+) = \frac{Z}{R}\sum_{i=2,4}\sum_{\rho=\pi,\nu}\beta_{0i\rho}^{\wedge} <J_f^+|\hat{n}_{di\rho}|J_i^+>\ldots\ldots\ldots\ldots(2-86)$$

Chapter Four
Conclusions and Suggestions for Future Work

Conclusions 4.1

In this work we have described various properties of the *Kr, Xe, Nd* and

.Ge isotopes in the framework of the IBM-2 model

1-   Kr isotopes :

a- From all figures of energy levels for $^{76\text{-}90}$Kr Isotopes we found that $^{76\text{-}90}$Kr isotopes changed from the vibrational SU(5) limit to transitional limit O(6) , because the value of the ratio E(4_1)/ E(2_1) is (2.44 ➤ 3.043)

b- The comparison of some B(E2), B(M1), mixing ratios   for these isotopes with the experimental data show that these isotopes exist along the   SU(5)-O(6) side of the IBM triangle.

c- In $^{76\text{-}90}$Kr isotopes we saw that when the states $J^{\pi}=2_2^+,2_4^+$ and 3_1^+ are strongly dominated by the F=F_{max}, the strongest contribution to the states is the one with F=F_{max}-1.

We also can see the states $J^{\pi}=2_3^+,3_2^+$ are mixed symmetry states in

$^{76\text{-}90}$Kr isotopes .

2-   **Xe isotopes :**

a- From all figures of energy levels for $^{124\text{-}134}$Xe Isotopes we found that $^{124\text{-}134}$Xe isotopes changed from the vibrational SU(5) limit to transitional limit O(6) because the value of the ratio E (4_1) / E(2_1) is (2 ➤ 2.5).

b- The study of the electromagnetic properties of the states together it that of energy spectra indicates that the following changes from an O(6)-like structure to an U(5) like-structure.

c- Often, the decay properties of the lowest excited 0^+ states are used as an additional signature of the E(5) structure. In the case of ^{132}Xe, the $R_{4/2}$ value 2.16 lies very close to the ideal value for the E(5) symmetry indicating that it lies more towards the U(5) side.

3-   **Nd isotopes :**

a- From all figures of energy levels for $^{144-154}$Nd Isotopes we found that $^{144-154}$Nd isotopes changed from the vibrational SU(5) limit to transitional limit SU(3) , because the value of the ratio E (41) / E(21) is (1.885 ► 3.281).

b- The X(5) analytic solutions for the critical point in the spherical to axially deformed phase/shape transition is closely manifested empirically in ^{150}Nd and in other N=90 isotones.

c- The 2_3^+ states in the N = 86 isotope show a similar behavior to the corresponding states in the N = 88 isotope and show that the mixed-symmetry states are sensitive to the residual proton-neutron interaction in this mass region.

4-   **Ge isotopes :**

a- From all figures of energy levels for $^{64-82}$Ge isotopes we found that $^{64-82}$Ge isotopes changed from the vibrational SU(5) limit to transitional limit O(6) , because the value of the ratio E (41) / E(21) is (2.28 ► 2.60).

b- The E2 transition rates, isotope shifts and results are in good agreement with those experimental values which are available, again indicating that the prescription of two mixed configurations works well.

4.2 Suggestions for Future Work

The use of the IBM-2 basis can be used for other calculations in addition to the energy levels and electromagnetic transitions. Same of these   extensions are suggested below :

1- One of the most significant recent developments in nuclear structure physics is the prediction that a Supersymmetry Model (*SSM*) may be realized in nuclei. The recognition of dynamical symmetries in even-even nuclei via the introduction of bosons has reoriented our directions nuclear spectroscopy. Therefore this suggests to use this model to study the level schemes in odd-even mass nuclei, and study the non-collective motion in transitional and deformed nuclei.

2- Study of the hexadecupole degree of freedom in transitional nuclei, by addition of a g-boson ($L = 4$), to test the important $K^\pi = 4^+$ band and *E4* transitions in this region.

3- Use the method to proposed of connecting of the interacting boson model and shell model is called interacting boson model-3 (IBM-3) to describe the light nuclei $(\pi\nu \, , T = 1)$.

4- The 2_M^+ states found so far in the A = 140 mass region give us an interesting glimpse into the behavior of mixed-symmetry states. The extent of the existence of these states and also their purity would test the limits of the validity of describing them as states of mixed proton-neutron symmetry. Efforts are continuing in the search of mixed-symmetry states in this mass region.

References :

[1] E. Rutherford. Philosophical Magazine, 21 (1911) 661.

[2] J. Chadwick. Nature,129 (1932) 312.

[3] P. A. M. Dirac. Proc. R. Soc. A 117(1928) 610.

[4] P. A. M. Dirac. Proc. R. Soc. A118 (1928) 351.

[5] C. Anderson. Phys. Rev. 43 (1933) 491.

[6] G. Gamow. Proc. R. Soc. A 126 (803) (1930) 632 .

[7] C. F. von Weiz¨acker. Zeits. F. Physik, 96 (1935) 431.

[8] M. Goeppert-Mayer. Phys. Rev. 75 (1969) 1949.

[9] O. Haxel, J. H. D. Jensen, and H. E. Suess. Zeits. F. Physik, 128 (1950) 295.

[10] J. Rainwater. Phys. Rev. 79 (1950) 432.

[11] A. Bohr. Kgl. Danske Videnskab. Selskab, Mat. Fys. Medd. 26 (1952) 14.

[12] A. Bohr and B. Mottelson. Kgl. Danske Videnskab. Selskab, Mat.fys.
     Medd. 27 (1953) 16.

[13] D. L. Hill and J. A. Wheeler. Phys. Rev. 89 (1953) 1102.

[14] S. G. Nilsson. Dan. Mat. Fys. Medd. 29 (1955) 16.

[15] A. Arima and F. Iachello. Phys. Rev. Lett. 35 (1975)1069.

[16] L. Eisenbud and E. P. Wigner. ′*Nuclear Structure*′. Princeton University
     Press, Princeton, New Jersey 1958.

[17] U. Kaup and A. Gellberg, Z. Phys. A293 (1979) 311.

[18] P. Hellmeister, J. Keinonen, K. P. Lieb , Phys. Lett. B 85 (1979) 34.

[19] A. R. Meyer, F. J. Wild and K. Esksla, Phys. Rev. C27 (1984) 2217.

[20] A. Giannutiempo, A. Nannini and A. Perego, Phys. Rev. C47 (1993) 521.

[21] H. Dejbakhsh, A. Kolomiets and S. Shlomo, Phys. Rev. C51 (1995) 573.

[22] A. Giannutiempo, A. Nannini and P. Sona, Phys. Rev. C62 (2000) 044302.

[23] Shi Zhu-Yi, Zhao Xing-Zhi and Tong Hong, China Phys. Soc. Vol. 12, No.7
     (2003) 0732.

[24] F. H. AL-Khudair and LONG Gui-Lu, High Energy Physics and Nuclear Physics
     Vol. 28, No. 6 (2004) 717.

[25] Nurettin Turkan, Davut Olgun, Ihsan Uluer and Sait Inan , Turk. J. Phys. 30
     (2006) 89.

[26] N. Turkan, T. Bascetin and I.Inci. Mom. 72, No. 6 (2009) 1004.

[27] A. Arima, F. Iachello, Ann. Phys. 99 (1976) 253 .

[28] A. Arima, F. Iachello, Ann. Phys. 111 (1978) 201.

[29] A. Arima, F. Iachello, Phys. Rev. Lett. 35 (1975) 1069 .

[30] A. Faessler, W. Greiner, and R. K. Sheline, Nucl. Phys. 417 (1965).

[31] A. S. Davydov and G. F. Filipov, Nucl. Phys. 8 (1958) 237.

[32] A. S. Davydov and A. A. Chaban, Nucl. Phys. 20 (1960) 499.

[33] S. G. Rohozinski, J. Dobaczewski, B. Nerlo-Pomorska, K. Pomorski, J. Srebrny,
     Nucl. Phys. A292 (1977) 66 .

[34] G. Puddu, O. Scholten, T. Otsuka, Nucl. Phys. A348 (1980) 109 .

[35] R. F. Casten, P. von Brentano, Phys. Lett. 152B (1985) 22.

[36] F. Iachello and A.Arima, *The Interacting Boson Model,* Cambridge University
     Press, Cambridge, 1987.

[37] A. Sevrin, K. Heyde, and J. Jolie, *Phys. Rev.* C 36 (1987) 2631.

[38] P. Von Brentano, A. Gelberg, S. Harissopulos and R. F. Casten, *Phys. Rev.* C
     38 (1988) 2386.

[39] X.-W. Pan, T. Otsuka, J.-Q. Chen and A. Arima, *Phys. Lett.* B 287 (1992) 1.

[40] T. Mizusaki and T. Otsuka, *Prog. Theor. Phys.* 125 (1996) 97.

[41] N. V. Zamfir, W. T. Chou, R. F. Casten, *Phys. Rev.* C 57 (1998) 427.

[42] C. L. Wu, D. H. Feng, X.-G. Chen, J.-Q.Chen and M. W. Guidry, *Phys. Rev.* C 36 (1987) 1157.

[43] X.-W. Pan, J. L. Ping, D. H. Feng, J. Q. Chen, C. L. Wu and M. W. Guidry, *Phys. Rev.* C 53 (1996) 715.

[44] N. Yoshinaga, T. Mizusaki, A. Arima and Y. D. Devi, *Prog. Theor. Phys.* 125 (1996) 65.

[45] N. Yoshinaga, Y. D. Devi and A. Arima, *Phys. Rev.*C 62 (2000) 024309.

[46] J. Q. Chen, *Nucl. Phys.* A626 (1997) 686.

[47]Y. A. Luo and J. Q. Chen, *Phys. Rev*C 58 (1998) 589.

[48]Y. M. Zhao, S. Yamaji, N. Yoshinaga and A. Arima, *Phys. Rev.* C 62 (2000), 014315.

[49] Y. A. Luo, J. Q. Chen and J. P. Draayer, *Nucl. Phys.* A 669 (2000) 101.

[50] R. Wyss *et al*., Nucl. Phys. A 505 (1989) 337.

[51] P. F. Mantica, Jr., B. E. Zimmerman, W. B. Walters, J. Rikovska and N. J. Stone, Phys. Rev. C 45 (1992) 1586.

[52] M. T. F. da Cruz and I. D. Goldman, Phys. Rev. C 42 (1990) 869.

[53] A. Christy, I. Hall, R. P. Harper, I. M. Naqib and B. Wakefield, Nucl. Phys. A142 (1970) 591.

[54] L. Prochniak, K. Zajac, K. Pomorski, S. G. Rohoziński and J. Srebrny, Nucl. Phys. A 648 (1999) 181.

[55] M. Beiner, H. Flocard, N. Van Giai and P. Quentin, Nucl. Phys. A 238 (1975) 29.

[56] E. W. Schneider, M. D. Glascock, and W. B. Walters, Phys. Rev. C 19 (1979) 1025.

[57] B. Singh, R. Iafigliola, K. Sofia, J. E. Crawford, and J. K. P. Lee, Phys. Rev. C 19 (1979) 2409.

[58] C Girit, W D Hamilton and E Michelakakis, J. Phys. G: Nucl. Phys. 6, (1980)1025.

[59] L. Goettig, Ch. Droste, A. Dygo, T. Morek, J. Srebrny, R. Broda and, J. Stycze , J. Hattula, H. Helppi and M. Jaaskelainen, , Nucl.Phys. A 357 (1981) 109.

[60] W. Gast, U. Kaup, H. Hanewinkel, R. Reinhardt, K. Schiffer, K. P.Schmittgen,K. O. Zell, J. Wrzesinski, A. Gelberg and P. v. Brentano, , Z.Phys. A 318 (1984)123

[61] R. Reinhardt, A. Dewald, A. Gelberg, W. Lieberz, K. Schiffer, K. P. Schmittgen, K. O. Zell and P. von Brentano, Z. Phys. A 329 (1988) 507.

[62] D. Jerrestam, S. Elfstrom, W. Klamra, Th. Lindblad, C.G. Linden, V. Barci, H. El-Samman and J. Gizon, , Nucl. Phys. A 481 (1988) 355.

[63] Rani Devi, S. P. Sarswat, Arun Bharti and S. K. Khosa, Phys. Rev. C 55 (1997) 2433.

[64] I. Maras1, R. Gumus and N. Turkan, Mathematical and Computational Applications, Vol. 15, No. 1 (2010) 79.

[65] Laurent Coquard, Ph. D Thesis " Evolution of the one qudrupole phonon $2_{1,ms}$ mixed symmetry state in $^{124-126-128-130\ 132}$Xe (2010) Darmstadt University.

[66] N. Turkan and I. Maras, Mathematical and Computational Applications, Vol. 16, No. 2 (2011) 467.

[67] Salah A. Eid and S. M. Diab, Progress in Physics, Vol.1 (2012) 54.

[68] G. Maino and A. Ventura, Lett. Nuovo Ciemento 34 (1982) 79.

[69] D. S. Chuu, C. S. Han, S. T. Hsieh and M. M. King Yen, Phys. Rev. C30 (1984) 1300.

[70] J. B. Gupta, J. Phys. G21 (1995) 565.

[71] A. G. Smith, W. R. Phillips, J. L. Durell, Phys. Rev. Lett. 73(1995) 2540.

[72] M. Hellstrom, H. Mach, B. Fogelberge *et al.*, Phys. Rev. C46 (1992) 86.

[73] A. G. Smith, W. R. Phillips, J. L. Durell, Phys. Rev. C47 (1993) 545.

[74] Long Guilu, ZHU Shengian, Zhang Jinyu, ZHAO Enguang and LIU Yuxin, Commun. Theor. Phys. 29 (1998) 65

[75] R.M. Clark *et al.*, Phys. Rev. C 67 (2004) 041302.

[76] R. F. Casten, N.V. Zamfir, R. Krucken, Phys. Rev. C 68 (2003) 059801.

[77] N. Turkan, I. Inci, Phys. Scr. 75 (2007) 515.

[78] S. Inan, N. Turkan, I. Inci and , D. Olgun, Mathematical and Computational Applications, Vol. 13, No. 2 (2008) 101.

[79] N. Turkan and I. Inci *Physics of Atomic Nuclei, Vol. 71, No. 11, (2008) 1918.*

[80] A. R. H. Subber and Falih H. Al-Khudair, *J. Basrah Researches (science)* 32 (2006) 12.

[81] E. Landulf, R. N. Saxena, C. B. Zamboni and A. L. Lapolli, *Phys. Rev.* C50 (1994) 733.

[82] M. Hasegawa, K. Kaneko and T. Mizusaki, *Phys. Rev.* C70 (2004), 031301.

[83] Zn. Podolyka et al., *International Journal of Modern Physics B* 13 (2004) 123.

[84] T. T. Hsieh, H. C. Chiang and De-San Chuu, *Phys. Rev. C* 46 (1992) 195.

[85] P. Duval, D. Goutte, and M. Vergnes, *Phys. Lett. B* 124 (1983) 297.

[86] E. Padilla-Rodal, Ph. D. Thesis, UNAM, Mexico (2004); E. Padilla-Rodal *et al. Phys. Rev. Lett.* 94 (2005) 122501.

[87] M. Vergnes *et al.*, *Phys. Lett. B* 72 (1978) 447.

[88] R. Lecomte *et al.*, *Phys. Rev. C* 22 (1980) 1530.

[89] Y. Toh *et al.* in *Nuclear Physics in the 21st century* INPC 2001, AIP Conf. Proc. 610 (2002) 793.

[90] R. Lecomte *et al.*, *Phys. Rev. C* 25 (1982) 2812.

[91] N. Turkan and I. Maras, *Mathematical and Computational Applications*, Vol. 15, No. 3, (2010) 428.

[92] A. R. H. Subber, Turk. J. Phys. 35 (2011) 43 .

,R. M. Clark , (2004) Paper LBNL-56419 , R. M. Clark *et al.*, Phys. Rev. C 69 [93] .064322 (2004)

.D. L. Hill and J. A. Wheeler, Phys. Rev. 89 (1953)1102 [94]

,D. Bonatsos, *Interacting Boson Models of Nuclear Structure*, (Clarendon Press [95] .(Oxford, 1988

.(A. Bohr and B. Mottelson, ′*Nuclear Structure*′ II, (Benjamin, Reading, 1975 [96]

. J.Wilets and M. Jean, Phys. Rev. 102 (1956) 788 [97]

.R. F.Casten, Romanian Reports in Physics, Vol. 57, No. 4 (2005) 515 [98]

,R. Bijker., Lecture notes: *IV International Balkan School on Nuclear Physics* [99] .Bodrum, Turkey, September (2004) 22

.(J. Lang, K. Kumar and J. H. Hamilton, Rev. Mod. Phys. Vol.54 No. 1 (1982 [100]

.E. L. Church and J. Weneser, *Phys. Rev*. 103 (1956), 1035 [101]

.R. Bijker, A. E. L. Dieperink and O.Scholten, Nucl. Phys. A 344 (1980) 207 [102]

.T. Otsuka, and O. Soholten, KVI Internal Report No. 253, 1979 [103]

.R. F. Casten, Nucl. Phys. A443 (1985) 1 [104]

.T. Otsuka, T. Matsuo, and D. Abe, Phys. Rev. Lett. 97 (2006) 162501 [105]

[106] D. Bohle, A. Richter, W. Steffen, A. E. L. Dieperink, N. Lo Iudice, F. Palumbo .and O. Scholten, Phys. Lett. 137B (1984) 27

[107] J. Enders, P. von Neumann-Cosel, C. Rangacharyulu, and A. Richter, .Phys. Rev. C71 (2005) 014306

 P. Van Isacker, K. Heyde, J. Jolie, and A. Sevrin, Ann. Phys. (NY) 171, 253 [108] .(1986)

[109] J. L. Wood, ˈin *Contemporary   research Topics in Nuclear Physics* .eds. D. H. Feng, *et al*., (Plenum Press, New York (1982) 451

[110] K. Heyde, P. Van Isacker, H. Waroquier, J. L. Wood, and R. A. Heyer, .Phys. Rep. 102 (1983) 291

.P. D. Duval, and B. R. Barrett, Nucl. Phys. A376 (1982)213 [111]

.P. D. Duval, Phys. Rev. Lett. 46, (1981)1504 [112]

.M. Sambataro and G. Molnar, *Nucl. Phys. A* 376 (1982) 201 [113]

[114] T. Otsuka, A. Arima and F. Iachello, Nucl. Pys. A309(1978) 1.

[115] R. F. Casten, A. I. Namenson, W. F. Davidson, D. D. Warner and H. G. Borner, Phys. Lette. 76B (1979) 280.

[116] N.A. Mansour ˝*Advances in Applied Science Research*˝, 2(5) (2011) 427.

[117] NSDF, http:// www.nndc.bnl.gov/ensdf, *National Nuclear Data Center*, (2011).

[118] A. R. Subber, P. Park, W. D. Hamilton, K. Kumar, K. Schreckenbach and G.   Colvin, J. Phys. G: Nuclear Phys. 12 (1986) 881.

[119] M. Sambataro, O. Scholten, A. E. L. Deperink and G. Piccitto, Nucl. Phys. A423(1984) 333.

[120] P. Van Isacker *et al*., Ann. Phys.2 (1985) 253.

[121] A. E.L.Dieperink, O.Scholten and D.D.Warner, Nucl. Phys. A469 (1987) 173.

[122] P. Van Isacker, K. Heyde , J. Jolie and A. Sevrin *Ann (NY)171. Phys (1986*) 253.

[123] O. Scholten , K. Heyde , P. Van Isacker and T. Otsuka *Phys. Rev.* C 32(1985) 1729.

[124] T. Otsuka and N. Yoshida, *the IBM-2 computer program NPBOS*, University of Tokyo (1985).

[125] G. Rainosvki, N. Pietralla, T. Ahn, L. Coquard, C. J. Lister, R. V. F. Janssens,M. P. Carpenter, S. Zhu, L. Bettermann, J. Jolie, W. Rother, R. V. Jolos, V. Werner, Phys. Lett. B683 (2010) 11.

[126] V. Werner, H. Meise, I. Wiedenhver, A. Gade, P. von Brentano, Nucl. Phys. A692 (2001) 451.

[127] A. Gade, I.Wiedenhver, J. Gableske, A. Gelberg, H. Meise, N. Pietralla, P.von Brentano, Nucl. Phys. A665 (2000) 268.

[128] D. Bonatsos, D. Lenis, N. Pietralla, P. A. Terziev, Phys. Rev. C 74 (2006) 44306.

[129] J. H. Hamilton, K. Kumar , L. Ramayya and P. E. Johnson Phys. Rev., 1974 C 10, 2540.

[130] W. D. Hamilton, A.Irback and P. Elliott, Phys. Rev. Lett. 53 (1984) 2469.

[131] S. Zerguine, P. Van Isacker, A. Bouldjedri, and S. Heinze, Phys. Rev. Lett. 101 (2008) 022502

الاهداء

الى مثلي الأعلى وقدوتي في الحياة *والدي

الى من صبرت وسهرت من اجل راحتي *والدتي

الى رمز المودة والوفاء وسندي *زوجتي

الى من شجعني في الشدائد *اخوتي

الى اصدقائي وكل من ساهم في انجاز هذا العمل

اليهم جميعا اهدي ثمرة جهدي عرفانا بفضلهم

عبد القادر سعد

بِسْمِ اللَّهِ الرَّحْمَنِ الرَّحِيمِ

إِنَّ فِي خَلْقِ السَّمَاوَاتِ وَالأَرْضِ وَاخْتِلَافِ اللَّيْلِ وَالنَّهَارِ وَالْفُلْكِ الَّتِي تَجْرِي فِي الْبَحْرِ بِمَا يَنْفَعُ النَّاسَ وَمَا أَنْزَلَ اللَّهُ مِنَ السَّمَاءِ مِنْ مَاءٍ فَأَحْيَا بِهِ الأَرْضَ بَعْدَ مَوْتِهَا وَبَثَّ فِيهَا مِنْ كُلِّ دَابَّةٍ وَتَصْرِيفِ الرِّيَاحِ وَالسَّحَابِ الْمُسَخَّرِ بَيْنَ السَّمَاءِ وَالأَرْضِ لَآيَاتٍ لِقَوْمٍ يَعْقِلُونَ .

الآية (164) مِن سورة البقرة

Committee Certification

We, the examining committee certify that we have read the thesis entitled "**Study of Nuclear Structure Properties and Electromagnetic Transitions for even – even Kr,Xe,Nd,Ge Nuclei in the Framwork of Interacting Boson Model**" and examined the student "**Abdulkader Saad Abdulkader**" in its contents and that is our opinion; it is accepted for the Degree of Master of Science in **Physics**.

Signature:
Name: **Dr. Raad A. Radhi**
Scientific Degree: **Professor**
Address: Dept. of Physics, College of Science /
Baghdad University
Date: 12/5 /2014
(Chairman)

Signature:
Name: **Dr. Muder Ahmed Abdulsattar**
Scientific Degree: **Chief . Researcher**
Address: Ministry of Science and
Technology
Date: 12/5/2014
(Member)

Signature: M. A. Z. Habeeb
Name: **Dr. M. A. Z. Habeeb**
Scientific Degree: **Assist. Professor**
Address: Dept. Physics, College of
Science/ Al-Nahrain University
Date: 11/5 /2014
(Member)

Signature: S. N. Abood
Name: **Dr. Saad N .Abood**
Scientific Degree: **Professor**
Address: Dept. of Physics, College of Science/
Al-Nahrain University
Date: 11 /5 /2014
(Member & Supervisor)

I, hereby certify upon the decision of the examining committee

Signature
Name: **Dr. Hadi M. A. Abood**
Scientific Degree: **Assistant Professor**
Title: Dean of the College of Science
Date: 10/5/2014

<u>List of Tables</u>

Abstract

Nuclear structure Properties and electromagnetic transitions of some even - even Kr, Xe, Nd and Ge isotopes have been studied in this work, by using the collective Interacting Boson Model-2 (IBM-2).

The Interacting Boson Model (IBM-2) has been very successful in describing the collective properties of nuclei. This work concerns a systematic applications of the model, involving configuration mixing of bosons.

There have been extensive IBM studies of low-lying positive parity bands, which are based on the ground state and the quadrupole degree of freedom.

The results for energy levels, B(E2), B(M1), mixing ratios $\delta(E2/M1)$, quadrupole and magnetic dipole moments and monopole transitions, were compared with some previous experimental and theoretical values. It was found that an acceptable degree of agreement between the predictions of the IBM-2 and the experiment can be achieved.

The Kr isotope (Z = 36) lies in the transitional region closer to the vibrational range of nuclei. Energy , levels B(E2), B(M1) and the mixing ratios δ(E2/M1) and X(E0/E2) for selected transitions in this isotope were calculated in the framework of the interacting boson model (IBM-2). All results were compared with experimental data. Some experimental X(E0/E2) ratios were calculated from available experimental data. Majorana parameters were found to have a great effect on the calculated energy levels of the $J_i^\pi = 2_3^+$, 3_2^+ , 2_4^+ and 1^+ states which indicates they have mixed symmetry properties.

The results of IBM-2 for Xe isotopes were compared with the theoretical predictions assuming a critical point symmetry E(5) which leads to conclude that ^{128}Xe is not an E(5) isotope as previously suggested. In this case of the ^{128}Xe the observable $R_{4/2} = 2.33$ is intermediate between the value for E(5) $\left(R_{4/2} = 2.2 \right)$ and gamma soft limit $\left(R_{4/2} = 2.5 \right)$. The ratio suggests that ^{128}Xe should lie between E(5) and O(6).

Similar test using ^{130}Xe as a most likely candidate amongst the Xe isotopes, conclusively demonstrate a how well E(5) is realized in the best case. The energy ratio confirmed that this isotope an E(5) critical point symmetry. The ^{132}Xe and ^{134}Xe show vibrational-like character (SU(5) limit).

Mixed symmetry states are also studied. It is found that some of the mixed symmetry states with moderate high spins change very fast with respect to the Majorana interaction. Under certain conditions, they become the yrast state or yrare state. These states are difficult to decay and become very stable. This study suggests that a possible new mode of isomers may exist due to the special nature in their proton and neutron degrees of freedom for these isotopes.

The mixed-symmetry 2_M (2_3^+) states or at least a fragment of it have been identified in Xe isotopes. This enables us to trace the evolution of the one-phonon 2_M states in the even-even xenon isotopic chain from the vibrators near N = 82 to the γ-soft nuclei towards mid-shell.

We have studied the nuclear properties of Neodymium isotopes with (A =144-154) in IBM-2. A good agreement results with the experimental data. $^{144-150}$Nd lie in the transitional region (virational - rotational limit SU(5)→SU(3)). For the $^{152-154}$Nd isotopes the energy ratio are well described by the rotational limit SU(3). The X(5) symmetry would take place when moving continuously from the pure U(5) symmetry to the SU(3) symmetry and it implies a definite relations among the level energies and among the E2 transition strengths. It was recently shown that a signature of phase transition is observed in the chain of Nd isotopes, ^{150}Nd display the predicted features of the X(5) symmetry and mark therefore the critical point. However, more detailed studies and experiments are needed to get ideas about this signature. At the end, we have concluded that some of Nd isotopes display X(5) symmetry features. The $2_3^+, 2_4^+$ and 1^+ are mixed symmetry states in Nd isotopes.

The even-even isotopes of germanium are of special interest because of the coexistence of two sets of bands, of very different character, in the lighter nuclei. The IBM-2 with configuration mixing provides a good description, both of states built on the normal ground state and of those associated with a proton pair excitation across the Z =28 closed-shell gap. Ge isotopes are studied, ranging from the middle of the neutron shell to very near the doubly closed shell at ^{82}Ge. Same Hamiltonian is used for all the nuclei studied, with parameters which are constant or smoothly varying.

الخلاصة

لقد تم في هذا البحث دراسة التركيب النووي والانتقالات الكهرومغناطيسية لبعض باستخدام النموذج الجماعي $\mathcal{G}e$ و $\mathcal{K}r$ ، $\mathcal{X}e$ ، $\mathcal{N}d$) النظائر (الزوجية – الزوجية $\mathcal{IBM_2}$) نموذج البوزونات المتفاعلة الثاني .

الانتقالات $B(E_2)$ ، تم الحصول على نتائج لمستويات الطاقة، والانتقالات الكهربائية وعزم رباعي القطب الكهربائي ، وعزم ، (E_2/M_1) ونسبة الخلط ، $B(M_1)$ المغناطيسية ثنائي القطب المغناطيسي ، والانتقالات احادية القطب . ولقد تم مقارنة النتائج مع القيم العملية المتوفرة وقد وجد انها متقاربة ومقبولة .

ان نظائر ال $\mathcal{K}r$ $(Z=36)$ تقع في المنطقة الانتقالية القريبة من التحديد الاهتزازي. لبعض $X(E_0/E_2)$ و (E_2/M_1) ، $B(M_1)$ ، $B(E_2)$ ، ولقد تم حساب مستويات الطاقة وان جميع النتائج $(\mathcal{IBM_2})$ الانتقالات المختارة باستخدام نموذج البوزونات المتفاعلة الثاني قد قورنت مع القيم العملية.

$$= 2^+_4$$

لقد كان لمعاملات ماجيرونا اثرا كبيرا في حساب مستويات الطاقة   ,, ,   التي حددت انها تمتلك صفات تناظر مختلطة .

$$(R_{4/2} = 2.5)$$

لقد تم مقارنة نتائج نظائر $\mathcal{X}e$ من نموذج   التي تم الحصول عليها من نموذج $\mathcal{IBM_2}$ التوقعات مع ان ^{128} وتبين $\mathcal{X}e$ ضمن يقع نظير ليس هو $\mathcal{E}(5)$ النظرية لتماثل النقطة الحرجة $\mathcal{E}(5)$. كما اقترح مسبقا . لذا فان نسبة الطاقة لنظير ال $\mathcal{X}e^{128}$ تقع بين O و حدود $\mathcal{E}(5)$ soft γ فان النسبة هذه فحسب وبذلك $\mathcal{X}e$ يجب ان يقع بين $\mathcal{E}(5)$ و $O(6)$. ^{128} .

بأفضل $E_{(5)}$ والذي يظهر خصائص ، X_e مناسب لنظائر X_eغالبا ما يكون اختبار [130]

اما بالنسبة لنظائر . $E_{(5)}$ حالته. كذلك فان مستويات الطاقة تعزز وجود هذا النظير ضمن

[132]X_e [134]و X_e فإنها تظهر صفات مشابهة للمحدد الاهتزازي . $SU_{(5)}$

$2_M^{}$

وهذا قد مكننا من X_e ان مستويات التناظر المختلطة   قد تم التعريف عليها من نظائر

تعقب تحرير فونون واحد لحالة في سلسلة النظائر (الزوجية – الزوجية) للزنون من

باتجاه منتصف القشرة γ_{-soft} الى نواة $N=82$ الاهتزازات القريبة من .

وتم الحصول IBM_2 في $(A=144-154)$ Nd لقد درسنا الخصائص النووية لنظائر

على نتائج جيدة مقارنة بالقيم العملية .

بينما . $(SU_{(5)} \to SU_{(3)})$ يقع في المنطقة الانتقالية (الاهتزازي – الدوراني $Nd^{144-150}$

نظائر Nd فإنها تقع ضمن التحديد الدوراني $(SU_{(3)})$. [154-152]

ان تناظر $X_{(5)}$ يستمر بحركته بين تناظر عندما يأخذ مكان او حيز سوف $U_{(5)}$ الى تناظر ال

$SU_{(3)}$ ويظهر ذلك بصورة واضحة ما بين مستويات الطاقة وقوى الانتقال رباعي القطب

. E_2

$1^+ , 2_4^+$

Nd^{150} تشير الى الانتقالات الطورية كما ان نظير Nd لقد وجد حديثا ان سلسلة نظائر

على العموم فان هناك عدة دراسات مفصلة بحاجة . $X_{(5)}$ يعرضا الخواص المتوقعة ل

تكتشف خواص $\mathcal{N}d$ للحصول على تلك المؤشرات . وبالنهاية نستنج بان بعض نظائر $\mathcal{X}(5)$. ان $\mathcal{N}d$, هي حالات تناظر مختلطة لنظائر

كان ناجحا بوصفه للخواص التجميعية للنواة . ان نموذج البوزونات المتفاعلة $\mathcal{IBM}_2$ وفي هذا البحث قد تم الاهتمام بالتطبيقات النظامية والمتضمنة اشكال البوزونات المختلطة.

ان النظائر الجرمانيوم (الزوجية – الزوجية) لها اهتمام خاص بسبب وجودها ضمن مجموعتين من الحزم ذات الخواص المعقدة للنواة الخفيفة . ان نموذج البوزونات المتفاعلة $\mathcal{IBM}_2$ مع التركيبات المختلطة يجهز توصيف جيد لكلا الحالات المبينة بالمستوى المغلق $\mathcal{Z}=28$ الارضي وللبروتونات الموجودة بالمستوى المتهيج عبر غلاف القشرة .

لقد تم دراسة نظائر الجرمانيوم وتبين انه يتدرج مابين وسط قشرة البروتون و القشرة ولقد وجد ان نظائر الجرمانيوم عند التشكيل $\mathcal{G}e$ المزدوجة القريبة من المغلقة عند ال ^{82} تأخذ الشكل الدوراني (ويزداد $\mathcal{N}_\pi=4$ تأخذ الشكل الاهتزازي وعند التشكيل $\mathcal{N}_\pi=2$ التشوه).

وفي هذا العمل استخدمت طرق حديثة جدا لتعيين الشحنات الفعلية $(effective$ $charge)$ للبوزونات وذلك باستخدام القيم العملية للانتقال رباعي القطب $(01+$

$21+$ $\mathcal{B}(\mathcal{E}_2;$

وكذلك استخدمت طرق جديدة لحساب المعاملات الجيرو مغناطيسية للبوزونات g_v ، g_π

وذلك بمعايرتها الى القيم العملية لـ (E_2/M_1) δ و $B(M_1)$.

Comparison between experimental and calculated energy levels for ^{80}*Ge* *($N_{\pi = 4}$)*

112

3 . 41

Comparison between experimental and calculated energy levels for ^{82}*Ge* *($N_{\pi = 4}$)*

113

3 . 42

The plot of the quantity M1 and M2 versus $e_{\pi} +$ $e_{\upsilon} N_{\upsilon} / N_{\pi}$ *for* $^{64\text{-}80}$*Ge*

114

Chapter One

Introduction

Chapter Two

Nuclear Collective Models

Chapter Three

Results and Discussion

Chapter Four

Conclusions and Suggestions

Contents

Chapter One : Introduction

Chapter two : Collective Models – General nuclear deformation

Chapter Three : Results and Discussion

Chapter Four: Conclusions and Suggestions

Republic of Iraq
Ministry of Higher Education
and Scientific Research
Al-Nahrain University
College of Science
Department of Physics
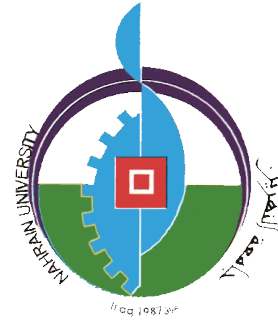
Study of Nuclear Structure Properties

and Electromagnetic Transitions for

even - even   Kr , Xe , Nd , Ge Nuclei in

the Framework of Interacting Boson

Model

A Thesis

Submitted to College of Science / Al-Nahrain University as

a partial fulfillment of the requirements for the degree of

. Master of Science in Physics

By

ABDULKADER SAAD ABDULKADER

B.Sc.2006 / College of Science / Al-Nahrain University

Supervised by

Prof. Dr. SAAD N . ABOOD

January , 2014   **Rabia Al awal ,1435**

دراسة الخصائص النووية التركيبية والانتقالات الكهرومغناطيسية الزوجية – الزوجية باستخدام Ge ، Nd ، Xe ، Kr لأنوية نموذج البوزونات المتفاعلة

رسالة مقدمة إلى
كلية العلوم – جامعة النهرين
وهي جزء من متطلبات نيل درجة الماجستير في الفيزياء

من قبل
عبد القادر سعد عبد القادر

بإشراف
الأستاذ الدكتور سعد ناجي عبود

Acknowledgments

At first, thanks to my God for helping me to complete this thesis. Then, I would like to express my sincere appreciation and deep gratitude to my supervisor, Prof.Dr. Saad N . Abood for suggesting the topic of this thesis, guidance, suggestions and continuous encouragement throughout the research work.

I would like to thank the Dean of the college of Science , the Head of Physics Department Dr .Thamir A.Jumaa , Dr . A.R.H.Subber / Al – Basrah University and all staff members of Physics Department at Al – Nahrain University.

Finally, I'm grateful to my dearest parents for their perpetual love, patience and encouragement, and to my brothers, also to anyone who helped me in one way or another, and who contributed in making this thesis possible particularly.

Abdulkader